The Physics of Non-spherical Compact Objects

Mert Mangut

Submitted to the
Institute of Graduate Studies and Research
in partial fulfillment of the requirements for the degree of

Doctor of Philosophy
in
Physics

Eastern Mediterranean University
September 2023
Gazimağusa, North Cyprus

Approval of the Institute of Graduate Studies and Research

Prof. Dr. Ali Hakan Ulusoy
Director

I certify that this thesis satisfies all the requirements as a thesis for the degree of Doctor of Philosophy in Physics.

Prof. Dr. İzzet Sakallı
Chair, Department of Physics

We certify that we have read this thesis and that in our opinion it is fully adequate in scope and quality as a thesis for the degree of Doctor of Philosophy in Physics.

Prof. Dr. Özay Gürtuğ
Co-Supervisor

Prof. Dr. İzzet Sakallı
Supervisor

Examining Committee

1. Prof. Dr. Muzaffer Adak
2. Prof. Dr. Tekin Dereli
3. Prof. Dr. Mustafa Gazi
4. Prof. Dr. Özay Gürtuğ
5. Prof. Dr. Mustafa Halilsoy
6. Prof. Dr. S. Habib Mazharimousavi
7. Prof. Dr. İzzet Sakallı

ABSTRACT

In this thesis, one of the well-known spacetimes named as Zipoy-Voorhees (ZV) or γ-metric is extended to its charged version via Ernst formalism and is called the charged ZV solution. This spacetime is then further investigated and the relevant geodesic equations, the Newtonian limit, the solution of Maxwell equations and the singularity analysis are all carried out in detail. These steps are later on followed by inspecting the physical properties of the consequent γ-metric, whose gravitational lensing effect is compared with the one for the stationary ZV solution. In this regard, the effect of deformation parameter γ on gravitational lensing and redshift is studied. With the help of Chandrasekhar-Xanthopoulos (CX) theorem and Ernst formalism, the charged and stationary version of ZV solution is also obtained. The metric functions of this new solution - which came out to be utterly complicated - are expanded up to the quadrupole terms. As a result, the closed time-like curves are examined. Another important compitation known as the singularity analysis is carried out for the uncharged and charged versions of ZV spacetime on $\theta = \pi/2$ and $\theta = \pi$ planes. In the end, it has been found that both solutions are quantum regular in s-mode on the $\theta = \pi$ plane for $1 < \gamma < 2$. Lastly, gravitational lensing analysis is conducted on another well-known spacetime of theoretical physics, Kerr-Newman Anti de Sitter metric, and the effect of rotation on black holes is studied by using observational data from $M87$ and $SgrA*$.

Keywords: Non-spherical Symmetry, Ernst Formalism, Gravitational Lensing, Gravitational Redshift, Quantum Singularity Analysis

ÖZ

Bu tezde literatürde Zipoy-Voorhees (ZV) uzayzamanı veya γ-metriği olarak bilinen ve fiziksel yapı parametresi sadece kütle olan küresel olmayan çözüm, Ernst formalizm yardımıyla yüklü hale getirilerek, yüklü ZV uzayzamanı elde edilmiştir. Bu yeni uzayzaman üzerinde, jeodezik analizi, Newton limiti, Maxwell denklemlerinin çözümü ve tekillik analizi yapılmıştır. Daha sonra ise ilgili uzayzamanın fiziksel özellikleri araştırılarak, bu yeni çözümde kütle-çekimsel mercekleme etkisi stasyoner ZV çözümüyle karşılaştırılmıştır. Bu bağlamda, γ ile ifade edilen geometrik deformasyon parametresinin, bahsi geçen fiziksel olay üzerindeki etkisi incelenmiştir. Elde edilen yeni yüklü ZV çözümü üzerinde kütleçekimsel kırmızıya kayma olayı da incelenmiştir. ZV çözümünün önemli başka bir sınıfı olan yüklü ve stasyoner ZV sınıfı, literatürde Chandrasekhar-Xanthopoulos (CX) teoremi olarak bilinen teorem kullanılarak, Ernst formalizm yardımıyla türetilmiştir. Bu oldukça karışık yeni çözümün metrik fonksiyonları, kuadrapol terimlere kadar açılarak bu çözümün kapalı zamansal jeodezik denklemleri incelenmiştir. Bir başka önemli analiz olan kuantum tekillik analizi, ZV ve yüklü ZV uzayzamanlarında $\theta = \pi/2$ ve $\theta = \pi$ düzlemlerinde yapılarak, her iki çözümün de $\theta = \pi$ düzleminde $1 < \gamma < 2$ aralığında, s-dalga modunda kuantumsal olarak düzenli olduğu bulunmuştur. Son olarak, teorik fiziğin tanınmış bir başka uzayzamanı olarak bilinen, küresel olmayan ve kara deliklere uygulanabilen Kerr-Newman Anti de Sitter metriğinde, kütleçekimsel mercekleme analizi yapılarak, dönmenin mercekleme üzerindeki etkisi; $M87$ ve $SgrA*$ kara deliklerinin gözlemsel verileri kullanılarak incelenmiştir.

Anahtar Kelimeler: Küresel Olmayan Simetri, Ernst Formalizmi, Gravitasyonel

Mercekleme, Kütleçekimsel Kırmızıya Kayma, Quantum Tekillik Analizi

... Dedicated to my wife Huriye

Je n'ais pas le temps

Évariste Galois (1811-1832)

ACKNOWLEDGMENTS

First of all, I would like to express my gratitude to my thesis supervisor, Prof. Dr. İzzet, and my co-supervisor, Prof. Dr. Özay Gurtuğ, who have consistently supported my academic development with both scholarly guidance and personal advice. I am deeply indebted to Prof. Dr. Mustafa Halilsoy for broadening my horizons with his scientific and humanitarian insights and for inspiring me to pursue research in non-spherical symmetries throughout my academic journey. Undoubtedly, my heartfelt thanks go to my dear wife, Assist. Prof. Dr. Huriye Gürsel Mangut, who has been my constant companion in this academic adventure, enriching my perspectives with emotional and scholarly discussions. Additionally, I would like to extend my appreciation to the dedicated instructors, teaching assistants, lab technician, Mr. Reşat Akoğlu, and our Administrative Assistant, Mrs. Çilem Aydıntan, from the Physics department, who have been like a second family to me during my assistantship.

Mert Mangut

Famagusta - Cyprus

September 2023

TABLE OF CONTENTS

LIST OF TABLES

LIST OF FIGURES

Figure 6.1: The plots illustrate the bending angles ε as a function of $x = R/R_*$ for both the $M87$ and $Sgr\ A^*$ black holes. In the case of $Sgr\ A^*$, the graphs are generated assuming a mass of $4.1 \times 10^6 M_\odot$. The Schwarzschild radius is taken as $1.27 \times 10^{10} m$, and the charge is approximately $10^{15} C$. For the $M87$ black hole, the graphs are plotted based on a mass of $6.5 \times 10^9 M_\odot$, an observable radius of $16.8 Mpc$, and a tidal charge of $9.35 \times 10^{22} C$. Additionally, as mentioned earlier, $j = 1$ represents the maximum-rotation scenario, while $j = 0$ corresponds to the non-rotating case. 105

LIST OF SYMBOLS

γ	ZV Parameter
Λ	Cosmological Constant
Ψ	Wave Function
α	Bending Angle
ε	One Sided Bending Angle
$\chi(\mathfrak{R})$	Euler-Poincare Characteristic
$\kappa_g(s)$	Geodesics Curvature
$\mathcal{K}$	Gaussian Curvature
$\mathcal{M}$	Quadrapole Moment
$\mathfrak{R}$	Generic Two Dimensional Surface
A	Spatial Wave Operator
b	Impact Parameter
g^{opt}	Optical Metric
g_{ij}	Metric Tensor
H	Electromagnetic Complex Potential
$H(L^2)$	Hilbert Space
R	Impact Parameter
r_0	Closest Distance of Approach
z	Gravitational Redshift Parameter
Z	Gravitational Complex Potential

LIST OF ABBREVIATIONS

AF	Asymptotically flat
BR	Bertotti-Robinson
BTZ	Bañados-Teitelboim-Zanelli
CX	Chandrasekhar-Xanthopoulos
em	Electromagnetic
EM	Einstein-Maxwell
GB	Gauss-Bonnet
HM	Horowitz-Marolf
KG	Klein-Gordon
KN(A)dS	Kerr-Newman (anti) de Sitter
NP	Newman-Penrose
NUT	Newman-Unti-Tamburino
PPON	Parallelly Propagated Orthonormal
RI	Rindler-Ishak
RN	Reissner-Nordström
S	Schwarzschild
ZAMO	Zero Angular Momentum Observer
ZV	Zipoy-Voorhees

Chapter 1

INTRODUCTION

Without any doubt, the Schwarzschild solution of Einstein's equations [3] plays an important role in the historical timeline of the concepts of general relativity. This specific solution possesses a spherical symmetry, and hence, despite its vast importance in the theory of black holes, can be considered to be trivial. Nevertheless, if the symmetry of concern is axial rather than spherical, the situation seems to be way more complicated. Such a case was examined in detail by Hermann Weyl, whose relevant ideas can be found in his article entitled "Zur Gravitationstheorie" [4] [1] .

During his study, Weyl first concentrates on the fundamental quantities mass m and electric charge e and rescales them (in c.g.s. units) as

$$a = \kappa m, \tag{1.1}$$

and

$$a' = \frac{\sqrt{\kappa} e}{c}. \tag{1.2}$$

In turn, he names a and a' as the gravitational radii of the mass and the electric charge, respectively. Then, he further introduces

$$a'' = \frac{e^2}{mc^2}, \tag{1.3}$$

[1] For the English-translated versions of Schwarzschild's and Weyl's papers, a reader is referred to [5] and [6], respectively.

which can be referred as the radius of an electron under appropriate conditions.

The mathematical equations constructed by Weyl relating the mass, charge and length at different scales can be considered as an attempt of using concepts of general relativity to explain atomic phenomena. This claim is supported by the words of Weyl himself, which go as follows [6]:

> *"The acquisition of exact solutions to the equations of gravity seems important to me with regard to the question of processes at work within the atom. After all, it is possible that at such scales it is essential to take the non-linearity of the exact laws of nature into account.*
>
> ....
>
> *To this end, granted, one that still lies in the distant future, it seems to me of interest to determine exactly the gravitational field of an axially symmetric distribution of masses and charges according to Einstein's theory. This will be done here for the static case; the study leads to surprisingly simple results."*

As can be seen from the statements above, Weyl solutions possess axial symmetry. Although one might find it tempting to use standard coordinates to study such solutions, there are good valid reasons to look for alternatives.

1.1 Deviating from Standard Symmetries

1.1.1 Observational Aspect

The universe is filled with a variety of astronomical objects with different fundamental properties. In a universe like ours (which is known to host a great many number of possibilities within itself), it would not be wise to assume perfect symmetries to exist for all its components. Although it is possible to create a list of astronomical objects with for instance spherical symmetry, there also exist a great many which can be treated as non-spherical compact objects. These can be thought as examples for objects of nature deviating from standard symmetries.

The geometrical shapes of compact objects deviating from standard symmetries are attained as a consequence of the strong gravitational effects. Non-spherical compact objects - which are the main objects of concern in this thesis - are good examples of such astronomical bodies. In outer space, neutron stars are generally treated as non-spherical compact objects. The majority of these stars are thought to have oblate shapes due to strong electromagnetic (em) and rotational effects.

Neutron stars are not the only astronomical examples we can give for non-spherical compact objects. Since deviations from standard symmetries are thought to arise due to immense physical effects, it is natural to treat black holes as candidates for having such geometrical deformations. Due to strong gravitational field, black holes are expected to exist in many different shapes, some of which can be categorised as flattened or oblate.

In the theory of general relativity, there are two familiar solutions that are treated as non-spherical compact objects. These are named as the Zipoy-Voorhees (ZV) [7, 8] and Kerr-Newman [9] solutions. ZV metric describes the gravitational field around a static, non-spherical mass distribution in empty space, whereas the Kerr-Newman solution has rotation and charge [10, 11, 12]. The ZV solution is also known as the γ-metric, since γ is the key parameter determining the geometrical shape of the associated compact object. For instance, if $\gamma > 1$, the solution is oblate; whereas $\gamma < 1$ refers to a prolate shape.

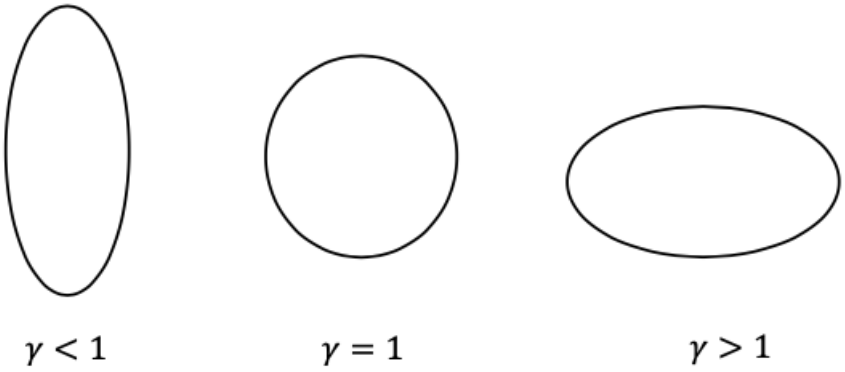

Figure 1.1: The diagrams above illustrate rough sketches of the prolate, sphere and oblate (from left to right).

It is also important to note that the concept of cosmological constant was first introduced in the Schwarzschild solution in 1918 by Kottler [13], and it was later on used in rotating black holes by Carter [14]. These were important steps in both theoretical and observational physics.

1.1.2 Theoretical Aspect

In 1966 [7], Zipoy declared that not being limited to cylindrical coordinates would be of advantage while searching for vacuum axially symmetric solutions of Einstein's equations. By then, picking alternative coordinate systems to solve Einstein's equations with less hassle was already a familiar viewpoint (for instance, check [15] for solutions in oblate spheroidal and toroidal coordinates). However, Zipoy's perspective differed in the sense that rather than concentrating on a variety of mass distributions, he ignored the entire concept as a whole and examined the case when there existed no mass in the vicinity. Eventually, he figured the mass term came into play as a mathematical consequence. In the end, via coordinate transformations, he obtained solutions for a specific class of Weyl spacetimes in prolate and oblate spheroidal coordinates.

Zipoy was not the only one seeking solutions of vacuum Einstein equations by using alternative coordinates. Voorhees also managed to obtain static axially symmetric solutions to the vacuum field equations. Zipoy's approach was criticized by Voorhees [8] in the following aspects:

Voorhees claimed that Zipoy's perspective was almost purely mathematical, lacking important physical implications. Furthermore, he claimed the logical path followed by Zipoy was not as straightforward as it should have been. Due to these reasons combined, Voorhees provided detailed physical explanations in his own work and the derivation steps also differed once compared with Zipoy's.

Voorhees expressed Schwarzschild line element in Weyl coordinates with the aid of transformations used by Ernst in his study entitled [16] "New Formulation of the Axially Symmetric Gravitational Field Problem".

Today, ZV solution is very frequently used by many physicists, some of which can be found in [17, 18, 19].

1.2 General Information on Gravitational Lensing, Redshift and Singularity

This section is reserved for concepts such as gravitational lensing, redshift and singularity. These events do not only carry importance in astronomy but also in theoretical physics, especially because they act as a bridge between theoretical concepts and observational evidences. Therefore, a brief introduction on them will be presented here. The mathematical details can be found in the upcoming chapter.

1.2.1 Gravitational Lensing

Einstein's theory of general relativity got its first empirical evidence in its favour after the famous astronomical effect observed by British astronomer Arthur Eddington in

1919. During the solar eclipse that occurred on 29^{th} of May in this year, observations of Eddington on bending of light due to gravity was compatible with theoretical work of Einstein[20, 21]. This is considered as the first observational confirmation of Einstein's theory of general relativity.

According to general relativity, the effect of gravity should also be distinctive in the vicinity of black holes. To be more specific, in theory, if the oscillations arising due to high temperature events occurring around a black hole cross the Earth's past light cone's caustics, one expects to see some observational effects encrypted in the X-rays emitted [22].

1.2.2 Redshift

Gravitational redshift can be defined as the Doppler effect arising due to the gravitational attraction experienced between light and a dense compact object. When light propagates in the vicinity of such an object, its wavelength decreases and the effect is seen as a shift toward the red spectrum. This effect got confirmed both in laboratory and with astrophysical observations. The laboratory confirmation was achieved by an experiment designed by Pound and Rebka in 1959 [23]. During this experiment, a gamma-ray beam was used rather than visible light and it was aimed to investigate what effects would be observed, once the gamma ray beam was set to travel close to a gravitational source. The recorded data was consistent with the expectation of gravitational redshift evaluations of general relativity. From the astrophysical aspect, the same affect was recognised in 1964, when the spectral lines of quasars $3C-48$ and $3C-273$ were studied by Greenstein and Schmidt in 1964 [24]. The associated spectral lines showed evidences for gravitational redshift with values 0.367 and 0.158, respectively.

1.2.3 Singularity

General theory of relativity contains a vast amount of information within itself. Although it covers a great range of possibilities and objects, there is a concept known as "singularity", which still remains as an unsolved mystery. Singularities are points in spacetime with infinite density and no volume of occupation. It is not that easy to picturize or mathematically or physically describe these regions with tools of general relativity, since the theory becomes insufficient at very small scales. For instance, if one attempts to write down geodesics at singularities, he or she would encounter problems. Furthermore, providing definitions for observables such as energy and gravitational force would also be problematic, as they would diverge at singularities. Due to these and many other reasons, one of the main goals of current theorists is to find some ways of dealing with singularities. As the theory foresees that at the centre of every black hole, there must lie a singular point in spacetime, it would not be insightful to not look for a precise definition of this peculiar concept. So far, quantum gravity seems to be a promising candidate that can coalesce principles of general relativity and quantum physics.

1.3 A Brief Prescription of The Thesis

In this thesis, a new solution to the Einstein-Maxwell (EM) equation that describes the charged version of the ZV spacetime is presented. It's physical properties are investigated in detail. In chapter 2, the required mathematical background is reviewed under the title of mathematical preliminaries. The Maxwell extension of ZV spacetime is presented in chapter 3, together with stationary generalizations. Chapter 4 is devoted for the investigation of the physical properties of the charged ZV spacetime. Geodesics, gravitational lensing and redshift analysis are considered in this section. Chapter 5 is devoted for the analysis of the singularity structure both for charged and uncharged ZV metrics. The singularity analysis is based on the principle

of quantum mechanics. The non trivial naked singularities are probed with quantum wave packets obeying the Klein-Gordon equation. In chapter 6, gravitational lensing is analysed for the Kerr-Newman (anti) de-Sitter spacetime with astrophysical application. The thesis is concluded with a conclusion in chapter 7.

Chapter 2

MATHEMATICAL PRELIMINARIENS

This section is devoted for the mathematical background used throughout the thesis.

2.1 Ernst Formalisim

Ernst formalism is a formalism that aims to express Einstein's equations in a more compact form. Furthermore, it can be treated as the process of deriving Ernst equations. The Ernst equations are a set of equations in general relativity that describe the gravitational and em fields of a stationary, axisymmetric spacetime. Frederick J. Ernst investigated the formalism in 1968 by using the Lagrangian formalism for gravitational and em spacetime [16, 25].

This subsection aims to provide steps that can be followed for deriving Ernst equations from the stationary axially symmetric metric with the Ernst Lagrangian.

Firstly, consider the line element

$$ds^2 = f(dt - \omega d\varphi)^2 - f^{-1}\left\{e^{2\gamma}\left[d\rho^2 + dz^2\right] + \rho^2 d\varphi^2\right\}, \tag{2.1}$$

which is known as the Weyl-Lewis-Papapetrou form of the stationary axially symmetric fields [4, 26, 27]. Here, $f = f(\rho, z)$, $\gamma = \gamma(\rho, z)$ and $\omega = \omega(\rho, z)$ and it is worthy to note that this metric admits two cyclic coordinates (t, φ).

Although it is possible for one to obtain the entire field equations by using methods

from exterior calculus, for our interest, we will only be concentrating on equations governing f and ω. These can be obtained by varying the Ernst Lagrangian, which is written as

$$\mathcal{L} = -\frac{1}{2}\rho f^{-2}\vec{\nabla} f \cdot \vec{\nabla} f + \frac{1}{2}\rho^{-1} f^2 \vec{\nabla}\omega \cdot \vec{\nabla}\omega. \tag{2.2}$$

Here, $ds_0^2 = d\rho^2 + dz^2 + \rho^2 d\varphi^2$ is the base manifold of the geometry. If we open the differential operators inside the Lagrangian according to the base manifold, Eq.(2.2) can be rewritten as

$$\mathcal{L} = -\frac{1}{2}\rho f^{-2}\left(f_\rho^2 + f_z^2\right) + \frac{1}{2}\rho^{-1} f^2 \left(\omega_\rho^2 + \omega_z^2\right), \tag{2.3}$$

where the coordinate index denotes the derivatives of the related coordinates. Now, let us find the necessary equations by taking variations with respect to f and ω using the Ernst Lagrangian, respectively. Varying $\mathcal{L}$ with respect to f leads to the following.

$$\frac{\partial \mathcal{L}}{\partial f} - \frac{\partial}{\partial \rho}\frac{\partial \mathcal{L}}{\partial f_\rho} - \frac{\partial}{\partial z}\frac{\partial \mathcal{L}}{\partial f_z} = 0. \tag{2.4}$$

When we substitute Eq.(2.3) into the varying equation of f, Eq.(2.4) becomes

$$f\nabla^2 f = \vec{\nabla} f \cdot \vec{\nabla} f - \rho^{-2} f^4 \vec{\nabla}\omega \cdot \vec{\nabla}\omega. \tag{2.5}$$

Varying equation of $\mathcal{L}$ with respect to ω implies

$$\frac{\partial \mathcal{L}}{\partial \omega} - \frac{\partial}{\partial \rho}\frac{\partial \mathcal{L}}{\partial \omega_\rho} - \frac{\partial}{\partial z}\frac{\partial \mathcal{L}}{\partial \omega_z} = 0. \tag{2.6}$$

Thus, Eq.(2.6) gives

$$\vec{\nabla} \cdot \left(\rho^{-2} f^2 \vec{\nabla}\omega\right) = 0. \tag{2.7}$$

For $\omega = 0$, Eq.(2.5) can be integrated easily and the attained results are referred as Weyl solutions.

Let us now focus on Eq.(2.7). From vector calculus, one can state that there exists a vector $\vec{A}$ such that

$$\vec{\nabla} \cdot \left(\vec{\nabla} \times \vec{A} \right) = 0 \tag{2.8}$$

is satisfied. If we compare Eq.(2.7) and Eq.(2.8), we can find

$$\rho^{-2} f^2 \vec{\nabla} \omega = \vec{\nabla} \times \vec{A}. \tag{2.9}$$

In cylindrical coordinates Eq.(2.9) can be written as

$$\begin{aligned} \rho^{-2} f^2 \left\{ \hat{e}_\rho \omega_\rho + \hat{e}_z \omega_z + \frac{1}{\rho} \hat{e}_\varphi \omega_\varphi \right\} = & \frac{1}{\rho} \left\{ \hat{e}_\rho \left[\rho A_{\varphi,z} - A_{z,\varphi} \right] - \hat{e}_z \left[A_\varphi + \rho A_{\varphi,\rho} - A_{\rho,\varphi} \right] \right. \\ & \left. + \rho \hat{e}_\varphi \left[A_{z,\rho} - A_{\rho,z} \right] \right\}, \end{aligned} \tag{2.10}$$

where "," represents derivative according to the coordinate that follows it. For achieving axial symmetry, one needs to set $\omega_\varphi = 0$. Due to this condition, the term including $\hat{e}_\varphi$ at the right hand side of Eq.(2.10) automatically vanishes. Furthermore, if one equates ω_ρ and ω_z in Eq.(2.10),

$$\omega_\rho = \rho f^{-2} \left[\rho A_{\varphi,z} - A_{z,\varphi} \right], \tag{2.11}$$

and

$$\omega_z = \rho f^{-2} \left[A_{\rho,\varphi} - A_\varphi - \rho A_{\varphi,\rho} \right]. \tag{2.12}$$

are obtained.

Suppose that, for simplicity, Eq.(2.11) and Eq.(2.12) are rewritten by introducing a new function Φ such that Eq.(2.11) and Eq.(2.12) become

$$\begin{aligned} \omega_\rho &= -\rho f^{-2}\Phi_z \\ \omega_z &= \rho f^{-2}\Phi_\rho. \end{aligned} \tag{2.13}$$

In this case, $-\Phi_z = \rho A_{\varphi,z} - A_{z,\varphi}$ and $\Phi_\rho = A_{\rho,\varphi} - A_\varphi - \rho A_{\varphi,\rho}$. However, one needs to make sure that the solution to ω from pair (2.13) satisfies the integrability condition

$$\omega_{\rho z} = \omega_{z\rho}. \tag{2.14}$$

With the introduction of Φ, Eq.(2.5) and Eq.(2.7) take the forms

$$f\nabla^2 f = (\nabla f)^2 - (\nabla\Phi)^2, \tag{2.15}$$

and

$$\vec{\nabla}\cdot\left(f^{-2}\vec{\nabla}\Phi\right) = 0. \tag{2.16}$$

If we further define $Z = f + |H|^2 - i\Phi$, combination of Eqs.(2.15) and (2.16) results in

$$\left(ReZ - |H|^2\right)\nabla^2 Z = (\nabla Z)^2 - 2\bar{H}\nabla Z.\nabla H, \tag{2.17}$$

$$\left(ReZ - |H|^2\right)\nabla^2 H = \nabla Z.\nabla H - 2\bar{H}(\nabla H)^2, \tag{2.18}$$

where a bar denotes complex conjugation, Z and H represent the gravitational and *em* complex potentials, respectively. Here, Eq.(2.17) and Eq.(2.18) are called Ernst equations for *em* spacetimes.

It is also possible to present Ernst equations in terms of new potential representations ξ

and η in which ξ stands for gravitational and η for *em* complex potential, respectively. This can be done by first letting

$$Z = \frac{1+\xi}{1-\xi}, \tag{2.19}$$

and

$$H = \frac{\eta}{1-\xi}. \tag{2.20}$$

Then, Ernst equations become

$$\left(\xi\bar{\xi} + \eta\bar{\eta} - 1\right)\nabla^2\xi = 2\nabla\xi\left(\bar{\xi}\nabla\xi + \bar{\eta}\nabla\eta\right), \tag{2.21}$$

$$\left(\xi\bar{\xi} + \eta\bar{\eta} - 1\right)\nabla^2\eta = 2\nabla\eta\left(\bar{\xi}\nabla\xi + \bar{\eta}\nabla\eta\right), \tag{2.22}$$

in which ξ and η are the gravitational and *em* complex potentials, respectively. If one wishes to get vacuum Ernst equation, η in Eq.(2.21) should be set to zero.

2.2 Quantum Singularities

A curved spacetime can be expressed using Riemann geometry. Einstein's general theory of relativity builds the spacetime using a C^∞ class Hausdorff manifold M with Lorentz metric $g_{\mu\nu}$. According to this purely mathematical definition, there seems to be no indication of any singularity in the geometry at the first glance. However, from the relativistic perspective, once the the exact solutions of Einstein's equations are studied, spacetime singularities start coming into existence. At these singular points, physical parameters break down and known physical laws lose their validity. In other words, they are holes in spacetime where the evolution of particles in time cannot be known, or they are the endpoints of geodesics. This is a major problem in classical physics.

Singularities of spacetime can be divided into two main groups: classical and quantum singularities. Classical singularities have been classified into three groups by G.F.R. Ellis and B.G. Schmidt [28]. From this viewpoint, spacetime singularities are further categorised as quasi-continuous, non-scalar curvature and scalar curvature singularities.

Now, suppose singularity z is a point. If all elements of Riemann tensor $R_{abcd,e_1e_2...e_k}$ in the PPON (Parallelly Propagated Orthonormal) frame derivative diverge at singularity z, this is called a quasi-continuous singularity. This type of singularities belong to the weakest class of singularities. If some components of Riemann tensor's derivative at singularity z are infinite, this is called a non-scalar curvature singularity. If all scalars of Riemann tensor are infinite at singularity z, this is called a scalar curvature singularity. These are the strongest among all singularities as they are inextendible and gravitational fields, energy density and tidal forces break down at these singularities.

In general, the singularities that we have been mentioning do not conflict with R. Penrose's yet unproven cosmic censorship hypothesis [29] as long as they are concealed by the horizon (horizons). However, in some definite solutions of Einstein's general theory of relativity, black holes do not form and the singular point is not covered by the horizon (horizons). These singularities are called naked singularities [30] and they violate R. Penrose's cosmic censorship hypothesis.

The analysis and understanding of naked singularities is one of the unresolved major problems in general relativity. Since currently a consistent quantum gravity theory does not exist, alternative methods are being developed. One of these can be considered

as the work of R.M. Wald [31] which was then further examined by G.T. Horowitz and D. Marolf (1995) [32]. They analyzed quantum test particles that obey the Klein-Gordon equation in static spacetimes with singularities. According to Horowitz and Marolf, the singular character of spacetime is defined as an uncertainty in the evolution of the wave function (ψ). This means that when the singular character of spacetime is in a definite uncertainty, the spatial differential operator obtained from the solution of the Klein-Gordon equation is self-adjoint in a Hilbert space, and in this case, the space is quantum mechanically singular. If the operator's extension is unique, the space is quantum mechanically regular for this case the spatial operator is called essentially self-adjoint operator. This analysis is known in the literature as the Horowitz-Marolf criterion [32].

In this context, we provide the standard mathematical definition of the Horowitz-Marolf criterion that we will use. For curved spacetime the Klein-Gordon (KG) equation is given by

$$\left(\frac{1}{\sqrt{-g}}\partial_\mu\left[\sqrt{-g}g^{\mu\nu}\partial_\nu\right]-m^2\right)\psi=0, \tag{2.23}$$

in which $g_{\mu\nu}$ denotes the metric tensor, $g=det(g_{\mu\nu})$, ∂ represents the partial derivation for the coordinates and m is the mass of the spinless (spin-0) particle. If we separate the time part of Eq.(2.23), the Klein-Gordon equation becomes

$$\frac{\partial^2\psi}{\partial t^2}=-A\psi, \tag{2.24}$$

where A is the spatial wave operator. Let $H(L^2)$, the Hilbert space, be formed by functions whose squares are integrable on manifold and the operator is real, positive and symmetric [32]. In this case, a self-adjoint extension of this operator always exists.

Then, the solution of Eq.(2.24) can be written as

$$\psi(t) = e^{-it\sqrt{A}}\psi(0). \tag{2.25}$$

If the operator is not essentially self-adjoint, solution (2.25) starts giving problems when its evolution in time is investigated. Consequently, waveform (2.25) is said to be quantum-mechanically singular according to the criteria proposed by Horowitz and Marolf (HM). Let us now concentrate on a different case. Suppose the operator has only one self-adjoint extension. Then, it becomes possible to find the time evolution of wave solution (2.25) provided that the initial conditions are known. As a result, one can conclude the spacetime is quantum mechanically regular. Shortly, the singularity analysis of our concern directly depends on whether the relevant operator is essentially self-adjoint or not.

Let us provide a mathematical theorem used to determine the essential self-adjointness of an operator. Weyl discovered the method for finding the number of self-adjoint extensions of operator A [33], and von Neumann expanded the method [34] . Now, we define the special subspaces of the spatial opherator mentioned in the mathematical method as defined below. The deficiency subspaces $N_{\pm}$ are given by

$$\begin{aligned} N_+ &= \{\psi \in D(A), \qquad A\psi = Z_+\psi, \qquad ImZ_+ > 0\}, \\ N_- &= \{\psi \in D(A), \qquad A\psi = Z_-\psi, \qquad ImZ_- < 0\}. \end{aligned} \tag{2.26}$$

The parameters $(n_+ = dim(N_+), n_- = dim(N_-))$ are known as the deficiency indices of operator A. These indices do not depend on the choice of Z_+ and Z_-, but instead on the location of Z in the upper or lower half of the complex plane. Usually, $Z_+ = i\lambda$ and $Z_- = -i\lambda$ are chosen, with λ being a positive constant used for dimensional purposes.

The calculation of the deficiency indices involve finding the number of solutions to $A\psi = Z\psi$ (when $\lambda = 1$),

$$A\psi \pm i\psi = 0. \tag{2.27}$$

Theorem 2.1 (The Criteria of Essentially Self-Adjointness): For an operator A with deficiency indices (n_+, n_-), there are three possibilities [35]:

(i) When $n_+ = n_- = 0$, A is essentially self-adjoint.

(ii) When $n_+ = n_- = n \geq 1$, A includes infinitely many self-adjoint extensions, represented by a unitary $n \times n$ matrix.

(iii) When $n_+ \neq n_-$,, A does no include any self adjoint extension.

According to Theorem 2.1, if there are no square integrable solutions (i.e. $n_+ = n_- = 0$) over the entire space $(0, \infty)$, operator A has a unique self-adjoint extension and is therefore essentially self-adjoint.

2.3 Tools for Exploring Gravitatinal Lens and Redshift Effects

In literature, there are different models for calculating the gravitational lensing angle based on the mathematical characteristics of spacetime. In this thesis, the gravitational lensing effect of ZV spacetimes that we have developed will be calculated using the Gauss-Bonnet theorem [36, 37], which is one of the most important theorems connecting discrete and continuous mathematics in the intrinsic geometry of surfaces and also the theorem is very popular in gravitational lensing analysis.

Now, let us mathematically state the Gauss-Bonnet theorem and reveal its connection with gravitational lensing angle by presenting it in sequence.

Theorem 2.2 (Gauss-Bonnet Theorem): Let $\mathfrak{R}$ be a regular region of an oriented surface and $\partial\Gamma_1, \partial\Gamma_2, ..., \partial\Gamma_n$ are simple, positively oriented, closed and piecewise regular boundary curves of the surface. Assuming that $\theta_1, \theta_2, ..., \theta_m$ are the set of all external angles (jump angles) of the boundary curves, one can write [38]

$$\sum_{i=1}^{n} \int_{\partial\Gamma_i} \kappa_g(s) ds + \iint_{\mathfrak{R}} \mathcal{K} d\sigma + \sum_{j=1}^{m} \theta_j = 2\pi\chi(\mathfrak{R}) \tag{2.28}$$

in which $\mathcal{K}$ is the Gaussian curvature, $\chi(\mathfrak{R})$ denotes the Euler-Poincare characteristic and $\kappa_g(s)$ represents the geodesics curvature of the boundary curvatures. Note that, s symbolizes the arc length of the boundary curves. Also, Fig. 2.1 shows the geometry in which the Gauss-Bonnet theorem is constructed.

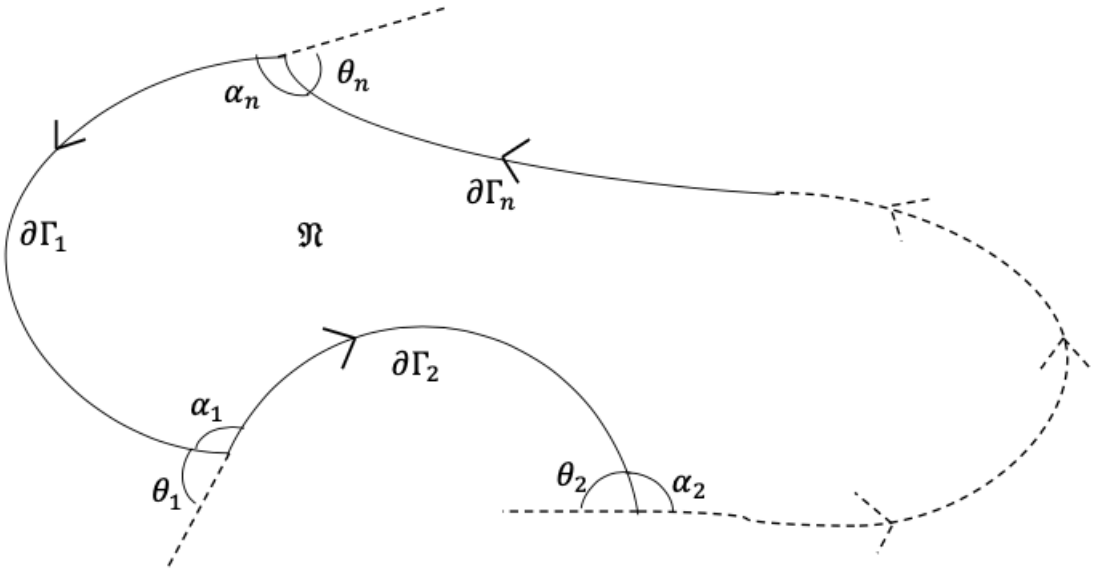

Figure 2.1: The generic geometry represented by the Gauss-Bonnet theorem. Here $\partial\Gamma_1, \partial\Gamma_2, ..., \partial\Gamma_n$ represent the curves that form the boundaries of the surface and $\alpha_1, \alpha_2, ..., \alpha_n$ are the interior angles.

Now, we will adopt the approach of Gibbons and Werner [36] to determine the deflection of light by gravity through the Gauss-Bonnet theorem. Let us define the most general static metric in which the gravitational lensing event will occur first on the equatorial plane ($\theta = \pi/2$) as follows.

$$ds^2 = g_{tt}dt^2 - g_{rr}dr^2 - g_{\varphi\varphi}d\varphi^2. \tag{2.29}$$

Here, g_{tt}, g_{rr} and $g_{\varphi\varphi}$ are generic metric functions. If we apply the null geodesic condition $ds^2 = 0$ for light traveling on null geodesics, Eq.(2.29) reduces to

$$g^{opt} = dt^2 = \bar{g}_{rr}dr^2 + \bar{g}_{\varphi\varphi}d\varphi^2, \tag{2.30}$$

in which $\bar{g}_{rr} = g_{rr}/g_{tt}$ and $\bar{g}_{\varphi\varphi} = g_{\varphi\varphi}/g_{tt}$. Here, g^{opt} is called the optical metric [36]. The geodesic curvature (κ_g) of the geometry represented by the optical metric is defined by [38]

$$\kappa_g = \frac{1}{2\sqrt{\bar{g}_{rr}\bar{g}_{\varphi\varphi}}}\left\{\frac{\partial\bar{g}_{\varphi\varphi}}{\partial r}\frac{d\varphi}{ds} - \frac{\partial\bar{g}_{rr}}{\partial\varphi}\frac{dr}{ds}\right\}. \tag{2.31}$$

The geodesic curvature, which is a measure of how much a curve deviates from being a geodesic, is zero if a curve is a geodesic [38]. If we look at the schematic representation of the Gibbons and Werner gravitational lensing analysis, Fig. 2.2, we see the boundary curves γ and C_R. Since γ curve is a geodesic, its geodesic curvature is zero, but the geodesic curvature of the C_R curve must be calculated. If the spacetime is asymptotically flat and is in the large r limit ($r \to \infty$), $\bar{g}_{\varphi\varphi}$ approaches r^2 and $\bar{g}_{rr}$ goes to 1 (In other words, if $r \to \infty$, the optical metric reduces to the metric, $g^{opt} \approx dr^2 + r^2d\varphi^2$), then κ_g approaches $\frac{d\varphi}{ds}$. Also, the Euler-Poincare characteristic is 1 for a two dimensional simply connected surface with non-empty boundary [38].

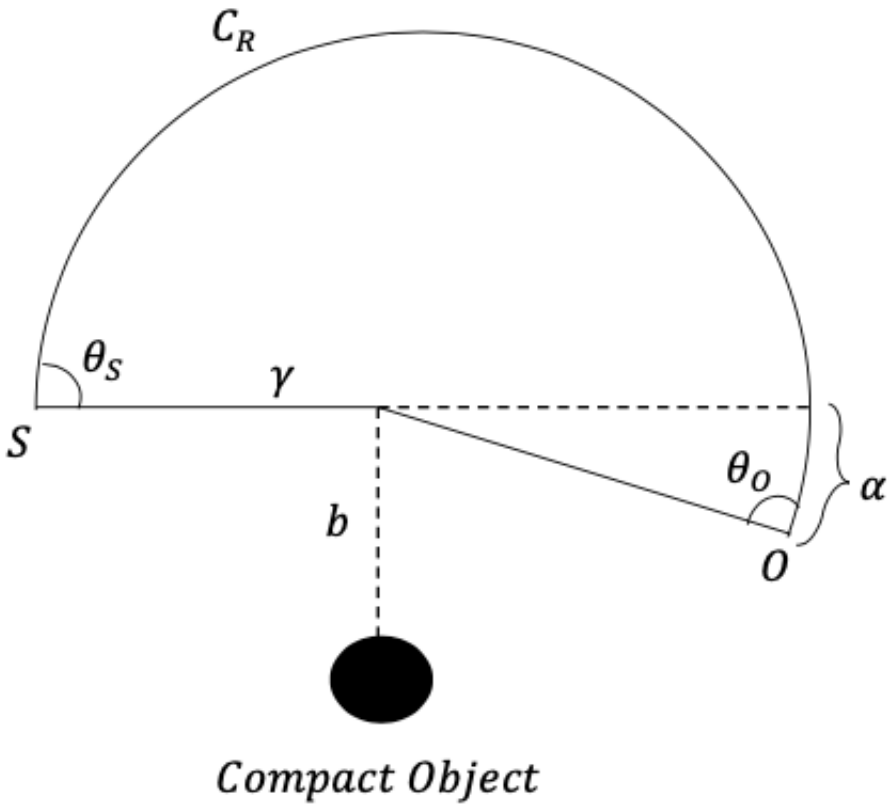

Figure 2.2: The representation of the propagation of light from a source (S) to an observer (O) in the equatorial plane $(\theta = \pi/2)$, which undergoes α deflection due to the presence of a massive object, with b being the impact parameter, where γ is the null geodesic and C_R represents the boundary curve between the jump angles.

Now, with all this information in mind, the general Gauss-Bonnet theorem transforms into

$$\int_0^{\pi+\alpha} d\varphi + \iint_{\mathfrak{R}} \mathcal{K} d\sigma + \theta_S + \theta_O = 2\pi \tag{2.32}$$

in which θ_S and θ_O show the interior angles of the source and the observer, respectively. When the spacetime is asymptotically flat, in the large r limit, each interior angle jump to $\pi/2$ [36, 37], so Eq.(2.32) is reduced to

$$\alpha = -\iint_{\mathfrak{R}} \mathcal{K} d\sigma \tag{2.33}$$

where the Gaussian curvature $(\mathcal{K})$ of the optical metric (g^{opt}) can be written as

$$\mathcal{K} = -\frac{1}{\sqrt{\bar{g}}}\left[\partial_r\left(\frac{1}{\sqrt{\bar{g}_{rr}}}\partial_r\sqrt{\bar{g}_{\varphi\varphi}}\right)+\partial_\varphi\left(\frac{1}{\sqrt{\bar{g}_{\varphi\varphi}}}\partial_\varphi\sqrt{\bar{g}_{rr}}\right)\right], \tag{2.34}$$

in which $\bar{g}$ is the determinant of the optical metric. Also note that, the generalized versions of Gauss-Bonnet theorem and the gravitational lensing analysis exist for non-asymptotically flat, rotating and similar spacetimes [37, 39, 40]. However, the application of the Gauss-Bonnet theorem in non-asymptotically flat spacetimes is mathematically complicated.

One of the intriguing questions related to cosmological constant is to figure out whether it is anyhow able to influence the path that light takes during its propagation through spacetime. Two scientists, Rindler and Ishak (RI), conducted research relevant to this field and the spacetime of their choice while doing so was Schwarzschild-de Sitter (SdS)[41]. RI method is now widely used when non-asymptotically flat spacetimes are of concern. This method is generalized for rotating spacetimes in [2]. For geometries with the inclusion of rotation, one can write

$$ds^2 = f(r)dt^2 + 2g(r)dtd\varphi - h(r)dr^2 - p(r)d\varphi^2. \tag{2.35}$$

It should be noted that the metric is written assuming a constant $\theta = \pi/2$. The RI method involves the generalization of the inner product to curved spaces, which allows for the determination of the invariant angle between two vectors. With this in mind, the angle between two coordinate directions d and δ, as depicted in Fig. 2.3 , can be expressed as

$$\cos(\psi) = \frac{d^i\delta_i}{\sqrt{(d^id_i)\left(\delta^j\delta_j\right)}} = \frac{g_{ij}d^i\delta^j}{\sqrt{\left(g_{ij}d^id^j\right)\left(g_{kl}\delta^k\delta^l\right)}}, \tag{2.36}$$

in which g_{ij} is the metric tensor of the constant time slice of metric (2.35).

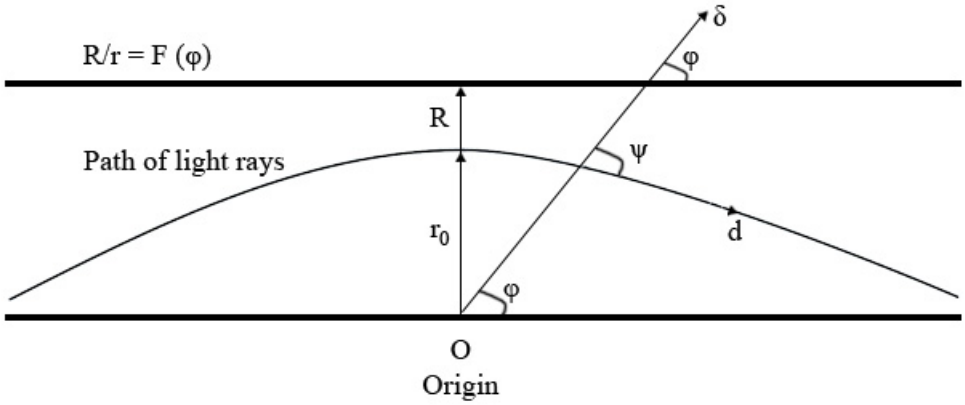

Figure 2.3: A graphical representation of the deflection of light caused by a massive object for RI method [2]. In this figure, R and r_0 represent the impact parameter and the closest distance of approach, respectively. Also, the solid straight line above shows the undistorted path of light rays, which is determined by the solution to the homogeneous part of the null geodesics equation.

Using Fig. 2.3, the lines d and δ are expressed in the coordinates (r,φ) as

$$d = (dr, d\varphi) = (A, 1)\, d\varphi \qquad d\varphi < 0,$$

$$\delta = (\delta r, 0) = (1, 0)\, \delta r, \tag{2.37}$$

where

$$A(r,\varphi) \equiv \frac{dr}{d\varphi}. \tag{2.38}$$

If we substitute the information in Eq. (2.37) into the invariant formula given in Eq.

(2.36) for using the generic line element (2.35), then Eq. (2.36) can be written as

$$\tan(\Psi) = \frac{\left[h^{-1}(r)p(r)\right]^{1/2}}{|A(r,\varphi)|}, \tag{2.39}$$

Moreover, the one-sided bending angle can be calculated as $\varepsilon = \Psi - \varphi$.

As discussed in the first chapter, gravitational redshift is also a very important concept which is the observed effect occuring due to loss of em energy, once it manages to leave the gravitational effect created by a dense source [42]. Fig. 2.4 can help to have a naive visualisation of this event.

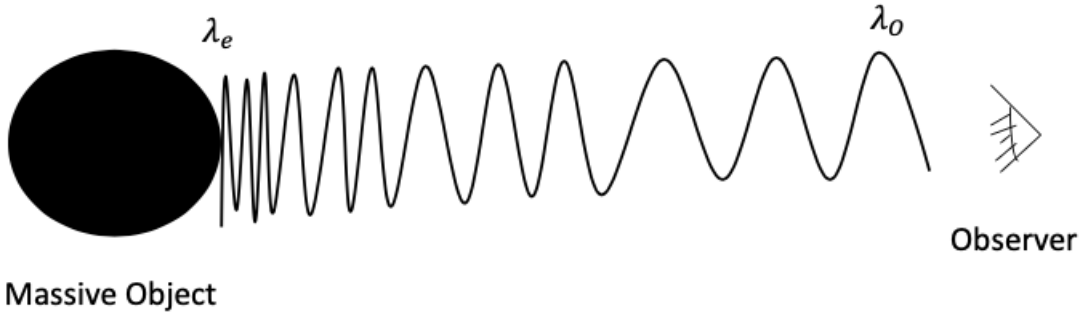

Figure 2.4: In this figure, λ_e represents the wavelength of the em radiation emitted from the surface of the source of gravity. An increase in the wavelength is expected to occur, as the radiation moves away from the source.

The gravitational redshift calculation will be based on the method developed for static cases as presented in references [43, 44]. This method states that the formula for gravitational redshift is given by

$$z = \frac{\lambda_o - \lambda_e}{\lambda_e} = \frac{\lambda_o}{\lambda_e} - 1 = \frac{\omega_o}{\omega_e} - 1 \tag{2.40}$$

in which

$$\frac{\omega_e}{\omega_o} = \sqrt{g_{tt}}. \tag{2.41}$$

where λ_e and λ_o represents emitted and observed wavelengths, respectively. Here, g_{tt} is the $-tt$ component of the related metric tensor. Equivalently, ω_e and ω_o denotes emitted and observed frequencies.

Chapter 3

MAXWELL EXTENSION OF ZV METRICS

3.1 Review of Uncharged ZV Metric

It has already been discussed that Weyl solutions carry a vital importance in general relativity. ZV spacetimes can be thought as an example of such solutions. These spacetimes are static, axially symmetric and asymptotically flat, therefore, they are considered as a specific case of Weyl solutions. ZV spacetimes also cover the familiar Schwarzschild solutions which attain spherical symmetry [7, 8].

In the prolate spheroidal coordinate system, which is represented by the variables (t,φ,x,y), the ZV metric can be expressed as

$$ds^2 = -F(x,y)dt^2 + G(x,y)d\varphi^2 + \Sigma(x,y)\left[\frac{dx^2}{x^2-1} + \frac{dy^2}{1-y^2}\right] \tag{3.1}$$

the metric functions are given by

$$\begin{aligned} F(x,y) &= \left(\frac{x-1}{x+1}\right)^{\gamma} \\ G(x,y) &= \left(\frac{m}{\gamma}\right)^2 \left(\frac{x+1}{x-1}\right)^{\gamma} (x^2-1)(1-y^2) \\ \Sigma(x,y) &= \left(\frac{m}{\gamma}\right)^2 \frac{(x+1)^{\gamma^2+\gamma}}{(x-1)^{-\gamma^2+\gamma}} \left(x^2-y^2\right)^{1-\gamma^2} \end{aligned} \tag{3.2}$$

where the parameter γ represents the distortion parameter. The quadrupole moment $\mathcal{M}$ can be written as [45]

$$\mathcal{M} = \frac{m^3\gamma(1-\gamma^2)}{3}. \tag{3.3}$$

As clearly seen in equation (3.3) , the quadrapole moment term is directly dependent on non-spherical symmetry. The solution's singularity structure has been analyzed in [46], and that the solution's singularities, which will be given by the Weyl scalar, Ψ_2, have been found as

$$\Psi_2 = \frac{\gamma(x-\gamma)(x^2-y^2)^{\gamma^2-1}}{2(x-1)^{\gamma^2-\gamma+1}(x+1)^{\gamma^2+\gamma+1}}. \tag{3.4}$$

Because Eq.(3.4) diverges at the points $x = \pm 1$, the singularities in spacetime occur at these points in prolate coordinates. The ZV metric can be rewritten in Schwarzschild coordinates by using the transformation

$$\begin{aligned} x &= \frac{r}{k} - 1 \\ y &= cos\theta, \end{aligned} \tag{3.5}$$

where $k = M/\gamma$. The prolate form of ZV metric (3.1) with the transformation (3.5) reduces to

$$ds^2 = -F(r)dt^2 + F^{-1}(r)\left[G(r,\theta)dr^2 + H(r,\theta)d\theta^2 + (r^2-2kr)sin^2\theta d^2\varphi\right]. \tag{3.6}$$

Here the new metric functions are

$$\begin{aligned} F(r) &= \left(1 - \frac{2k}{r}\right)^{\gamma} \\ G(r,\theta) &= \left(\frac{r^2-2kr}{r^2-2kr+k^2sin^2\theta}\right)^{\gamma^2-1} \\ H(r,\theta) &= \frac{(r^2-2kr)^{\gamma^2}}{(r^2-2kr+k^2sin^2\theta)^{\gamma^2-1}}. \end{aligned} \tag{3.7}$$

Also, we can find the singularity locations of line element (3.6) by using the help of the expression (3.5). In this context, $r = 2k$ and $r = 0$ are the singular points of the metric at these coordinates. Another interesting feature of the ZV solution is that it is a non-integrable system, and as a result, it can generate chaos [47]. For the quantum probe analysis to be conducted, the singular surface needs to be time-like according to

the HM criteria. Penrose diagrams prove to be useful to achieve this. We can start our process by transforming t and r in Eq. (3.6) to T and R via

$$\begin{aligned} T &= tan^{-1}(t+r^*)+tan^{-1}(t-r^*) \\ R &= tan^{-1}(t+r^*)-tan^{-1}(t-r^*), \end{aligned} \tag{3.8}$$

where

$$r^* = \int \sqrt{\frac{g_{rr}}{g_{tt}}} dr. \tag{3.9}$$

To check if the singularity is timelike or nulllike, we can carry out the following analysis.

$$r^* = \int \left(1-\frac{2m}{r}\right)^{-\gamma} \left(\frac{r^2-2mr}{r^2-2mr+m^2 sin^2\theta}\right)^{\frac{\gamma^2-1}{2}} dr, \tag{3.10}$$

in which $k = m$. Since it is not possible to find an exact solution of this integral, we expand the integrand near the singular surface $r_+ = 2m$ by considering only the first term. This leads to

$$r^* \approx \frac{2^{\gamma^2}(r-r_+)^{\frac{(\gamma-1)^2}{2}} r_+^{\gamma-\frac{\gamma^2}{2}+\frac{1}{2}} sin^{1-\gamma^2}\theta}{(\gamma-1)^2}. \tag{3.11}$$

The singularity at $r = r_+ = 2m$ is timelike, since the singularity appears on the vertical axis (T- axis) of the Penrose diagram.

3.2 Charged Extension of ZV Metric

We will demonstrate in this subsection [2] how to obtain charged version of the ZV metric by using the Ernst formalism. To be more precise, the field equations will be solved in prolate coordinate system which is found very useful for describing colliding

[2] The material of this subsection was published in [17]

gravitational waves. Once the field equation one solved in prolate coordinates then the resulting solution is interpreted in another coordinate system. In doing so, we employ the metric introduced by Chandrasekhar and Xanthopoulos (CX) [48, 49] and using the method given in [50]. This allows us to describe the spacetime of colliding em waves using a specific line element (Chandrasekhar and Xanthopoulos line element)

$$ds^2 = \sqrt{\Delta}e^N \left(\frac{d\eta^2}{\Delta} - \frac{d\mu^2}{\delta} \right) - \sqrt{\Delta\delta} \left(\chi dx^2 + \chi^{-1} dy^2 \right) \tag{3.12}$$

in which N and χ are dependent on η and μ with $\Delta = 1-\eta^2$ and $\delta = 1-\mu^2$. This choice can provides solutions of Ernst equations (2.21) and Eq. (2.22) with real coefficients p and q.

Then, the particular set of solutions read

$$\xi = p\xi_0, \tag{3.13}$$

and

$$\eta = q\xi_0, \tag{3.14}$$

in which $\xi_0 = \bar{\xi}_0$ and the real coefficients satisfy

$$p^2 + q^2 = 1. \tag{3.15}$$

Note that q denotes the charge and $\xi_0 = tanhX$ solves to the Euler-Darboux equation provided that X is a function of η and μ.

$$(\Delta X_{,\eta})_{,\eta} - \left(\delta X_{,\mu}\right)_{,\mu} = 0, \tag{3.16}$$

where a comma represents partial derivative, satisfies the Ernst system in the real

domain. Note that, X is called the seed function. Let us choose the harmonic function below that satisfies Eq. (3.16)

$$e^{2X} = \left(\frac{1-\eta}{1+\eta}\right)^{\gamma}. \tag{3.17}$$

In the following sections, we will identify the constant γ as the $ZV-$ parameter. If we compare the metric function (2.1), which is the general metric defined by the Ernst Lagrangian, with equation (3.12), which is the general colliding wave metric given in prolate coordinates, and map the $y-$coordinate in metric (3.12) to the $t-$ coordinate in metric (2.1), and also consider $f \to \Psi$, then we can define the metric function χ as follows

$$\chi = \frac{\sqrt{\Delta\delta}}{\Psi}. \tag{3.18}$$

The expression $Z = f + |H|^2 - i\Phi$, defined in the chapter 2 to the above analogy, becomes

$$Z = \Psi + H^2. \tag{3.19}$$

If we substitute the harmonic function (3.17) from previous chapter expressed in terms of ξ and η as Z and H using Eqs. (3.13) and (3.14) into Eq.(3.19), we can solve for the Ψ function. As a result of all these operations, the Ψ function is

$$\Psi = \frac{1-\eta^2}{(1+\eta p)^2}. \tag{3.20}$$

We obtain the other unknown generic metric function N by solving the integrability equations of metric (3.12) [50]

$$(N + ln\Psi)_{,\eta} = \frac{2\eta}{\delta-\Delta} + \frac{\eta}{\Delta} + \frac{2\delta}{\delta-\Delta}\left[2\mu\Delta X_{,\eta}X_{,\mu} - \eta\left(\Delta X_{,\eta}^2 + \delta X_{,\mu}^2\right)\right], \tag{3.21}$$

$$(N+ln\Psi)_{,\mu}=\frac{2\mu}{\Delta-\delta}+\frac{2\Delta}{\Delta-\delta}\left[2\eta\Delta X_{,\eta}X_{,\mu}-\mu\left(\Delta X_{,\eta}^{2}+\delta X_{,\mu}^{2}\right)\right], \tag{3.22}$$

where the comma represents the derivative with respect to the coordinate that comes after it. When we put the harmonic function X and Ψ into the integrability equations, we can integrate the metric function N. To sum up the final form of the line element can be written as

$$ds^{2}=M^{2}(\eta)\left[\Delta^{\gamma^{2}}(\delta-\Delta)^{1-\gamma^{2}}\left(\frac{d\eta^{2}}{\Delta}-\frac{d\mu^{2}}{\delta}\right)-\Delta\delta dx^{2}\right]-\frac{dy^{2}}{M^{2}(\eta)}, \tag{3.23}$$

in which

$$M(\eta)=coshX-psinhX. \tag{3.24}$$

It is important to note that the line element being considered as a solution to the problem of colliding em waves must meet the appropriate boundary conditions in both the incoming and interaction regions. Unfortunately, the factor $(\delta-\Delta)$ in Eq.(3.23) does not satisfy the necessary boundary conditions, so it is not a viable option. This difficulty can be overcome only by redefinition of (μ,η) coordinates in terms of the null coordinates (u,v) at the cost of introducing light-like sources to accompany the *em* wave. However, in the interaction region alone, it can be useful as a solution, as we will demonstrate later.

After performing the Schwarzschild coordinate ($S-$coordinate) transformation,

$$\begin{aligned} p\eta+1&=\frac{r}{m} \quad , \quad x=\varphi, \\ \mu&=cos\theta \quad , \quad y=\tau, \end{aligned} \tag{3.25}$$

by supplementing the condition $(-1)^{\gamma} = -1$ and appropriately rescaling time $(\tau \to t)$ in the line element (3.23), we express the metric in the form

$$ds^2 = \frac{\Delta^{\gamma}}{K^2}dt^2 - \frac{K^2}{\Delta^{\gamma}}\left[\Delta^{\gamma^2}\Sigma^{1-\gamma^2}\left(\frac{dr^2}{\Delta} + r^2 d\theta^2\right) + r^2\Delta sin^2\theta d\varphi^2\right]. \tag{3.26}$$

where m is the mass of resulting metric. The related metric functions are

$$\Delta(r) = 1 - \frac{2m}{r} + \frac{m^2q^2}{r^2}, \tag{3.27}$$

$$\Sigma(r,\theta) = 1 - \frac{2m}{r} + \frac{m^2}{r^2}\left(q^2 + p^2 sin^2\theta\right), \tag{3.28}$$

and

$$K(r) = (1+p)\left(1 - \frac{m(1-p)}{r}\right)^{\gamma} - (1-p)\left(1 - \frac{m(1+p)}{r}\right)^{\gamma}. \tag{3.29}$$

We have confirmed that the line element (3.23) satisfies the *EM* equations and reduces to the *ZV*-metric for $q = 0$ $(p = 1)$. However, we must exclude the case of $p = 0$ $(q = 1)$ since the metric function K becomes zero in such a limit. Although we initially imposed the condition $(-1)^{\gamma} = -1$ on the parameter γ, we have found that the metric is valid for all values of γ as this condition can be relaxed. In particular, we can incorporate the transformation for γ even through an analytic continuation $y \to i\tau$ and $x \to i\varphi$, while leaving the other coordinates as in the previous transformation. We note that previous versions of charged metrics were only valid for integer parameters [51], but the new solution (3.23) describes charged, deformed *ZV* objects that are valid for all values of γ. Since most planetary objects are charged, especially magnetized ones, this metric is likely to have important astrophysical applications

3.3 Stationary Charged/Uncharged ZV Metrics

Let us first consider the colliding *EM* wave metric that contains the rotational term in order to generate the solution for the rotating and charged ZV [3] . The line element is given by [49, 50, 53]

$$ds^2 = e^N\sqrt{\Delta}\left(\frac{d\eta^2}{\Delta} - \frac{d\mu^2}{\delta}\right) - \sqrt{\Delta\delta}\left[\chi dx^2 + \frac{1}{\chi}(dy - q_2 dx)^2\right]. \tag{3.30}$$

The only difference between metric (3.30), which is used to produce the solution for the charged ZV in metric (3.12), is that it includes the $q_2(\eta,\mu)$ function that generates the rotation. We will follow a slightly different approach than the one we used to obtain the charged ZV in the previous section when producing the solution for the stationary charged ZV. Firstly, starting with the complex potential that satisfies the vacuum Ernst equation, i.e. $H = 0$, which contains the complex rotation potential, we will use a method known in the literature as the Chandrasekar-Xanthopoulos (CX) theorem to convert the metric into a charged metric.

The satisfying complex potential of vacuum Ernst equation with base metric, $ds_0^2 = \frac{d\mu^2}{\Delta} - \frac{d\nu^2}{\delta} + \Delta\delta d\phi^2$ is given by [54]

$$Z = \Psi - i\Phi = \frac{1 - i\sin\alpha\cosh 2X}{\cosh 2X\sqrt{1+\sin^2\alpha} - \sinh 2X}. \tag{3.31}$$

Here, α represents the integration constant (for colliding *EM* waves case, α measures the second polarization of the waves in collision.) and $X(\eta,\mu)$ is a harmonic function that satisfies Eq. (3.16). Let us now state the CX theorem, which transfers an uncharged solution to a charged one, for us.

[3] The material of this subsection was published in [52]

Theorem 3.1 (CX− Theorem): When we denote the Ernst potentials and metric functions of the vacuum case as (Z,Ψ,Φ,χ,N,q_2) respectively, the charged versions of the expressions represented by $(Z_e,\Psi_e,\Phi_e,\chi_e,N_e,q_{2e})$ can be obtained using the relations of the following transformation [49, 55].

$$
\begin{aligned}
Z_e &= \Psi_e + |H|^2 - i\Phi_e, \\
\Psi_e &= \left(\frac{4}{\Omega^2}\right)\Psi, \\
\Phi_e &= \left(\frac{4p}{\Omega^2}\right)\Phi, \\
\chi_e &= \left(\frac{\Omega^2}{4}\right)\chi, \\
N_e &= N + ln\left(\frac{\Omega^2}{4}\right) \\
q_{2e,\mu} &= \frac{1}{4}(1+p)^2 q_{2,\mu} + \frac{\delta}{4}\left[\frac{(\Phi^2-\Psi^2)\Phi_\eta}{\Psi^2} + \frac{2\Phi\Psi_\eta}{\Psi}\right](1-p)^2, \\
q_{2e,\eta} &= \frac{1}{4}(1+p)^2 q_{2,\eta} + \frac{\Delta}{4}\left[\frac{(\Phi^2-\Psi^2)\Phi_\mu}{\Psi^2} + \frac{2\Phi\Psi_\mu}{\Psi}\right](1-p)^2.
\end{aligned}
\tag{3.32}
$$

in which

$$
\begin{aligned}
H &= q\frac{(\Psi - i\Phi - 1)}{(1-p)(\Psi - i\Phi) + p + 1}, \\
\Omega^2 &= q^4(\Psi^2+\Phi^2) + 2q\Psi + (1+p)^2, \\
p^2 + q^2 &= 1.
\end{aligned}
\tag{3.33}
$$

If we put the vacuum Ernst potentials into the q_{2e} equations for using Eq. (3.31), q_{2e} expressions can be written as

$$
\begin{aligned}
q_{2e,\mu} &= (1+p^2)\delta X_\eta \sin\alpha, \\
q_{2e,\eta} &= (1+p^2)\Delta X_\mu \sin\alpha.
\end{aligned}
\tag{3.34}
$$

Furthermore, the other metric functions (N) are obtained using the integrability

equations given in Eq. (3.21) and (3.22) in the previous section.

If we select the ZV seed function (Eq.(3.17)) and the seed function is substituted into all equations with necessary integrations made, the resulting rotating and charged metric can be found as follows:

$$ds^2 = \frac{D\Omega^2}{4}\left[\Delta^{\gamma^2}(\delta-\Delta)^{1-\gamma^2}\left(\frac{d\eta^2}{\Delta}-\frac{d\mu^2}{\delta}\right)-\Delta\delta dx^2\right]-\frac{4}{D\Omega^2}\left(dy+q_0\gamma(1+p^2)\mu dx\right)^2, \tag{3.35}$$

in which

$$\begin{aligned}\Omega^2 &= \left(\frac{1-p}{D}+1+p\right)^2+(1-p)^2\left(\frac{q_0}{D}\cosh 2X\right)^2,\\ D &= \sqrt{1+q_0^2}\cosh 2X-\sinh 2X \;\; (q_0\equiv\sin\alpha).\end{aligned} \tag{3.36}$$

Also, the em complex potential H can be written as

$$H = q\frac{(1-p)(\Psi^2+\Phi^2)+2p\Psi-(1-p)-2i\Phi}{(1-p)^2(\Psi^2+\Phi^2)+2q^2\Psi-(1+p)^2}. \tag{3.37}$$

Note that, the vector potential $A_\mu=(0,A_x,A_y,0)$ components are given by

$$\begin{aligned}A_y &= Re(H),\\ A_x &= Im(H).\end{aligned} \tag{3.38}$$

We should note that the metric (3.35) can be regarded as a solution to the problem of colliding em waves, provided that the boundary conditions are satisfied and do not generate current sources at the junctions. However, since our goal here is not to search for specific incoming wave profiles, we will ignore this aspect of the problem. Alternatively, by reversing the direction of time, we can determine the waves that collide and give rise to the metric (3.35) of the interaction region.

3.3.1 Stationary Charged $ZV-$ Metric in $S-$ Coordinates

The important thing now is to look for an isometry that maps the coordinates $\{\mu,\eta,x,y\}$ in metric (3.35) to the $S-$coordinates $\{t,r,\theta,\varphi\}$. To achieve this purpose, we utilize the transformations (3.25). As $(-1)^{\gamma}=-1$ needs to be met and the metric signature should remain to be (-2), the distortion parameter needs to be determined accordingly.

When $(-1)^{\gamma}=1$ is chosen, it is noticed that $\gamma=\frac{2n+1}{2k+1}$ and the signature of the metric comes out as $(-,+,+,+)$. In contrary, if $\gamma=\frac{2n}{2k+1}$ is picked, the metric signature then becomes $(+,-,-,-)$. In this case, k and n can be any integer including zero. Accordingly, line element (3.35) becomes

$$ds^2=\frac{4}{D\Omega^2}\left(dt+q_0 m\gamma p(1+p^2)\cos\theta d\varphi\right)^2-\frac{D\Omega^2}{4}\left\{\Sigma^{1-\gamma^2}\Delta_0^{\gamma^2}\left(\frac{dr^2}{\Delta_0}+r^2d\theta^2\right)+r^2\Delta_0\sin^2\theta d\varphi^2\right\} \tag{3.39}$$

where

$$\begin{aligned}
\Delta_0&=1-\frac{2m}{r}+\frac{m^2q^2}{r^2},\\
\Sigma&=1-\frac{2m}{r}+\frac{m^2}{r^2}\left(q^2+p^2\sin^2\theta\right),\\
D&=\frac{1}{2\Delta_0^{\gamma}}\left\{(k-1)\left[1-\frac{m}{r}(1+p)\right]^{2\gamma}+(k+1)\left[1-\frac{m}{r}(1-p)\right]^{2\gamma}\right\},\\
\Omega^2&=\left(\frac{1-p}{D}\right)^2\left(1+q_0^2\cosh^2 2X\right)-\frac{2q^2}{D}+(1+p)^2,\\
\cosh 2X&=\frac{1}{2\Delta_0^{\gamma}}\left[\left(1-\frac{m}{r}(1+p)\right)^{2\gamma}+\left(1-\frac{m}{r}(1-p)\right)^{2\gamma}\right],
\end{aligned} \tag{3.40}$$

where $k=\sqrt{1+q_0^2}$. Also, the em vector fields can be expressed as $A_\mu=(A_t=Re(H),0,0,A_\varphi=Im(H))$. The $S-$ coordinate representation of complex potential H can be written as

$$H=q\frac{(1-p)\left[1+(q_0\cosh 2X)^2\right]-D\left(2p+(1+p)D\right)+2iq_0D\cosh 2X}{\left[(1-p)-(1+p)D\right]^2+\left(q_0(1-p)\cosh 2X\right)^2}. \tag{3.41}$$

The associated parameters are m, q, q_0 and γ which respectively represent the mass, charge, NUT-type and distortion (ZV) parameter.

The important limits of new metric (3.39) are

i) $q_0 = 0 = q \rightarrow$ ZV limit

ii) $q_0 \neq 0 = q \rightarrow$ NUT-type stationary limit [4]

iii) $q_0 = 0 \neq q, \gamma = 1 \rightarrow$ Reissner-Nordström (RN) limit

iv) $q_0 = 0 = q, \gamma = 1 \rightarrow$ Schwarzschild limit

v) $q_0 = 0 \neq q, 0 < \gamma < \infty \rightarrow$ Charged ZV limit [17]

Our metric is not asymptotically flat due to the presence of the cross term $g_{t\varphi} \neq 0$. Similar to the NUT-metric [57, 58], it only exhibits asymptotic flatness in the plane $\theta = \pi/2$. We want to emphasize that metric (3.39) is quite complex and challenging to analyze analytically. Even the expression for $\sqrt{-g}$ in the analysis of wave equations or Maxwell equations appears to be almost beyond analytical reach. However, the solution given can reproduce all known limiting cases. Additionally, it is possible to incorporate additional contributions to the metric by multiplying the choice for e^{2X} in (3.17) with an exponential factor involving a quadrupole term, for example.

3.3.2 Asymptotic Form of The Metric, Closed Time-Like Curves

3.3.2.1 Metric Functions for $r \rightarrow \infty$

We can introduce a new radial variable, denoted by $R = r_0 r$, which is applicable for large values of r. Here, r_0 is given by

$$r_0 = (k+1)p^2 + k - 1. \tag{3.42}$$

[4] A minor scaling property of the parameters in Ref. [56]

If we expand all metric functions up to the third order of $1/R$, we can obtain

$$\begin{aligned} g_{tt} &\approx 1+\sum_{n=1}^{3} a_n R^{-n} \\ g_{t\varphi} &\approx b_0\left(1+\sum_{n=1}^{3} b_n R^{-n}\right) \\ g_{rr} &\approx c_0\left(1+\sum_{n=1}^{3} c_n R^{-n}\right) \\ g_{\theta\theta} &\approx \sum_{n=-2}^{3} d_n R^{-n} \\ g_{\varphi\varphi} &\approx \sum_{n=-2}^{3} e_n R^{-n} \end{aligned} \tag{3.43}$$

in which all coefficients are given in the Appendix A. And, we can expand the vector potential $A_\mu = (A_t, 0, 0, A_\varphi)$ up to the same order as shown below.

$$\begin{aligned} A_t &\approx \alpha_0\left(-1+\sum_{n=1}^{3} \alpha_n R^{-n}\right) \\ A_\varphi &\approx \beta_0\left(1+\sum_{n=1}^{3} \beta_n R^{-n}\right) \end{aligned} \tag{3.44}$$

In Appendix A, more information about α_n, β_n can be found. If $k = 1$ and $p = 1$ are picked, ZV line element is obtained, whereas $\gamma = 1$ results in the Schwarzschild spacetime.

3.3.2.2 Possible Existence of Closed, Time-Like Curves

Well known Gödel's approach [59], closed time-like curves can be explored in stationary metrics by projecting the metric onto the (t, φ) sector through the selection of $r = const.$ and $\theta = const.$. This process is carried out as follows.

$$ds^2 = e^{2\Psi}(dt - \omega d\varphi)^2 - e^{-2\Psi} r^2 \Delta_0 sin^2\theta d\varphi^2 \tag{3.45}$$

Note that $e^{2\Psi} = \frac{4}{\Omega^2 D}$ and $\omega = -q_0 mp\gamma(1+p^2)cos\theta$. Moreover, $t = -a\varphi$ in which a represents a positive parameter such that $a << 1$. By this way, it has been ensured that

$\varphi = 0$ and $\varphi = 2\pi$ are achieved. Hence, the Killing vectors ∂_t and ∂_φ turn out to be proportional. Finally,

$$(a+\omega)^2 - r^2\Delta_0 e^{-4\Psi} sin^2\theta > 0 \tag{3.46}$$

is achieved. By satisfying equation (3.46), a closed time-like curve can be obtained, given that r is constant and $0 < \gamma < \infty$. In Figure 3.1, we depict the plot of $e^{-2\Psi}$ versus γ for small r, and the area enclosed between the two curves represents a possible range for the variables. It is worth noting that a particular instance of the stationary metric, referred to as the NUT-Curzon metric without charge [60], was also previously shown to exhibit analogous closed time-like curves.

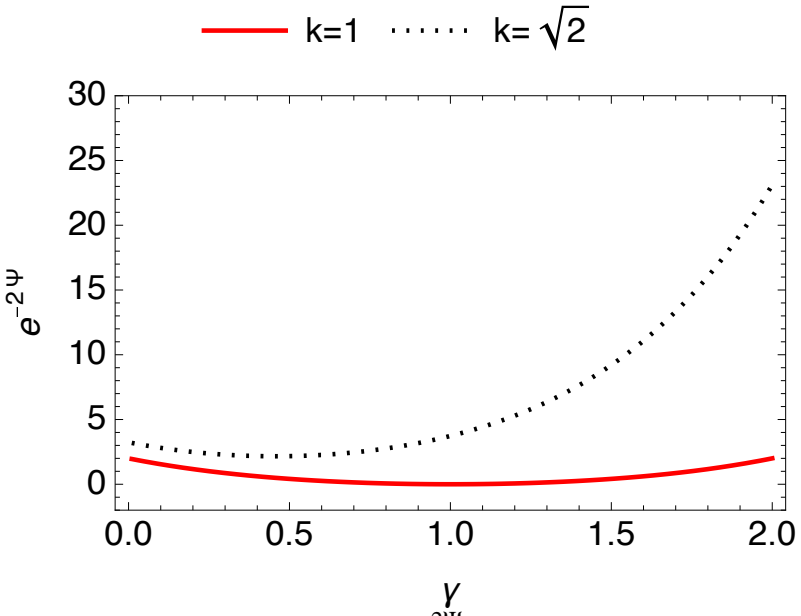

Figure 3.1: The plot of $e^{-2\Psi}$ versus γ takes into account the minimum $(k = 1)$ and maximum spin $(k = \sqrt{2})$ values. The region between the two curves indicates that our inequality can be satisfied by choosing a small value of r and a reasonable value of γ. Moreover, it is possible to satisfy the addition of a constant to the metric function ω.

Chapter 4

PHYSICAL PROPERTIES OF CHARGED ZV-METRICS

In this chapter, we will perform astrophysical applications and analyze important physical properties of the newly obtained class, charged ZV solution.[5]

4.1 Newtonian Limit

To observe the Newtonian limit, as is customary, we extract the g_{tt} component of metric (3.26) and represent it in a certain form

$$g_{tt} = \frac{\Delta^{\gamma}}{K^2} \approx 1 + 2\phi. \tag{4.1}$$

Here, The asymptotic form of the Newtonian potential is given by $\phi = \phi(r)$, and when we expanded to the order of r^{-3}, the weak potential can be written as

$$\phi(r) \approx -\frac{m\gamma}{r} + \frac{\gamma m^2}{2r^2}\left[\gamma q^2 + 2(\gamma-1)\right] - \frac{\gamma(\gamma-1)}{3}\left(\frac{m}{r}\right)^3\left[(1+4\gamma)q^2 + 2(\gamma-2)\right] + O\left(\frac{1}{r^4}\right). \tag{4.2}$$

In equation (4.2), the first term includes monopole-related concepts, whereas the second and third are linked to dipole and quadrupole terms, respectively. In addition, if there is no charge in the vicinity, the second term vanishes due to transformation of r [56]. The chargeless case however is out of scope of this thesis.

There are a couple of points worth mentioning at this point. When potential (4.2) is examined in detail, it is seen that one can obtain RN potential by taking the distortion

[5] All the analyses to be performed in this chapter have been published in [17]

parameter as 1. Additionally, Bertotti-Robinson (BR) potential [61, 62] also seems to be a special case of (4.2), provided that the pure em limit is applied [50].

4.2 Electromagnetic Sources for The Metric

In this subsection, we will analyze the solutions of the Maxwell equations under the assumptions of pure magnetic and pure electric sources for the charged ZV metric.

4.2.1 Pure Magnetic Case

The choice of vector potential is

$$A_\mu = (0,0,0,C_0 cos\theta). \tag{4.3}$$

Here, C_0 represents the magnetic charge, which is directly proportional to q. The magnetic field writes $F_{\theta\varphi} = -C_0 sin\theta$ from $F_{\mu\nu} = \partial_\mu A_\nu - \partial_\nu A_\mu$, which satisfies the only relevant source-free Maxwell equation

$$\nabla_\mu F^{\mu\nu} = 0. \tag{4.4}$$

The magnetic field invariant can be written as

$$I = F_{\mu\nu}F^{\mu\nu} = \frac{2C_0^2}{r^4K^4}\Delta^{-(\gamma-1)^2}\Sigma^{\gamma^2-1}, \tag{4.5}$$

When $\gamma = 1$, the expression simplifies to the case of *RN*. The presence of any divergence in the em field can be readily detected by analyzing this invariant, which is significantly influenced by γ. Moreover, directional singularities in the *em* field can be identified by examining the zeros of Σ at specific γ values ($\gamma^2 < 1$).

It is noteworthy that even though the *em* invariant diverges at $r = 0$, it remains regular for $\gamma \neq 1$, in contrast to the case when $\gamma = 1$. This can be demonstrated by expressing K as $K = r^{-\gamma}K_0$, and upon substituting $r = 0$, the invariant becomes $I = \frac{2C_0^2}{K_0^4}(m^2q^2)^{-(\gamma-1)^2}(m^2q^2 + m^2p^2\sin^2\theta)^{\gamma^2-1} < \infty$, where $K_0 \neq 0$. Additionally, we

observe that the constant C_0 can be fixed as $C_0^2 = 8m^2\gamma^2 p^2 q^2$ using the Einstein equations $R_{\mu\nu} = -T_{\mu\nu} = \frac{1}{4} g_{\mu\nu} F_{\alpha\beta} F^{\alpha\beta} - F_{\mu\alpha} F^{\alpha}_{\nu}$, which results in $T^{\nu}_{\mu} = \frac{I}{4} diag(-1,-1,1,1)$. Although this solution does not correspond to a magnetic dipole, we recall that at large distances, the magnetic charge q plays the role of a dipole, as shown by the expansion (4.2) multiplied by the Legendre polynomial $P_1 = cos\theta$.

4.2.2 Pure Electric Case

For this case, we select the vector potential as

$$A_\mu = (f(r), 0, 0, 0), \tag{4.6}$$

in which the function $f(r)$ is unknown and must be obtained by fulfilling the Maxwell equation $\nabla_r F^{rt} = 0$. When we put the vector potential of this case into the em tensor, the radial component of Eq.(4.4) becomes

$$\partial_r \left(\sqrt{-g} g^{rr} g^{tt} f' \right) = 0, \tag{4.7}$$

where $'$ denotes derivation with respect to r. If we write the related metric functions into the Eq.(4.7), the non-zero component of the pure electric vector potential is

$$f(r) = C_1 \int^r \frac{\Delta^{\gamma-1} dr}{r^2 K^2}, \tag{4.8}$$

in which C_1 is the integration constant. It can be observed that determining the precise expression for $f(r)$ is entirely dependent on the value of γ. When we select the spherically symmetric case with $\gamma = 1$, it is straightforward to note that the potential of the pure electric *RN* solution is obtained.

The invariant of the field can be calculated as

$$I = F_{\mu\nu}F^{\mu\nu} = -\frac{2C_1^2}{r^4K^4}\Delta^{-(\gamma-1)^2}\Sigma^{\gamma^2-1}, \tag{4.9}$$

The expression for the electric invariant, up to an anticipated change in sign, is consistent with the magnetic invariant. Similar to the magnetic case, the value of the constant C_1 can be obtained as $C_1^2 = 8m^2\gamma^2p^2q^2$, and the energy-momentum tensor is given by $T_\mu^\nu = \frac{I}{4}diag(1,1,-1,-1)$. By substituting the constant C_1 into the integral (4.8) and performing the integration, the electric potential can be expressed as

$$A_0(r) = \frac{\sqrt{2}q\left(1-\frac{m(1+p)}{r}\right)^\gamma}{(1+p)K(r)}. \tag{4.10}$$

Below, one can find graphical representations showing how electric potential varies in terms of the radial distance. There exist four different graphs, each with a fixed charge but changing γ values. The plots show that the effect of distortion parameter is inversely proportional with the radial distance.

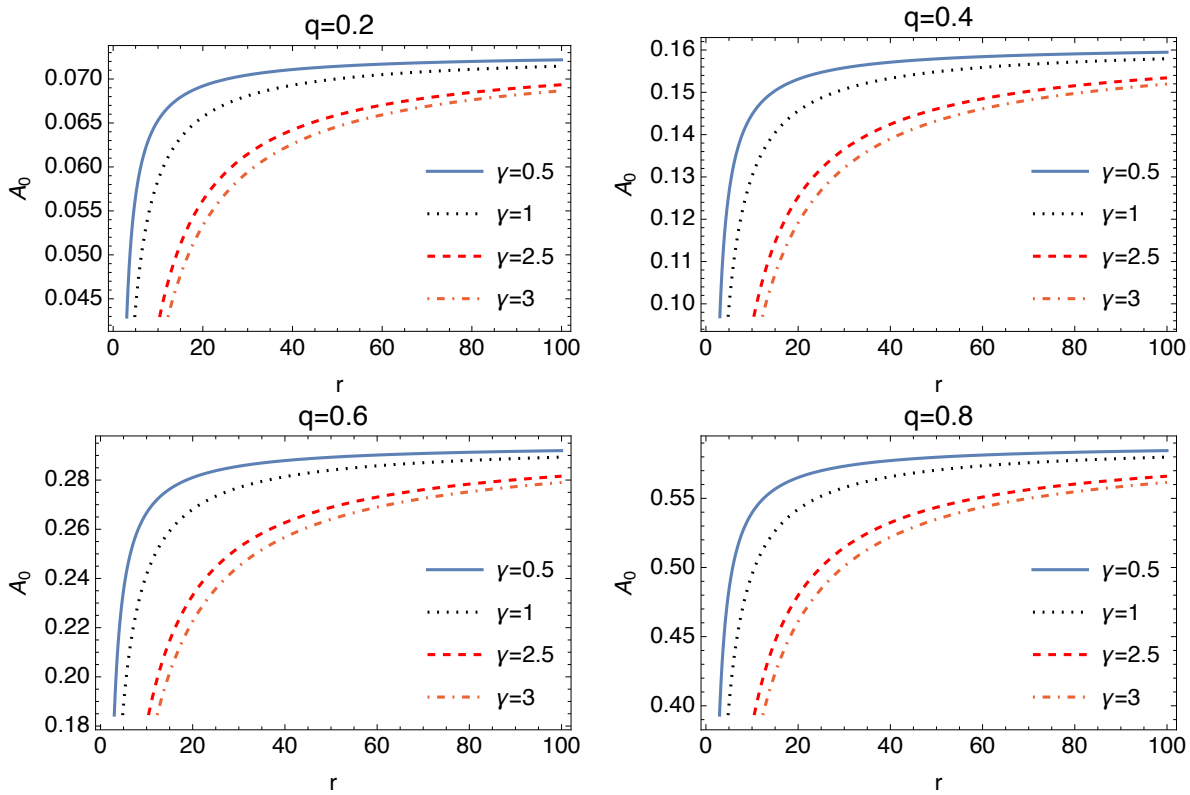

Figure 4.1: These figures represent how electric potential varies with radial distance within a charged ZV spacetime. For each case, mass is taken as $m = 1$ and q is fixed for within each figure as 0.2, 0.4, 0.6 and 0.8, respectively.

4.3 Singularity Structure

To understand the singularities in our metric, we need to compute the Kretchmann scalar $R_{\mu\nu\alpha\beta}R^{\mu\nu\alpha\beta}$. However, due to technical difficulties, we are using an alternative approach that involves investigating the Newman-Penrose (NP) component [63] Ψ_2 within the null-tetrad formalism. Typically, the singularities of Ψ_2 can give us an indication of the overall spacetime singularities. However, even this approach is not straightforward and presents significant challenges. To accomplish this, we have opted a null-tetrad basis of $1-$ forms.

$$
\begin{aligned}
\sqrt{2}l &= A(r)dt - C(r)sin\theta d\varphi = \sqrt{2}l_\mu dx^\mu, \\
\sqrt{2}n &= A(r)dt + C(r)sin\theta d\varphi = \sqrt{2}n_\mu dx^\mu, \\
\sqrt{2}m &= B(r,\theta)\left(\frac{dr}{\sqrt{\Delta}} + ird\theta\right) = \sqrt{2}m_\mu dx^\mu, \\
\sqrt{2}\bar{m} &= B(r,\theta)\left(\frac{dr}{\sqrt{\Delta}} - ird\theta\right) = \sqrt{2}\bar{m}_\mu dx^\mu,
\end{aligned}
\tag{4.11}
$$

in which $A(r)$, $B(r,\theta)$ and $C(r)$ are given by

$$
\begin{aligned}
A(r) &= \Delta^{\gamma/2}K^{-1}, \\
C(r) &= Kr\Delta^{\frac{1-\gamma}{2}}, \\
B(r,\theta) &= K\Delta^{\frac{\gamma^2-\gamma}{2}}\Sigma^{\frac{1-\gamma^2}{2}}.
\end{aligned}
\tag{4.12}
$$

The non-zero spin coefficients in the null-tetrad $(l_\mu, n_\mu, m_\mu, \bar{m}_\mu)$ of NP can be written as

$$
\begin{aligned}
\alpha &= \frac{1}{2\sqrt{2}B}\left[\sqrt{\Delta}\left(\frac{1}{r} + \frac{d}{dr}(ln(B))\right) - \frac{i}{r}\frac{d}{d\theta}(ln(B))\right], \\
\beta &= -\frac{1}{2\sqrt{2}B}\left[\sqrt{\Delta}\left(\frac{1}{r} + \frac{d}{dr}(ln(B))\right) + \frac{i}{r}\frac{d}{d\theta}(ln(B))\right], \\
\tau &= \frac{\sqrt{\Delta}}{2\sqrt{2}B}\frac{d}{dr}(ln(AC)) + \frac{icot\theta}{2\sqrt{2}rB}, \\
\pi &= -\frac{\sqrt{\Delta}}{2\sqrt{2}B}\frac{d}{dr}(ln(AC)) + \frac{icot\theta}{2\sqrt{2}rB}, \\
\kappa &= \frac{\sqrt{\Delta}}{2\sqrt{2}B}\frac{d}{dr}\left(ln\left(\frac{A}{C}\right)\right) - \frac{icot\theta}{2\sqrt{2}rB}, \\
\nu &= -\frac{\sqrt{\Delta}}{2\sqrt{2}B}\frac{d}{dr}\left(ln\left(\frac{A}{C}\right)\right) - \frac{icot\theta}{2\sqrt{2}rB}.
\end{aligned}
\tag{4.13}
$$

The Weyl Ψ_2 calculated as

$$\Psi_2(r,\theta) = \frac{\Delta^{1+\gamma-\gamma^2}}{4K^2}\Sigma^{\gamma^2-1}\left\{\frac{\Delta'}{2r\Delta} - 3\left(\frac{K'}{K}\right)^2 + \frac{1}{4}\gamma(\gamma-1)(\gamma-\gamma^2-2)\left(\frac{\Delta'}{\Delta}\right)^2 \right.$$
$$+\frac{1}{4}(1-\gamma^2)(\gamma^2-2)\left(\frac{\Sigma'}{\Sigma}\right)^2 + \gamma(2-\gamma)\frac{K'}{K}\frac{\Delta'}{\Delta} + (\gamma^2-1)\frac{K'}{K}\frac{\Sigma'}{\Sigma}$$
$$+\frac{1}{4}(1-\gamma^2)(1+2\gamma-2\gamma^2)\frac{\Sigma'}{\Sigma}\frac{\Delta'}{\Delta} - \frac{2}{r}\frac{K'}{K} + \frac{\gamma^2}{2r}\frac{\Delta'}{\Delta} + \frac{K''}{K} + \frac{1}{2}\gamma(\gamma-1)\frac{\Delta''}{\Delta}$$
$$\left.+\frac{1}{2}(1-\gamma^2)\frac{\Sigma''}{\Sigma} + \frac{(1-\gamma^2)p^2m^2}{r^4\Sigma^2}\left(cos2\theta - \frac{p^2m^2}{\Delta r^2}sin^2\theta\right)\right\}, \tag{4.14}$$

in which prime represents derivative with respect to r of the related metric functions.

If we put the metric functions into the Eq.(4.14), Ψ_2 can be written as

$$\Psi_2(r,\theta) = \frac{\Delta^{1+\gamma-\gamma^2}}{4K^2}\Sigma^{\gamma^2-1}\left\{\frac{m}{r^4\Delta}\left[(r-mq^2)(1-\gamma^2-2\gamma)+m\gamma q^2(\gamma-1)\right] + \frac{3(1-\gamma^2)}{r^2}\right.$$
$$+\frac{\gamma(\gamma-1)(\gamma-\gamma^2-2)m^2(r-mq^2)^2}{r^6\Delta^2} + \frac{(1-\gamma^2)(\gamma^2-2)m^2\left[m(sin^2\theta+q^2cos^2\theta)-r\right]^2}{r^6\Sigma^2}$$
$$-\frac{(1-\gamma^2)(1+2\gamma-2\gamma^2)m^2(mq^2-r)\left[r-m(sin^2\theta+q^2cos^2\theta)\right]}{r^6\Delta\Sigma} + \frac{(1-\gamma^2)(4m-3r)}{r^3\Sigma}$$
$$+\frac{K''}{K} + \frac{K'}{K}\left[-3\frac{K'}{K} + \frac{2}{r}\left(-\gamma^2 + \frac{m\gamma(2-\gamma)(r-mq^2)}{r^2\Delta} + \frac{(1-\gamma^2)(r-m)}{r\Sigma}\right)\right]$$
$$\left.+\frac{(1-\gamma^2)p^2m^2}{r^4\Sigma^2}\left(cos2\theta - \frac{p^2m^2}{\Delta r^2}sin^2\theta\right)\right\}. \tag{4.15}$$

Analyzing $\Psi_2(r,\theta)$ shows that singularities occur at $r=0$, as well as the roots of $\Delta(r)=0$ and $\Sigma(r,\theta)=0$. Notably, we observed that the outermost singularity arises from the root of $\Delta(r)=0$, which is given by

$$r_\Delta = m(1+p). \tag{4.16}$$

The root of $\Sigma(r,\theta)=0$ is

$$r_\Sigma = m(1+pcos\theta), \tag{4.17}$$

which is inside of r_Δ. Thus, it should be noted that any investigation into the singularities of the metric must first encounter $r_\Delta = m(1+p)$ as the outermost

singularity. Furthermore, it is worth mentioning that $K(r)$ is non-zero for $r > 0$ and $0 < p < 1$, and therefore, the presence of $K(r)$ in the curvature expression does not give rise to any additional singularities. We would like to highlight that $K(r)$ is the metric function that arises when the Maxwell field is added to the gravitational $ZV-$ metric, and that $K(r)$ becomes a constant when there is no em source present. Lastly, it is interesting to observe that directional singularities occur for $\gamma^2 < 3$ based on the behaviour of the power of $\Sigma(r,\theta)$, which becomes positive beyond this interval in order to avoid any divergence. Also, we can prove that the surface represented by $S(r) = r - r_+$ for $r_+ = m(1+p)$ is timelike by analyzing the normal vector to the surface in the limit of $r \to r_+$:

$$\begin{aligned}(\nabla S)^2 = g^{rr}\left(\frac{dS}{dr}\right)^2 &= -\frac{\Sigma^{\gamma^2-1}}{K^2}\Delta^{1+\gamma-\gamma^2}|_{r\to r_+} \\ &= -\frac{1}{K^2}\left(\frac{m^2p^2sin^2\theta}{r_+^2}\right)^{\gamma^2-1}\left(\frac{(r-r_+)(r-r_-)}{r_+^2}\right)^{1+\gamma-\gamma^2} < 0,\end{aligned} \tag{4.18}$$

in which $r_- = m(1-p)$ and $K = (2p)^{\gamma}(1+p)^{1-\gamma} < \infty$, in the limit of $r \to r_+$. Since $(\nabla S)^2 < 0$, normal vector to singular surface S is spacelike means that the singular surface S is timelike.

4.4 Restricted Geodesic Analysis for The ZV Spacetime

Since the gravitational lensing effect that we will calculate in the following section will be analysed in the equatorial plane, it is necessary to find null geodesics within this plane. In order to check if there are specific limitations on the distortion parameter, we will concentrate on the case when $\theta = \pi/2$. With this choice, the effect of q on the time-like circular geodesics will be studies. Afterwards, the specific condition $\dot{r} = 0$, $\dot{\theta} \neq 0$ will be studied, which will correspond to circular null-geodesics, via linear approximation.

4.4.1 Charge Effect on The Time-Like Geodesics with $\dot{r} = \dot{\theta} = 0$

The space-time line element, when subjected to these limitations, becomes

$$ds^2 = A(r)dt^2 - r^2 C_0(r) sin^2\theta d\varphi^2, \tag{4.19}$$

in which $A(r)$ and $C_0(r)$ can be determined from the general form of metric (3.26), a simplified Lagrangian can be formulated to depict the system as follows

$$\mathcal{L} = \frac{1}{2}A\dot{t}^2 - \frac{1}{2}r^2 C_0(r) sin^2\theta\dot{\varphi}^2, \tag{4.20}$$

where a dot denotes derivative with respect to an affine parameter. Regarding the time-like circular geodesics, the square of the angular velocity can be expressed as

$$\omega^2 = \frac{\dot{\varphi}^2}{\dot{t}^2} = \frac{A'}{r^2 C_0' sin^2\theta}, \tag{4.21}$$

in which a prime shows derivative with respect to r. If we select $K \approx 1$, and scale the asymptotic expansion of each term (detailed expansions of which are provided in the next section), we obtain the following outcome

$$\omega^2 \approx \frac{m\gamma}{r^3 sin^2\theta}\left(1 + \frac{3m}{r}(1-\gamma) + \frac{m\gamma}{r}q^2 + ...\right). \tag{4.22}$$

It is possible to derive Kepler's law under certain conditions. This becomes possible when the distortion parameter and θ are chosen as 1 and $\pi/2$, respectively. Additionally, when there is no charge, our results match with ref. [64].

4.4.2 The Circular Null-Geodesics

In this case, by setting the reduced line element (4.19) to zero, it follows that the magnitude of the angular frequency squared is

$$\omega^2 = \frac{\dot{\varphi}^2}{\dot{t}^2} = \frac{A}{r^2 C_0 sin^2\theta}. \tag{4.23}$$

After substituting the values from the metric (3.26), we get

$$\omega^2 = \frac{1}{r^2 K^4 sin^2\theta}\left(1 - \frac{2m}{r} + \frac{m^2 q^2}{r^2}\right)^{2\gamma-1} \tag{4.24}$$

Alternatively, we can express this as

$$\omega^2 = \frac{(r-r_1)^{2\gamma-1}}{r^{4\gamma} K^4 sin^2\theta}\,(r-r_\Delta)^{2\gamma-1} \tag{4.25}$$

in which $r_1 = m(1-p)$ and $r_\Delta = m(1+p)$. For the case where $p = 1$ and $q = 0$, the findings correspond to those of the uncharged ZV model. This indicates that in order to assign a meaningful value to ω^2, it is necessary to have $\gamma > 1/2$. If $\gamma < 1/2$, then ω^2 becomes infinite at the outer root $r = r_\Delta$, and we need to avoid this scenario. It is worth noting that this conclusion applies not only to $\theta \neq \pi/2$, but also to $\theta = \pi/2$.

4.4.3 The Linearized Circular Geodesics with $\dot{r} = 0$, in The Vicinity of $\theta = \pi/2$

We can now express the geodesic Lagrangian in the following form

$$\mathcal{L} = \frac{1}{2}A\dot{t}^2 - \frac{1}{2}r^2 B(r,\theta)\dot{\theta}^2 - \frac{1}{2}r^2 sin^2\theta C_0(r)\dot{\varphi}^2. \tag{4.26}$$

The Euler-Lagrange equations yields

$$\dot{t} = \frac{E}{A}, \tag{4.27}$$

$$\dot{\varphi} = \frac{l}{C_0(r) r^2 sin^2\theta}, \tag{4.28}$$

in which E and l are integration constants. When we apply the null condition $ds^2 = 0$, we arrive at the constraint

$$r^2 B(r,\theta)\dot{\theta}^2 = \frac{E^2}{A} - \frac{l^2}{C_0(r) r^2 sin^2\theta}. \tag{4.29}$$

To derive the $\theta-$equation in terms of the affine parameter, we differentiate the

aforementioned equation. Our approach involves assuming that $\dot{\theta}^2 \approx 0$ holds true for $\theta \approx \pi/2$. After carrying out the derivation, the constraint condition is expressed as a relation between the constants of motion, which is given by

$$\frac{E^2}{l^2} \approx \frac{(r-r_1)^{2\gamma-1}(r-r_\Delta)^{2\gamma-1}}{K^4 r^{2+4\gamma}}, \tag{4.30}$$

This expression is valid when $\gamma > 1/2$. It should be pointed out that when we choose $\theta \approx \pi/2$, we obtain

$$\Sigma \approx 1 - \frac{2m}{r} + \frac{m^2}{r^2} \approx \Delta + \frac{m^2 p^2}{r^2}. \tag{4.31}$$

By making certain expansions, we can express the second-order equation for θ in the following form

$$(r-r_1)^{2(1-\gamma)}(r-r_\Delta)^{2(1-\gamma)}\left(1+(1-\gamma^2)\frac{m^2p^2}{r^2\Delta}\right)\ddot{\theta} \approx \frac{l^2 cos\theta}{K^4 r^{2(2\gamma-1)} sin^3\theta}. \tag{4.32}$$

The upper limit of distortion parameter needs to be $\gamma < 1$ in order for achieving finiteness for the term at the left hand side of equation (4.32). We had previously stated that $\gamma > 1/2$ is also a necessary condition meaning one is constraint to the region with $1/2 < \gamma < 1$ in the the equatorial plane. Therefore, this range will be used throughout the gravitational lensing analysis for $\theta = \pi/2$.

4.4.4 The Particle Motion in The Equatorial Plane

In this subsection, we will examine the motion of electrically and magnetically charged test particles in the charged ZV spacetime separately.

4.4.4.1 The Magnetic Case

The Lagrangian that governs the movement of a test particle, possessing a charge of Q and unit mass, is described as

$$\mathcal{L} = \frac{1}{2} g_{\mu\nu} \frac{dx^\mu}{d\tau} \frac{dx^\nu}{d\tau} + QA_\mu \frac{dx^\mu}{d\tau}. \tag{4.33}$$

In the equation above, τ represents proper time. Therefore, the differentiations are carried out with respect to proper time. The vector potential of our choice is $A_\mu = (0,0,0,C_0 cos\theta)$, which yields to the following Euler-Lagrange equations.

$$g_{00}\left(\frac{dt}{d\tau}\right) = E = const. \tag{4.34}$$

$$g_{\phi\phi}\left(\frac{d\phi}{d\tau}\right) + QC_0 cos\theta = l = const. \tag{4.35}$$

The $\theta-$ equation is automatically fulfilled in the equatorial plane. We now decide to set $\theta = \pi/2$, which eliminates the test particle's coupling term with the metric. As a result, the analysis will be equivalent to that of a neutral particle. The time-like geodesics condition provides us with the following expression

$$1 = \frac{E^2}{g_{00}} + g_{rr}\left(\frac{dr}{d\tau}\right)^2 + \frac{l^2}{g_{\phi\phi}} \tag{4.36}$$

which is identical to

$$E^2 = \Delta^{\gamma^2-1}\Sigma^{1-\gamma^2}\left(\frac{dr}{d\tau}\right)^2 + \frac{\Delta^\gamma}{K^2}\left(1 + \frac{l^2\Delta^{\gamma-1}}{K^2 r^2}\right). \tag{4.37}$$

As we have selected $\theta = \pi/2$, we can infer that

$$\Sigma = \left(1 - \frac{m}{r}\right)^2, \tag{4.38}$$

$$\Delta = \left(1 - \frac{m}{r}\right)^2 - \frac{m^2 p^2}{r^2}. \tag{4.39}$$

For circular geodesics, the derivative of r with respect to τ is equal to zero, indicating from equation (4.37) that the condition $V = E$ must be satisfied. The potential acting on

a neutral particle (or a charged particle under the influence of a magnetically charged ZV star) can be expressed as

$$V(r) = \frac{\Delta^{\gamma/2}}{K}\left(1 + \frac{l^2\Delta^{\gamma-1}}{K^2 r^2}\right)^{1/2}. \tag{4.40}$$

In order to be able to make comments about the allowed values for the angular momenta, one needs to make sure that $\frac{dV}{dr} = 0$ is satisfied. Furthermore, for achieving circular geodesics, $V = E$ is a necessity. Although circular geodesics are not of interest in this context, we will adhere to the overall structure of an effective potential, which can be defined as

$$2V_{eff} = E^2 - 1 - \left(\frac{dr}{d\tau}\right)^2 \tag{4.41}$$

After substituting $\left(\frac{dr}{d\tau}\right)^2$ with the expression given in equation (4.37), the effective potential can be written as

$$V_{eff} = \frac{1}{2}(E^2 - 1) + \frac{1}{2}\left(\frac{\Delta}{\Sigma}\right)^{1-\gamma^2}\left[-E^2 + \frac{\Delta^{\gamma}}{K^2}\left(1 + \frac{l^2\Delta^{\gamma-1}}{K^2 r^2}\right)\right]. \tag{4.42}$$

As a special case, we can examine the scenario when $\gamma = 1$ (RN geometry) and $p = \frac{1}{2}$. In this case, the effective potential reduces to

$$V_{eff} = -\frac{m}{r} + \frac{l^2}{r^2}\left(1 - \frac{2m}{r}\right). \tag{4.43}$$

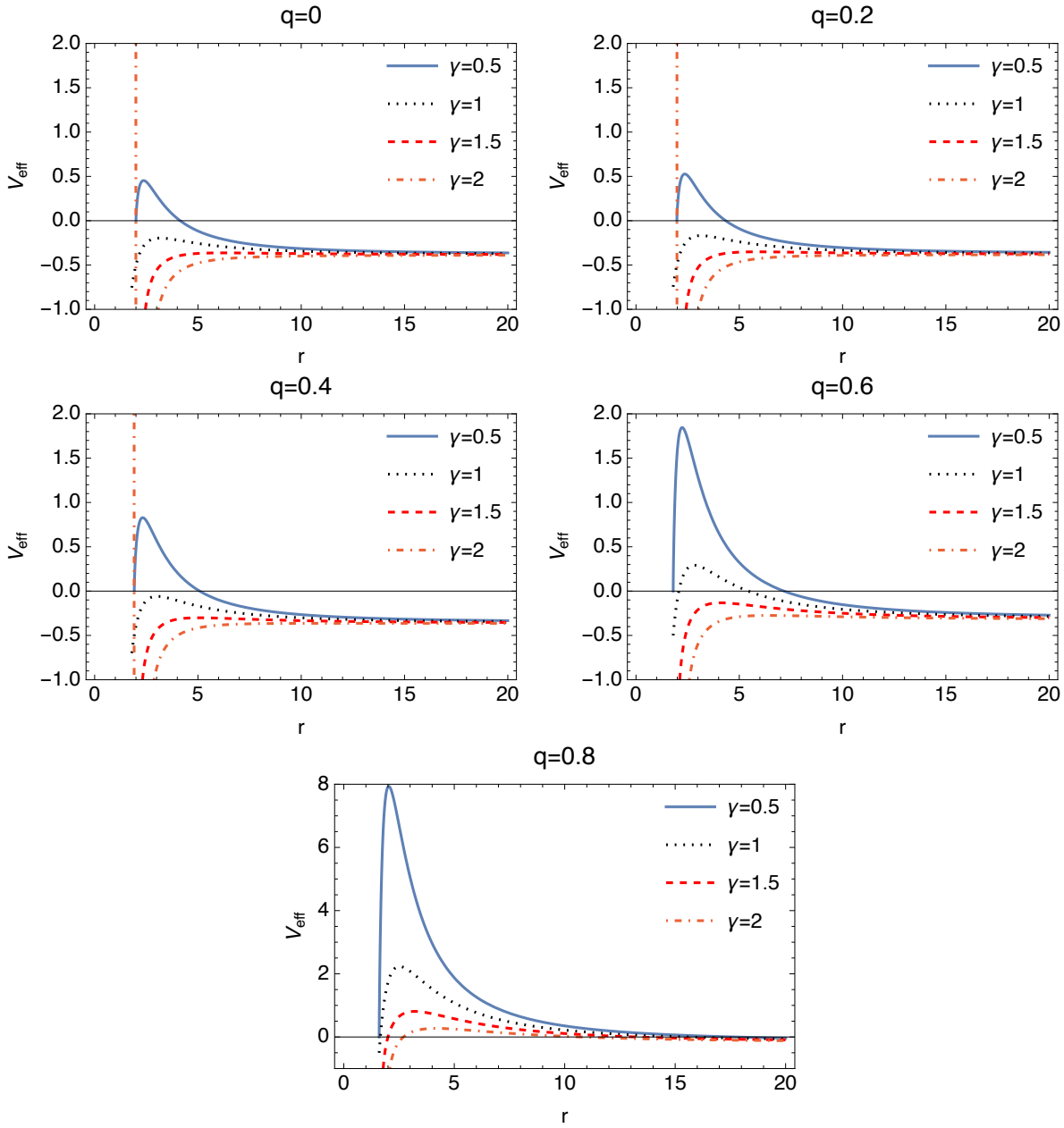

Figure 4.2: Produce a plot of the effective potential (4.41) using specific parameters $m = 1$, $E = 1$, and $l = 15$. Additionally, include the special parameter $\gamma = 1$ for comparison with the spherical case.

Fig. 4.2 displays the radial variation of the effective potential (4.42) for various γ values, while keeping E, l, and m constant. The figure also reveals that as the distance approaches infinity, the impact of γ weakens. In contrast, the effect of γ is stronger in closer regions. Additionally, an important consequence of the charge is that an increase in its value leads to a rise in the potential barrier.

4.4.4.2 The Electric Case

Assuming an electrically charged particle with a charge of Q and a mass of one unit, the Lagrangian that describes its motion for $\theta = \pi/2$ is given by

$$\mathcal{L} = \frac{1}{2} g_{\mu\nu} \frac{dx^\mu}{d\tau} \frac{dx^\nu}{d\tau} + QA_0 \frac{dt}{d\tau}, \tag{4.44}$$

in which expression (4.6) provides the value of $A_0(r)$. Applying the Euler-Lagrange equations yields

$$\dot{t} = \frac{K^2}{\Delta^\gamma}(E - QA_0), \tag{4.45}$$

and

$$\dot{\varphi} = \frac{l^2 \Delta^{\gamma-1}}{r^2 K^2}. \tag{4.46}$$

Here, we have two integration constants, E and l, representing energy and angular momentum respectively. It is worth noting that for $\theta = \pi/2$, the equation involving θ becomes trivially satisfied. By following a similar process as in the magnetic scenario, we arrive at the effective potential

$$V_{eff} = \frac{1}{2}(E^2 - 1) + \frac{1}{2}\left(\frac{\Delta}{\Sigma}\right)^{1-\gamma^2} \left[-(E - QA_0)^2 + \frac{\Delta^\gamma}{K^2}\left(1 + \frac{l^2 \Delta^{\gamma-1}}{K^2 r^2}\right)\right]. \tag{4.47}$$

The effective potential is represented by the equation given above, where Σ and Δ correspond to the values in equations (3.27) and (3.28) respectively.

Fig. 4.3 displays plots of the effective potential against the radial distance r. As expected, the influence of the deformation parameter γ becomes weaker at larger distances, with more pronounced effects in the closer regions. Similar to the magnetic case, an increase in the electric charge results in a higher potential barrier.

Interestingly, when the charge Q equals zero, the effective potential for the electric case coincides with that of the magnetic case.

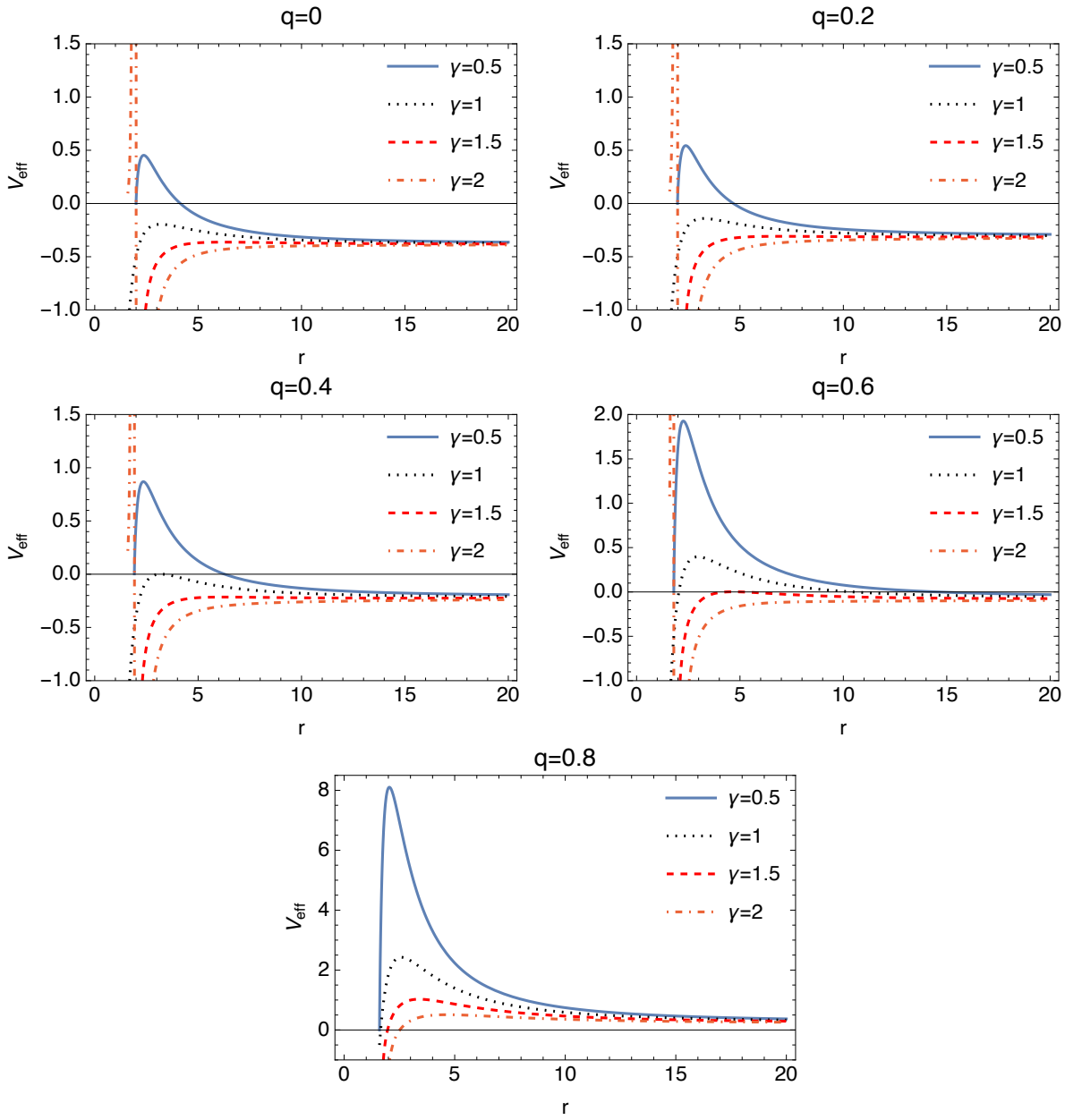

Figure 4.3: The radial variation of the effective potential for a test particle carrying a charge of $Q = 1$, situated on the equatorial plane, is shown for various γ and q values. The plots are generated for fixed values of $m = 1$, $E = 1$, and $l = 15$.

4.4.5 Gravitational Lensing in Charged *ZV* Spacetime

In this subsection, we will calculate the lensing angle of the charged ZV solution using the Gauss-Bonnet theorem, whose mathematical and physical foundations were

provided in the previous section (section 2.3). In the preceding section, we focused on circular, null geodesics that can be projected onto the $\theta = \pi/2$ plane. It should be noted that $\theta = \pi/2$ is the symmetry plane of ZV objects and geodesics can be projected onto this plane. The existence of circular geodesics also allows for their perturbation into elliptical orbits, which will be utilized in this section. To this end, we introduce the optical metric of the spacetime (3.26), which is projected onto the $\theta = \pi/2$ plane

$$dt^2 = \bar{g}_{rr}dr^2 + \bar{g}_{\varphi\varphi}d\varphi^2, \tag{4.48}$$

in which

$$\bar{g}_{rr} = K^4\Delta^{\gamma^2-2\gamma-1}\Sigma^{1-\gamma^2}, \tag{4.49}$$

$$\bar{g}_{\varphi\varphi} = r^2K^4\Delta^{1-2\gamma}. \tag{4.50}$$

The square root of determinant for this metric can be written as

$$\sqrt{\bar{g}} = rK^4\Delta^{\frac{\gamma^2}{2}-2\gamma}\Sigma^{\frac{1-\gamma^2}{2}}. \tag{4.51}$$

As shown in section 2.3, total deflection angle δ is given by

$$\int_0^{\pi}\int_{r_g}^{\infty}\mathcal{K}dS = -\delta, \tag{4.52}$$

where $dS = \sqrt{\bar{g}}drd\varphi$.Here, the value of the lower limit r_g in the integral depends on the angle and represents the minimum distance from the source, which can be determined using the null geodesic equation. Specifically, for the problem invariant (4.52) gives

$$\int_0^{\pi}\int_{r_g}^{\infty}\mathcal{K}dS = -\int_0^{\pi}\int_{r_g}^{\infty}\partial_r\left[\Delta^{1-\frac{\gamma^2}{2}}\Sigma^{\frac{\gamma^2-1}{2}}\left(1+2r\frac{K'}{K}+r\left(\frac{1}{2}-\gamma\right)\frac{\Delta'}{\Delta}\right)\right]drd\varphi. \tag{4.53}$$

To evaluate $\mathcal{K}$, we require expansions for the metric functions, which are provided as follow

$$\begin{aligned}\Delta^n \simeq & 1-\frac{2nm}{r}+\frac{nm^2}{r^2}\left[q^2+2(n-1)\right]-\frac{2m^3}{3r^3}n(n-1)(3q^2+2)\\ & +\frac{m^4}{r^4}n(n-1)\left[\frac{1}{2}q^4+2q^2+\frac{2}{3}(n-2)\right]+\dots,\end{aligned} \tag{4.54}$$

$$\Sigma^n \simeq \Delta^n(q=1), \tag{4.55}$$

$$K \simeq 2p\left[1-\frac{m^2q^2}{2r^2}\gamma(\gamma-1)\right]+\dots, \tag{4.56}$$

$$\frac{\Delta'}{\Delta} \simeq \frac{2m}{r^2}\left(1-\frac{mq^2}{r}\right)\left[1+\frac{2m}{r}-\frac{m^2}{r^2}(q^2-4)\right]+\dots, \tag{4.57}$$

$$\frac{\Sigma'}{\Sigma} \simeq \frac{2m}{r^2}\left(1+\frac{m}{r}+\frac{m^2}{r^2}\right)+\dots, \tag{4.58}$$

$$\frac{K'}{K} \simeq \frac{q^2m^2}{r^3}\gamma(\gamma-1)\left(1-\frac{m}{r}(\gamma-2)\right)+\dots, \tag{4.59}$$

in which "a prime" showes $\frac{d}{dr}$. Note that the higher-order expansions are presented in the event that additional corrections are necessary.

To find the minimum value of r_g, we can solve the null geodesics equation. For this purpose, we rewrite the line element in the following form (for $\theta=\pi/2$)

$$ds^2 = A(r)dt^2 - B(r)dr^2 - r^2C(r)d\varphi^2, \tag{4.60}$$

where $A(r), B(r)$ and $C(r)$ are metric functions to be wrote from (3.26). By defining the geodesic Lagrangian with respect to an affine parameter λ

$$\mathcal{L} = \frac{1}{2}A\dot{t}^2 - \frac{1}{2}B\dot{r}^2 - \frac{1}{2}r^2C\dot{\varphi}^2. \tag{4.61}$$

Here, $\dot{} \equiv \frac{d}{d\lambda}$, results in the first integrals

$$A\frac{dt}{d\lambda} = E = const.\,, \tag{4.62}$$

$$Cr^2\frac{d\varphi}{d\lambda} = L = const.\,, \tag{4.63}$$

so that

$$\frac{A}{Cr^2}\left(\frac{dt}{d\varphi}\right) = \frac{1}{b} = \frac{E}{L}, \tag{4.64}$$

in which b denotes the impact parameter. Now, if we switch to the new variable $u = 1/r$, and solve for $\left(\frac{dr}{d\lambda}\right)^2$ using the expression for ds^2, we obtain

$$\left(\frac{du}{d\varphi}\right)^2 = \frac{C}{B}\left(\frac{C}{Ab^2} - u^2\right), \tag{4.65}$$

The derivative of this expression with respect to φ gives us the equation for geodesics. If we put the related charged ZV metric functions in to the Eq.(4.65), the null geodesic equation of charged can be written as

$$\begin{aligned}\frac{d^2u}{d\varphi^2} + u =& 3mu^2 + \frac{16m(\gamma-1)p^4}{b^2}\left\{2 - 3mu\left[1 - 3\gamma + (1+\gamma)q^2\right]\right. \\ &\left. + m^2u^2\left[-3 - 3q^2(3+\gamma)(-1+2\gamma)\right] + \gamma(3 + 12\gamma + 2p^2(-4+5\gamma))\right\}.\end{aligned} \tag{4.66}$$

It can be observed from this equation that when $\gamma = 1$, the contribution of the charge is of order $1/b^3$, which is neglected. After solving the homogeneous equation

$$\frac{d^2u}{d\varphi^2} + u = 0. \tag{4.67}$$

Here, the solution of Eq.(4.67) is $u = \sin\varphi/b$. If we substitute $u = \sin\varphi/b$ into Eq.(4.66) and solve, we can find a term of order $1/b^2$

$$u = \frac{sin\varphi}{b} + \frac{32mp^4}{b^2}(\gamma-1) + \frac{m}{b^2}\left(1 + cos^2\varphi\right). \tag{4.68}$$

Eq. (4.68) can be identified as $1/r_g$.

Upon revisiting Eqs. (2.33) and (2.34) and utilizing the aforementioned limit for the GB integral, we can derive the deflection angle (up to the order of $1/b^2$) as

$$\delta = \frac{4m\gamma}{b} + \frac{\pi}{b^2}(m\gamma)^2 \left[64p^4\left(1-\frac{1}{\gamma}\right) + \frac{4}{\gamma} - \frac{1}{4} - \frac{3}{4}q^2\right]. \tag{4.69}$$

When $\gamma = 1$, $q = 0$ ($p = 1$) is applied, the deflection angle δ_S of Schwarzschild can be retrieved

$$\delta_S = \frac{4m}{b} + \frac{15m^2\pi}{4b^2}. \tag{4.70}$$

Similarly, in the *RN* limit where $\gamma = 1$ and $q \neq 0$, the deflection angle can be expressed as δ_{RN}:

$$\delta_{RN} = \frac{4m}{b} + \frac{15m^2\pi}{4b^2} - \frac{3Q^2\pi}{4b^2}, \tag{4.71}$$

in which $Q = mq$. Eq. (4.69) reveals that by introducing the distortion parameter γ, the new mass can be defined as $M = m\gamma$.

4.4.5.1 Gravitational Lensing in Stationary Uncharged ZV Spacetime

Now, let us compare the gravitational lensing effect created by the pure rotating *ZV* solution with the absence of gravitational lensing effect created by the pure charged *ZV* solution. To do so, we will utilize the metric from [19], but adjust the sign convention to match our own

$$\begin{aligned} ds^2 =& e^{2\psi}dt^2 - \frac{e^{2\lambda-2\psi}\Sigma}{\Delta}dr^2 - e^{2\lambda-2\psi}\Sigma r^2 d\theta^2 \\ &- \left(e^{-2\psi}\Delta r^2 sin^2\theta - \omega^2 e^{2\psi}\right)d\varphi^2 - 2\omega e^{2\psi}dtd\varphi, \end{aligned} \tag{4.72}$$

in which

$$
\begin{aligned}
e^{-2\psi} &= \frac{1}{2}\left[(1-p_0)\Delta^{\gamma}+(1+p_0)\Delta^{-\gamma}\right], \\
e^{2\lambda} &= \left(\frac{\Delta}{\Sigma}\right)^{\gamma^2}, \\
\omega &= -2m\gamma q_0 cos\theta.
\end{aligned}
\tag{4.73}
$$

Here, $p_0^2+q_0^2=1$ and

$$
\begin{aligned}
\Delta &= 1-\frac{2m}{r} \\
\Sigma &= 1-\frac{2m}{r}+\frac{m^2}{r^2}sin^2\theta.
\end{aligned}
\tag{4.74}
$$

In here, q_0 is called the NUT-like parameter and it needs to obey $0<q_0<1$. This parameter contributes to the rotation of the spacetime and disappears for $\theta=\pi/2$. To avoid confusion with the charged metric parameter p, we denote it as p_0 (and q_0) in reference to Refs. [19, 56]. When $p_0=1$, this metric reduces to the well-known *ZV* metric. It is worth mentioning that Ref. [19] refers to p_0 as the 'quasi-NUT' parameter, which is related to $q_0=\sqrt{1-p_0^2}$, while Ref. [56] introduces it as a differential 'spinning' parameter. The reason behind this is that unlike the NUT parameter l (with $0<l<\infty$), p_0 is strongly bounded by $p_0\leq 1$. From a physical perspective, this parameter may be applicable only to large-scale astrophysical systems, such as spiral galaxies.

When we fix $\theta=\pi/2$, the optical metric of line element (4.72) becomes

$$
ds^2 = e^{-4\psi}\left(\frac{e^{2\lambda}\Sigma}{\Delta}dr^2+\Delta r^2 d\varphi^2\right),
\tag{4.75}
$$

otherwise

$$
dt^2 = \bar{g}_{rr}dr^2+\bar{g}_{\varphi\varphi}d\varphi^2.
\tag{4.76}
$$

For this case GB theorem gives

$$\delta = \int_0^{\pi} \int_{r_g}^{\infty} \left[\partial_r \left(\frac{1}{\sqrt{\bar{g}_{rr}}} \partial_r \sqrt{\bar{g}_{\varphi\varphi}} \right) \right] dr d\varphi. \tag{4.77}$$

We would like to highlight that this simplification is feasible because even though the optical metric (4.76) is not asymptotically flat (AF) in general, it becomes AF when $\theta = \pi/2$.

To establish the value of the lower limit of integration r_g, we employ the null geodesics equation from (4.65) with the variable $u = 1/r$. By utilizing the impact parameter b and differentiating once again, we arrive at the following result

$$\begin{aligned} \frac{d^2u}{d\varphi^2} + u =& 3mu^2 + \frac{m^2}{b^2} \left[3 + \gamma(5\gamma + 4p_0(p_0\gamma - 3)) \right] u \\ &+ \frac{2m}{b^2}(p_0\gamma - 1) + O\left(\frac{1}{b^3}\right). \end{aligned} \tag{4.78}$$

By using the homogeneous solution, as in the case of the charged ZV, we can calculate the lower limit of the $r-$ integral up to the order of $\sim \frac{1}{b^2}$, which is given by

$$\frac{1}{r_g} = \frac{sin\varphi}{b} + \frac{m}{b^2} \left(2p_0\gamma - sin^2\varphi \right). \tag{4.79}$$

After integrating (4.77) and setting the limits for r, followed by an additional integration with respect to φ, we can derive the deflection angle

$$\delta = \frac{4m\gamma p_0}{b} + \frac{m^2 p_0 \gamma\pi}{b^2}(4p_0\gamma - 1) + \frac{m^2\gamma\pi}{4b^2}(4p_0 + 7\gamma - 8p_0^2\gamma) \tag{4.80}$$

It should be noted that the deflection angle derived is only applicable for $\theta = \pi/2$. It is worth noting that when $\gamma = 1$ (spherical symmetry) and $p_0 = 1$ ($q_0 = 0$ - zero NUT-like parameter), the result reduces to δ_S.

4.4.6 Gravitational Redshift in Charged *ZV* Spacetime

According to Eq.(2.41) the explicit expression for the gravitational redshift of charged ZV spacetime is found as

$$z=\frac{(1+p)\left(1-\frac{m(1-p)}{r}\right)^{\gamma}-(1-p)\left(1-\frac{m(1+p)}{r}\right)^{\gamma}}{\left(1-\frac{2m}{r}+\frac{m^2q^2}{r^2}\right)^{\gamma/2}}-1. \tag{4.81}$$

4.4.7 Applications in Astrophysics

This subsection is reserved for calculation of bending angles for the compact stars listed in Table 4.1 whose physical parameter values are given. The lensing analyses are conducted for charged and stationary uncharged ZV spacetimes [65, 66].

Another goal of this subsection is to provide graphical representations of our gravitational lensing calculations. However, for practical purposes, sticking to standard international (SI) units for the plots sound more reasonable. Therefore, it has been made sure that in all relevant equations, the necessary conversions are made by multiplying M with Gc^{-2}, in which $G = 6.67408 \times 10^{-11} m^3 kg^{-1} s^{-2}$ and $c = 3 \times 10^8 ms^{-1}$. It is important to record that the bending angle comes out in radians.

Table 4.1: Compact star masses and radii numerical values [1]. Here, $M_\odot$ is the mass of the sun

Compact Stars	M	Radius (km)
Vela X-1	$1.77M_\odot$	9.56
SAXJ 1808.4-3658	$0.9M_\odot$	7.95
Her X-1	$0.85M_\odot$	8.10
4U 1538-52	$0.87M_\odot$	7.86

Below, one can find graphs of δ versus b/R_{star} with different distortion parameter values. In the plots, R_{Star} and δ stand for the estimated radius of the charged compact

object and the associated bending angle, respectively. On the x-axis, instead of using b directly, it was replaced by b/R_{star}, since for gravitational lensing analysis, we are interested in the path of light around the star, not the ones that may reach beyond R_{star}.

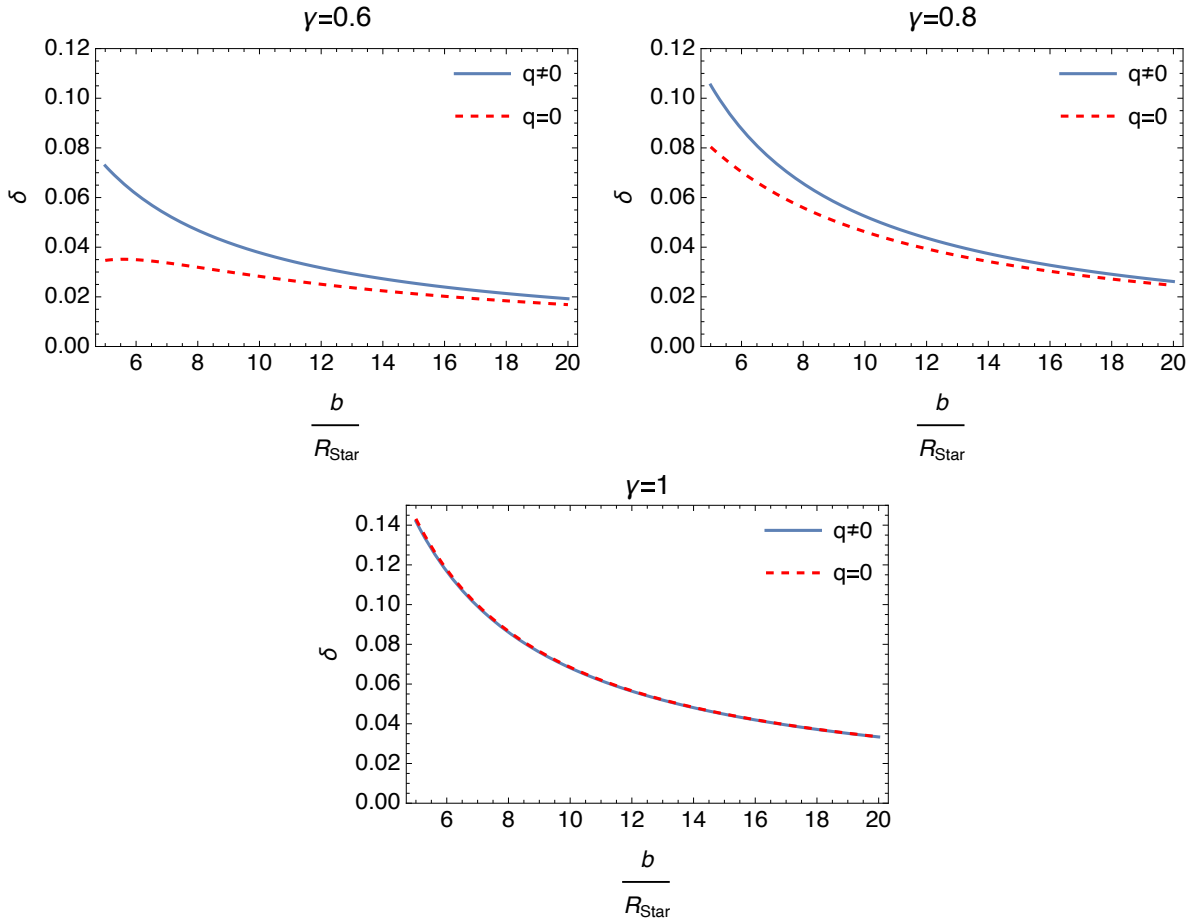

Figure 4.4: The graph shows how the deflection angle δ varies with b/R_{Star} for the astronomical object 4U 1538-52. There are different curves on the plot, which correspond to different values of γ, ranging from $\gamma = 0.6$ on the left to $\gamma = 1$ on the right. It is important to note that for all curves, the charge parameters have been set to $q = p = 1/\sqrt{2}$. The solid line represents the charged case, while the dashed line represents the uncharged case.

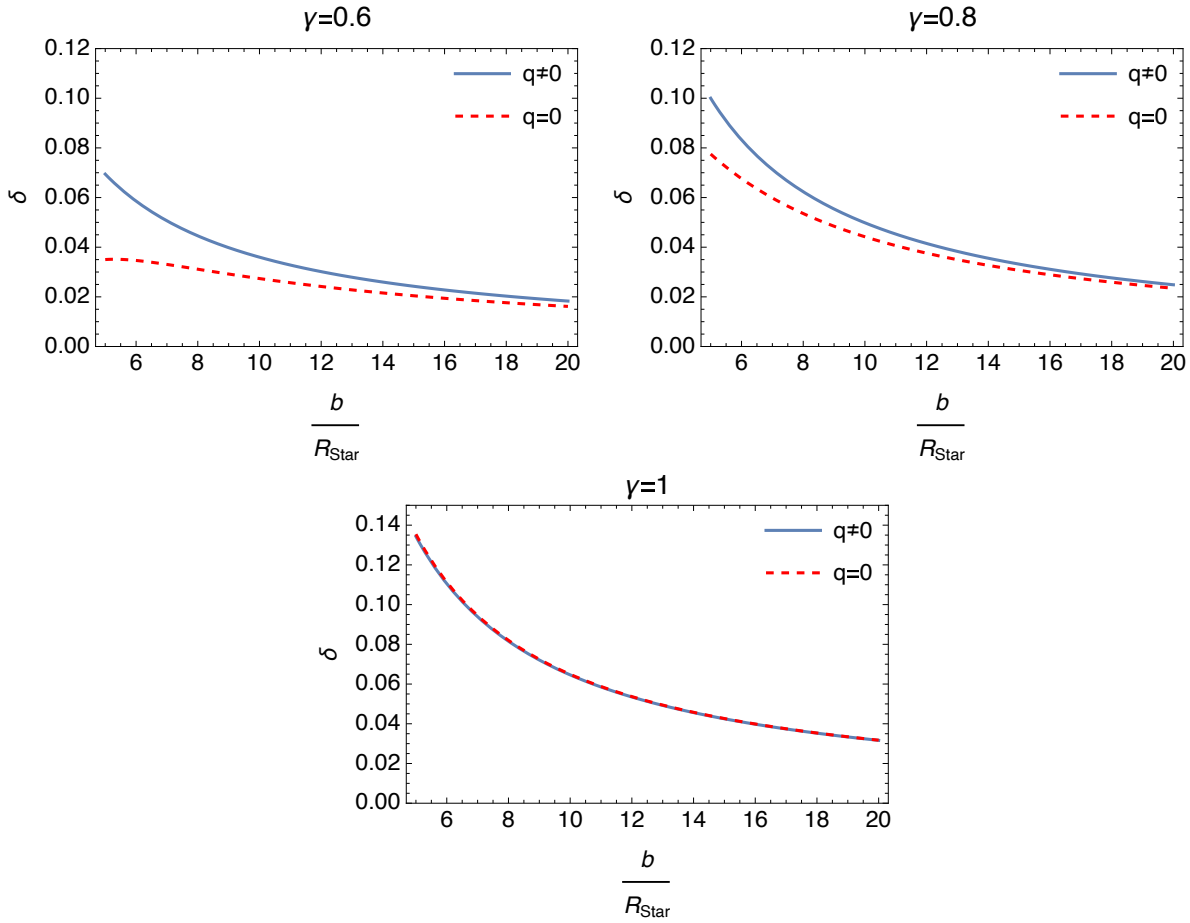

Figure 4.5: The plot shows how the deflection angle δ changes with b/R_{star} for the astronomical object HerX-1, with separate curves for the charged (solid line) and uncharged (dashed line) cases.

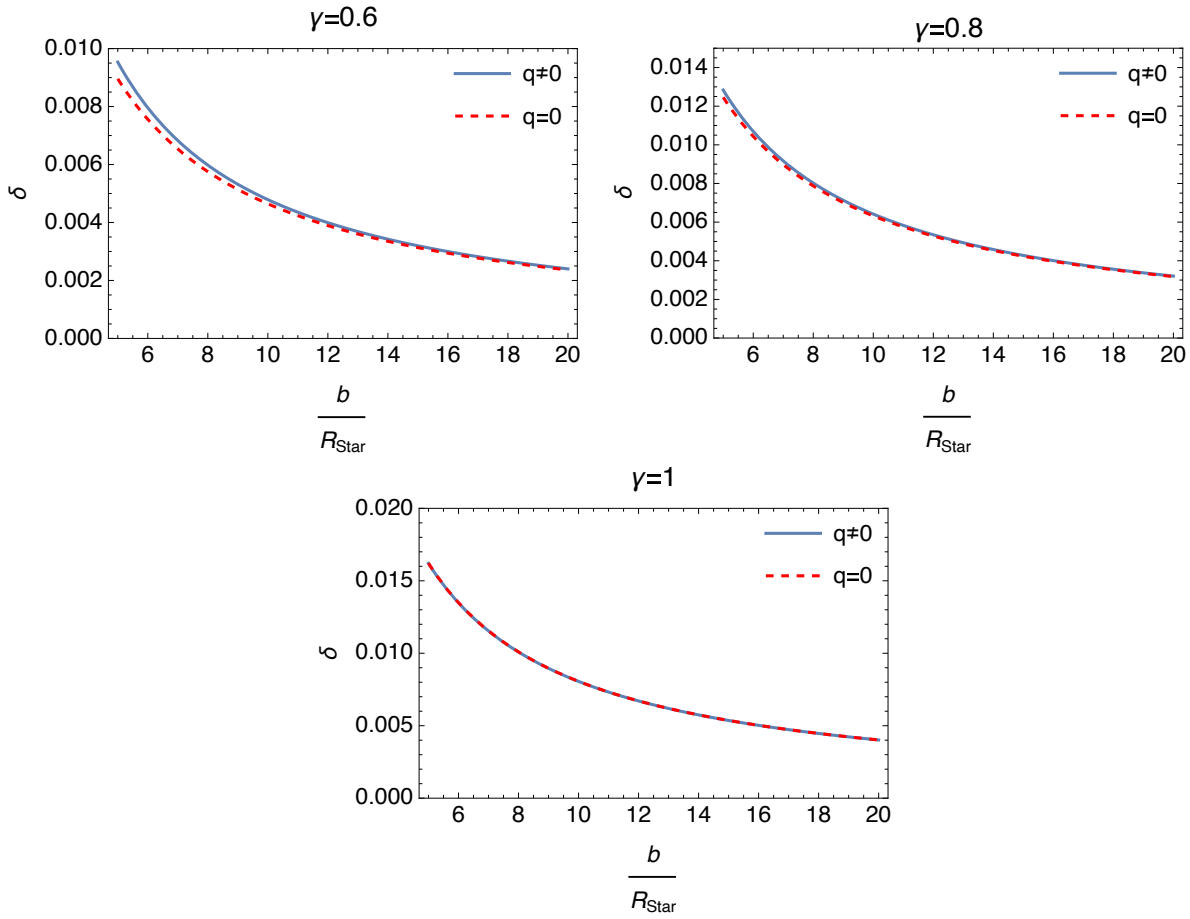

Figure 4.6: Here is a plot of the deflection angle δ as a function of b/R_{star} for the astronomical object SAXJ1808.4-3658 with the charged (solid line) and uncharged (dashed line) cases.

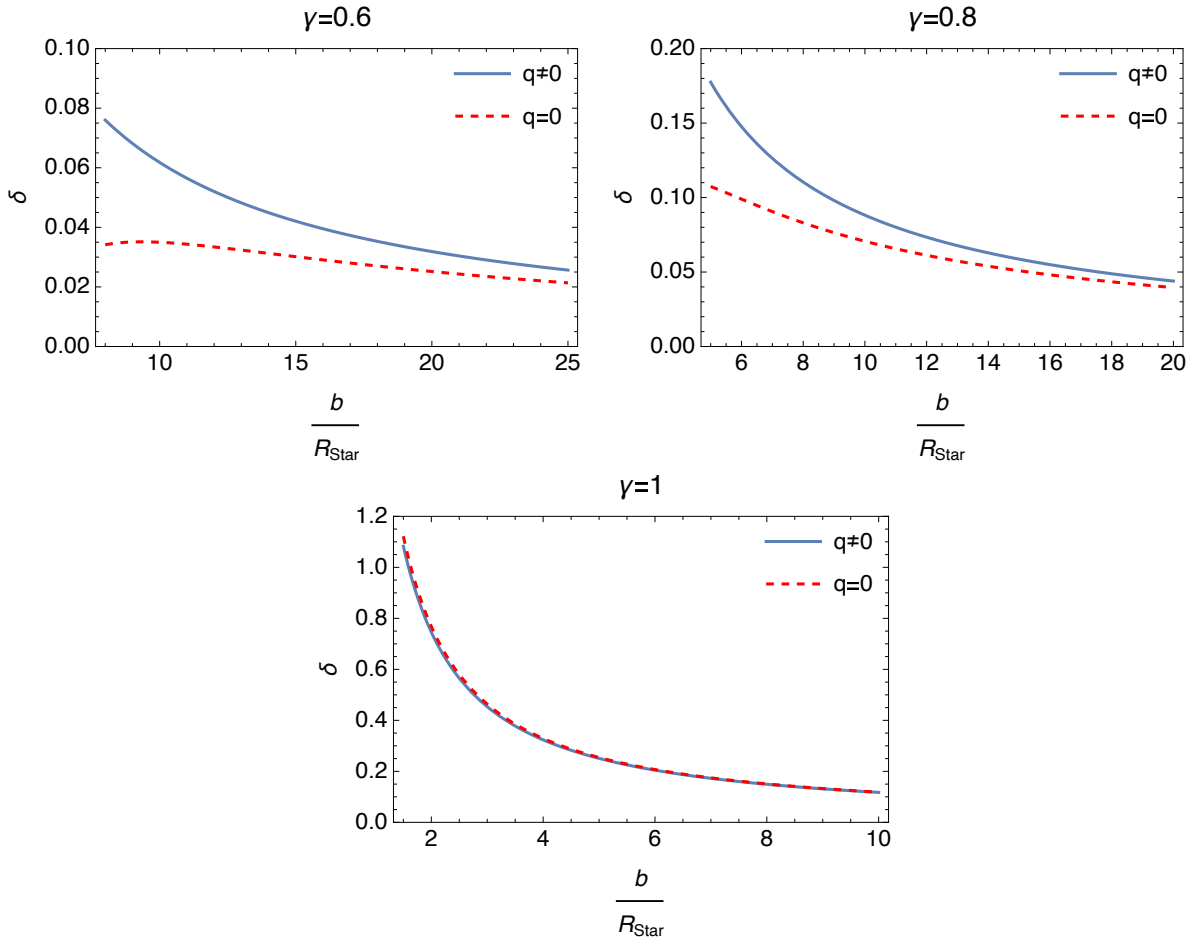

Figure 4.7: The plot illustrates how the deflection angle δ varies with b/R_{star} for the astronomical object VelaX-1. The graph displays separate curves for the charged case (solid line) and uncharged case (dotted line), allowing for a direct comparison between the two scenarios.

If Figures 4.4-4.7 are examined in detail, it can be observed that for the spherically symmetrical case, the charged and uncharged cases have the same bending angle curve. This must carry importance in the sense that the path that light follows seems to be unaffected by the charge in the vicinity.

On the other hand, in the upcoming figure (Figure 4.8), one can see the effect of distortion parameter on the bending angle in an easier way.

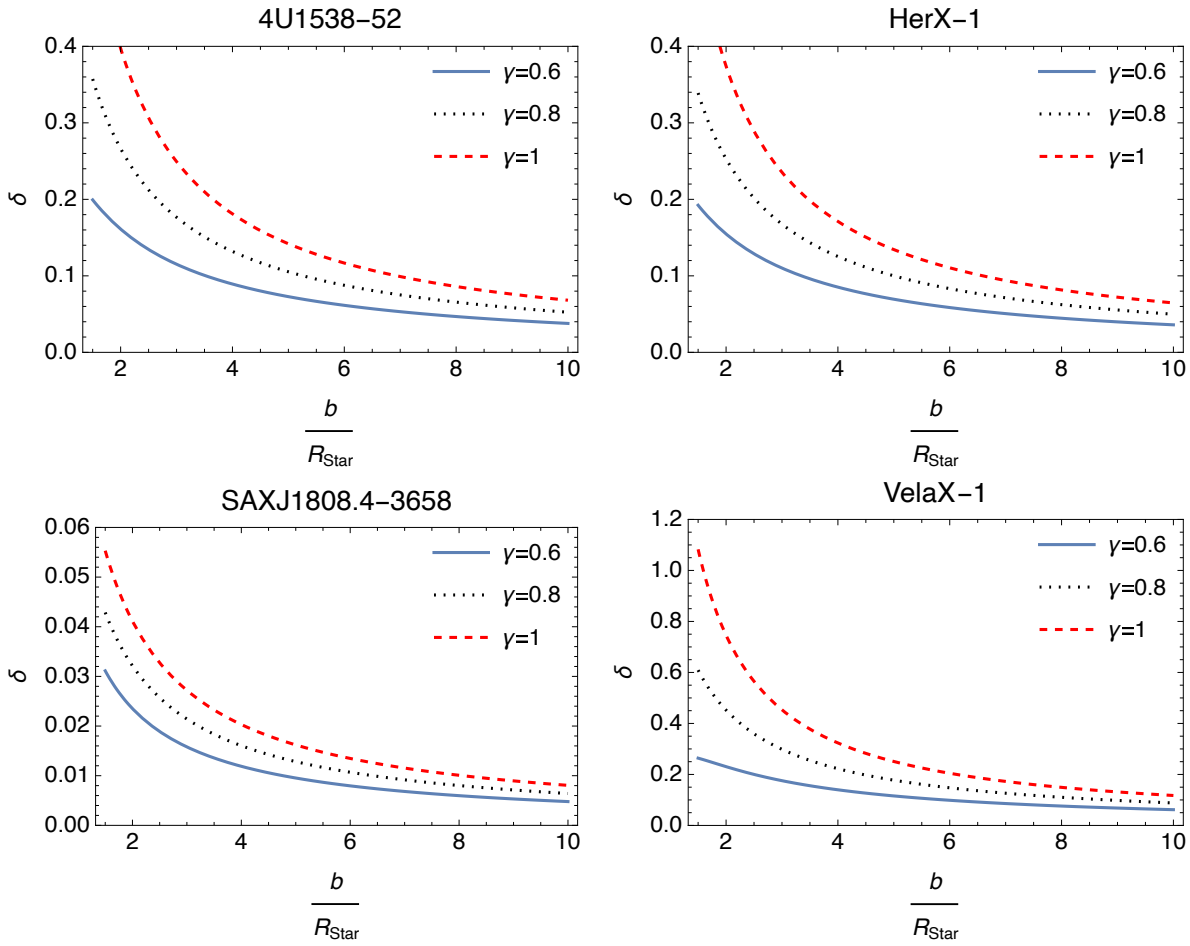

Figure 4.8: The plots with overlapping curves of δ vs b/R_{star} for all objects listed in Table 4.1, choosing $p = q = \frac{1}{\sqrt{2}}$ for charged ZV. The graphs plotted different distortion values $(\gamma's)$ for understanding effect of geometric distortion on gravitational lensing.

It is crucial to investigate the gravitational lensing effects that arise when a non-spherical compact object is in a stationary case. To accomplish this, we numerically study the bending angle calculated in Eq. (4.80) for the compact objects listed in Table 4.1.

Figures 4.9-4.12 exhibit the variation in bending angle as a function of idealized radial distance for different values of the γ parameter. These plots display the bending angles for the uncharged stationary case, as well as for the uncharged and charged ZV cases. By displaying these plots together, the "spin" of the non-spherical compact objects can be better understood.

There seems to be no significant distinction between the charged and uncharged cases of ZV line elements, based on the figures drawn for the $\gamma = 1$ choice. Additionally, an inverse relationship between the spin of the spacetime and the bending angle is observed.

It is important to note that the plots for the stationary uncharged case were generated using a specific value of $p_0 = q_0 = \frac{1}{\sqrt{2}}$. Similarly, the plots for the static charged case were generated using $p = q = \frac{1}{\sqrt{2}}$.

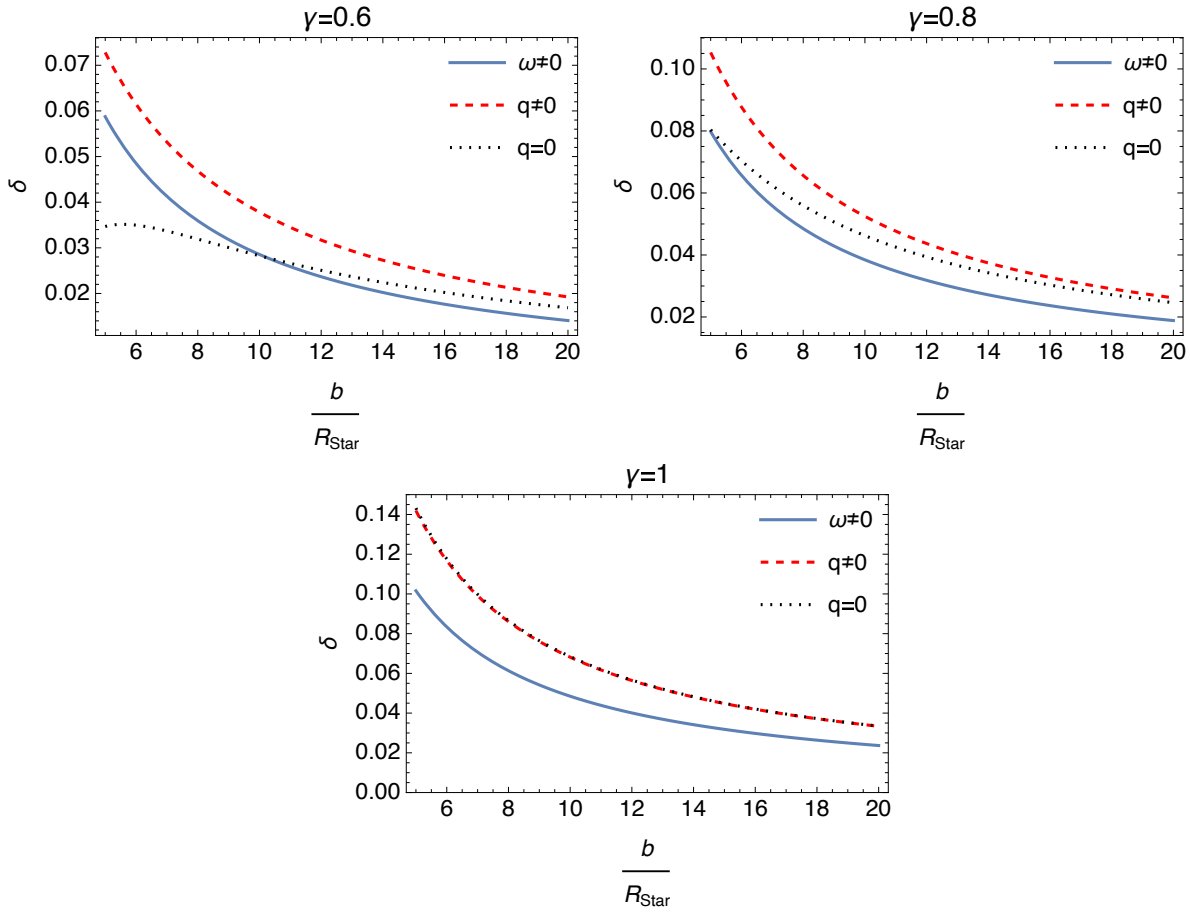

Figure 4.9: These figures represent how the bending angle δ changes with respect to b/R_{star} for 4U1538-52. Within each graph, one can notice the specific conditions $\omega \neq 0$, $q \neq 0$, and $q = 0$ are applied. These correspond to uncharged stationary, static charged and static uncharged spacetimes, respectively. The deformation parameter γ is kept fixed at each graph.

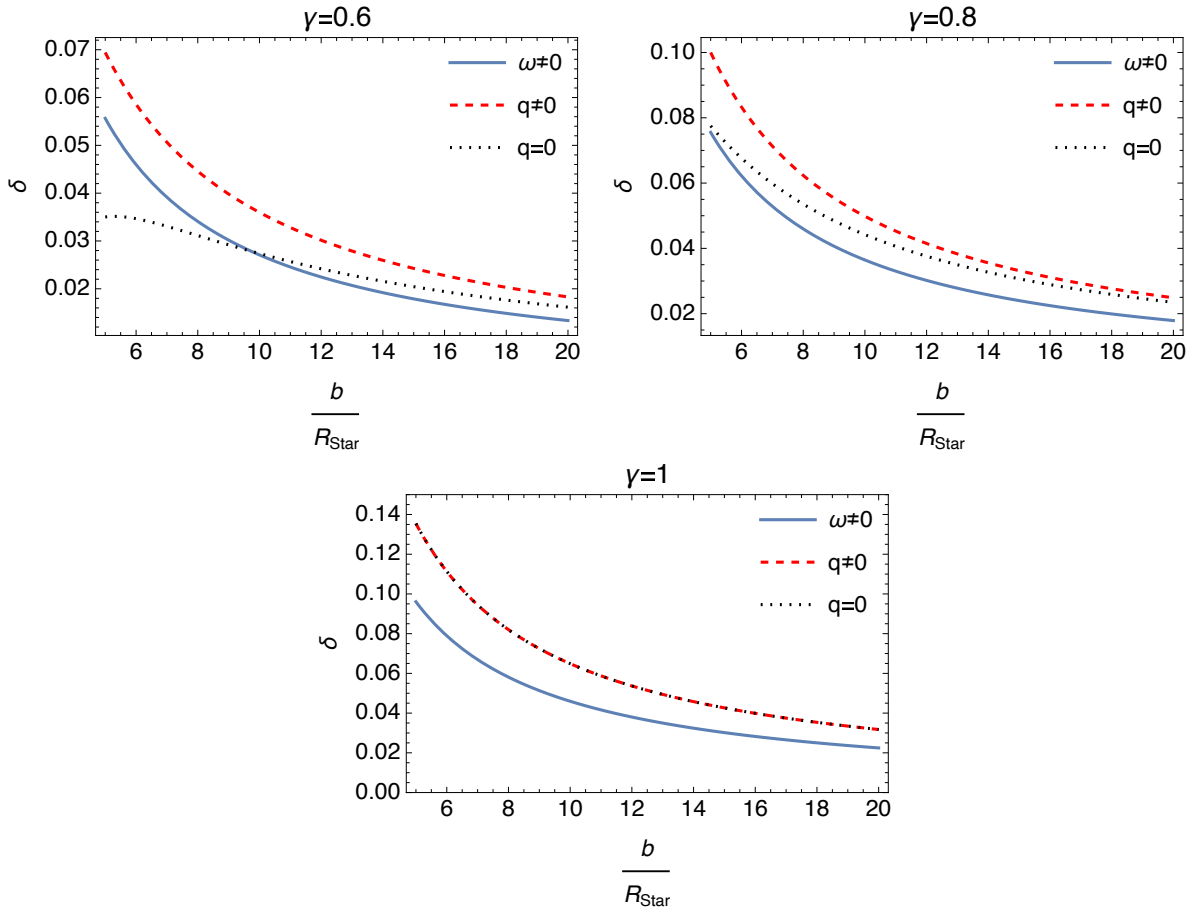

Figure 4.10: These figures represent how the bending angle δ changes with respect to b/R_{star} for HerX-1. Within each graph, uncharged stationary, static charged and static uncharged spacetimes are drawn, respectively. The deformation parameter γ is kept fixed at each graph.

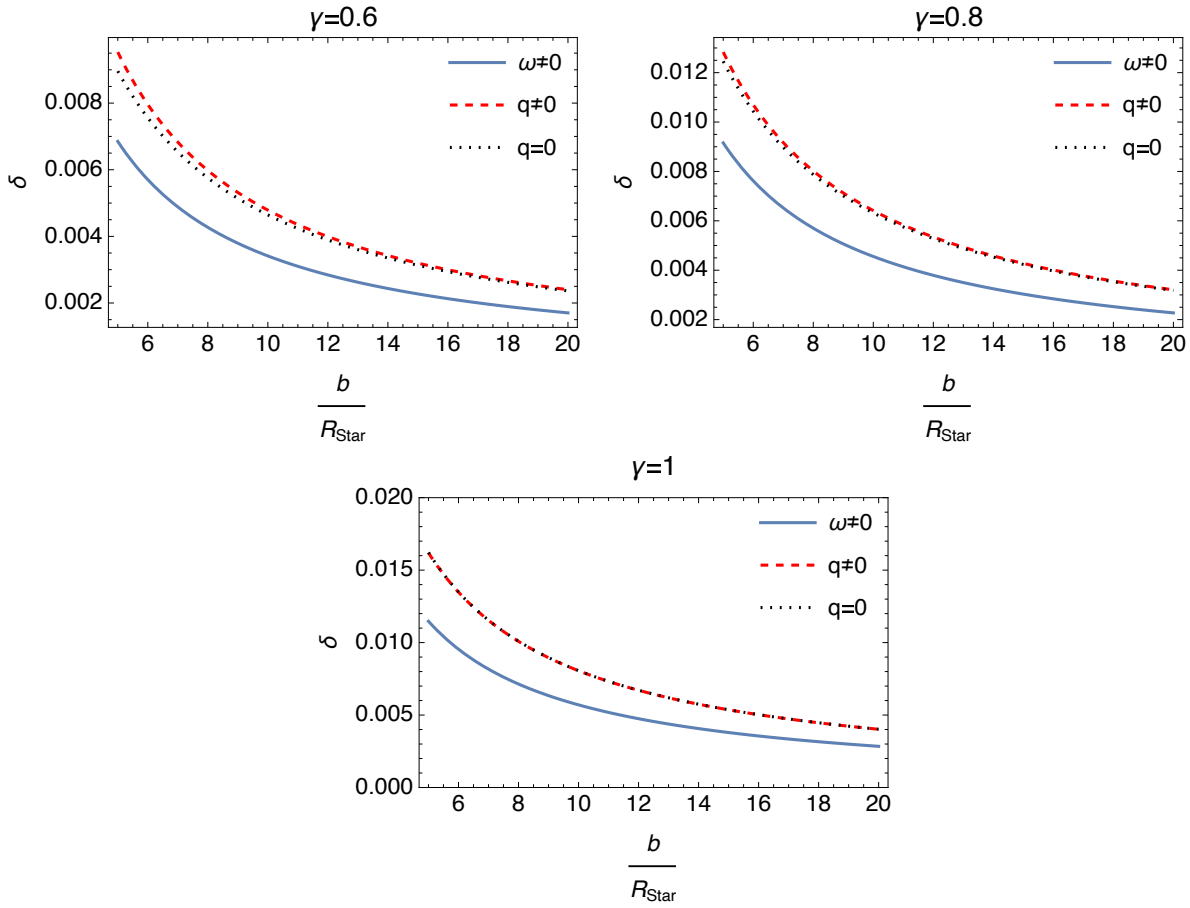

Figure 4.11: The graphs are created to depict the variation in bending angle δ with respect to b/R_{star} for the compact object SAXJ1808.4-3658. The star is analyzed under three different scenarios: uncharged stationary $(\omega \neq 0)$, static charged $(q \neq 0)$, and static uncharged $(q = 0)$. It should be noted that the bending angle for the stationary state is lower than the static cases for each specific γ value.

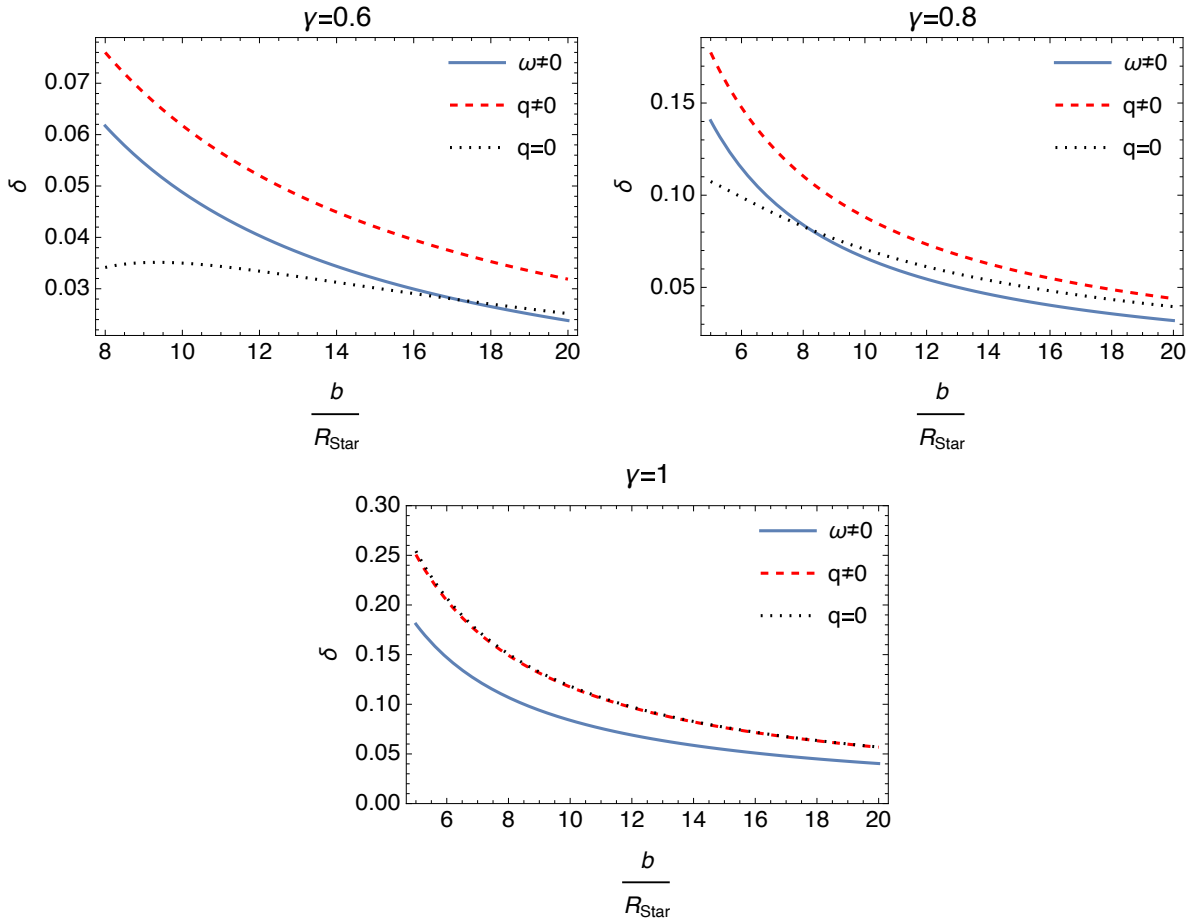

Figure 4.12: These figures represent how the bending angle δ changes with respect to b/R_{star} for VelaX-1. Within each graph, uncharged stationary, static charged and static uncharged spacetimes are drawn, respectively. The deformation parameter γ is kept fixed at each graph.

Figure 4.13 shows the role of γ on the bending angle for two different ZV cases.

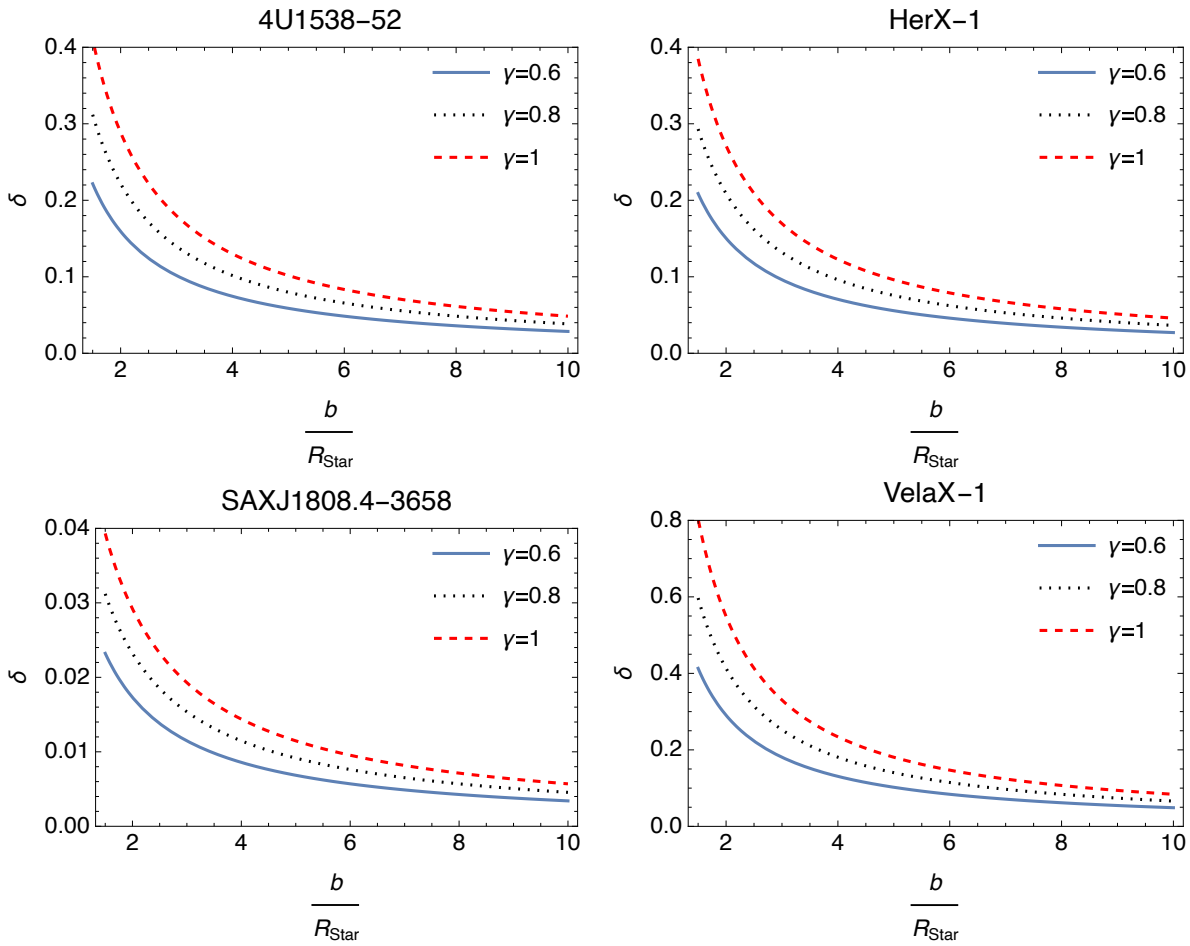

Figure 4.13: These diagrams show the graphical representations of the bending angle δ against the normalized radial distance b/R_{star}. The astronomical objects of concern are compact stars that can be found in Table 4.1. Here, the distortion parameter is not fixed and the graphs are drawn for the stationary state of the uncharged ZV line element.

The graphs are produced for different values of the deformation parameter γ. Additionally, the impact of charge is demonstrated by comparing the gravitational redshift with the uncharged scenario.

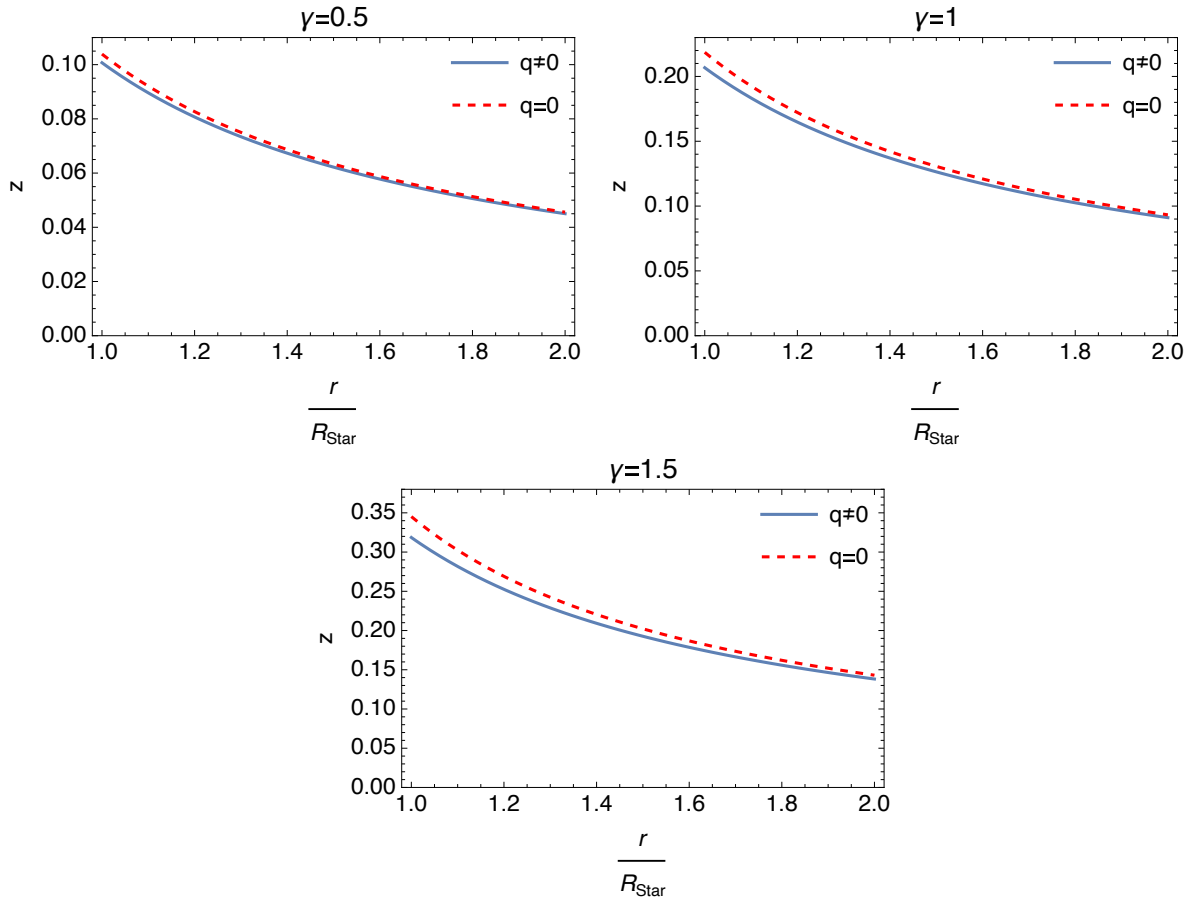

Figure 4.14: The redshift values of 4U1538-5 are drawn as a function of $\frac{r}{R_{Star}}$ with different γ values for both the static charged $(q \neq 0)$ and static uncharged $(q = 0)$ cases.

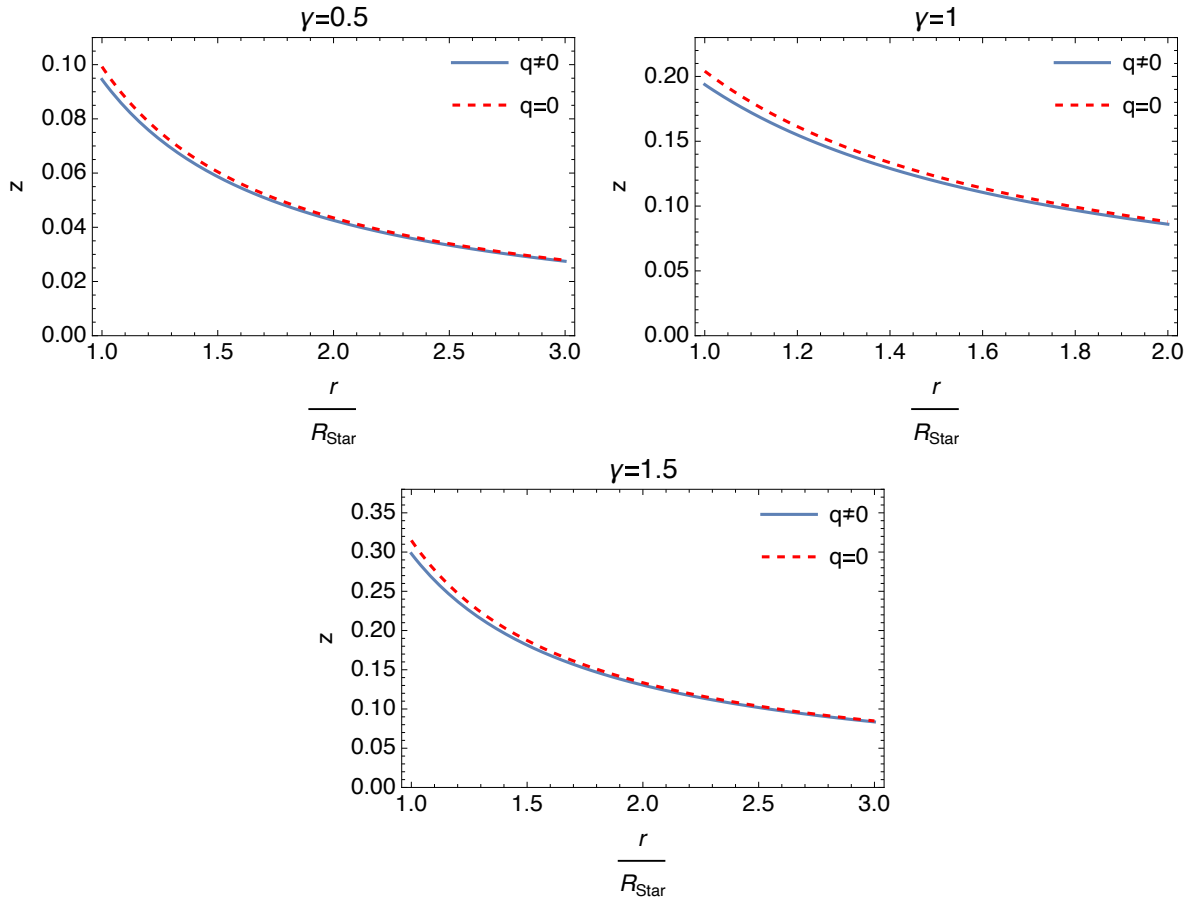

Figure 4.15: The redshift values of HerX-1 are drawn as a function of $\frac{r}{R_{Star}}$ with different γ values for both the static charged $(q \neq 0)$ and static uncharged $(q = 0)$ cases.

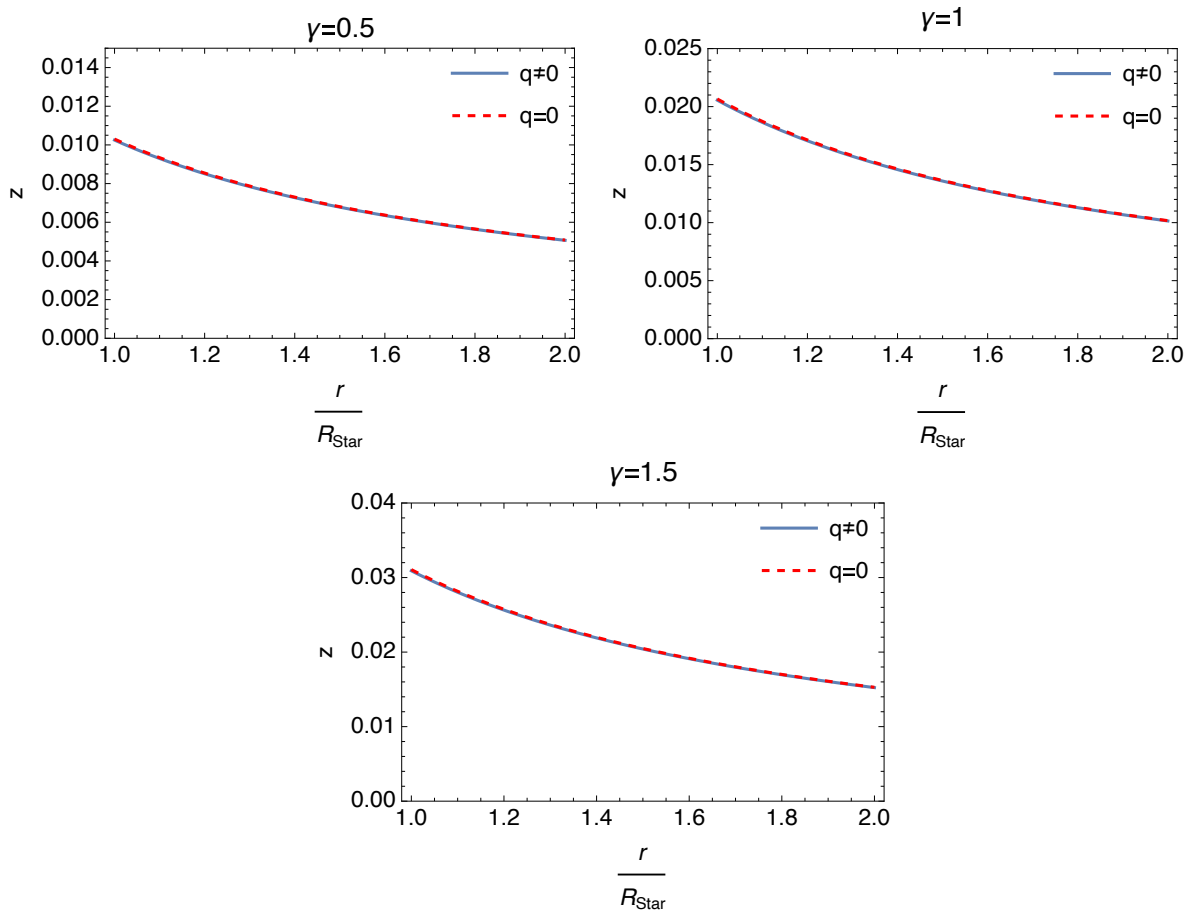

Figure 4.16: The redshift values of SAXJ1808.4-3658 are drawn as a function of $\frac{r}{R_{Star}}$ with different γ values for both the static charged $(q \neq 0)$ and static uncharged $(q = 0)$ cases.

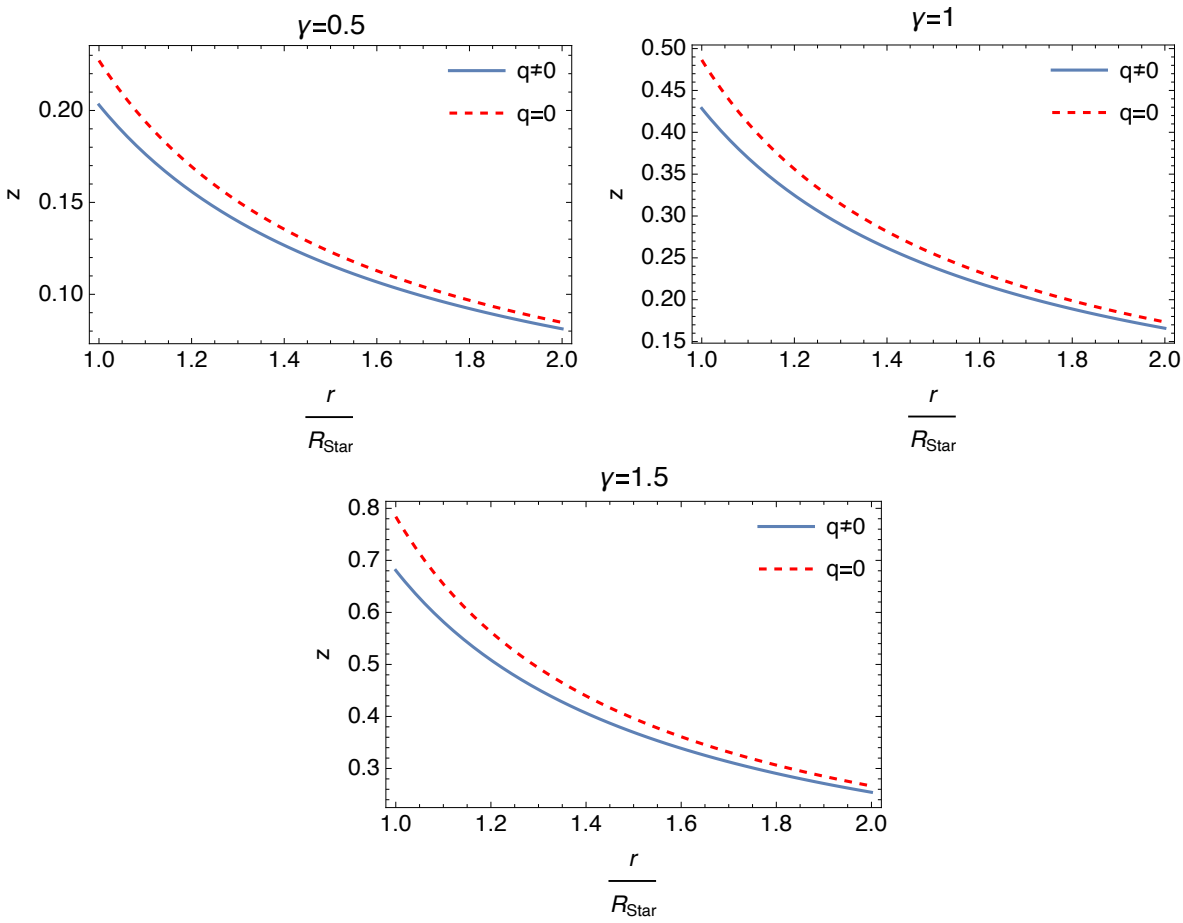

Figure 4.17: The redshift values of VelaX-1 are drawn as a function of $\frac{r}{R_{Star}}$ with different γ values for both the static charged $(q \neq 0)$ and static uncharged $(q = 0)$ cases.

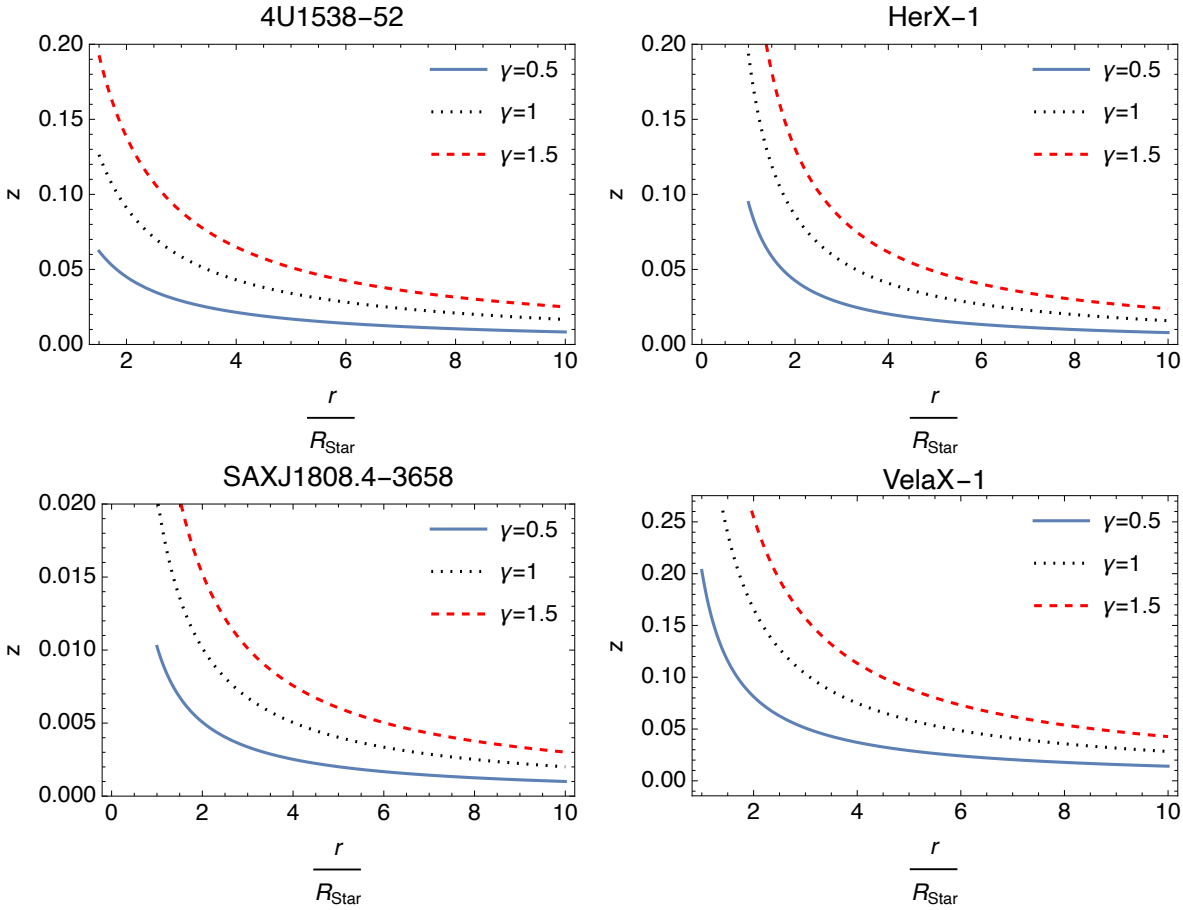

Figure 4.18: These figures illustrate how redshift z varies as a function of $\frac{r}{R_{Star}}$. The astronomical bodies chosen here can be found in Table 4.1. from the figures, one can check how γ affects z. The line element picked is the charged ZV case and we have chosen $p = q = \frac{1}{\sqrt{2}}$.

Chapter 5

SINGULARITY ANALYSIS

In this chapter, we will examine the quantum regularity of the naked singularity of the charged ZV spacetime that we found using the Ernst formalism, using the HM criterion that we defined both physically and mathematically in Chapter 2, with the aid of spinless waves [6] .

The spatial component of the massive KG equation (Eq.(2.23)) can be derived for the metric specified in Eq.(3.26) can be written as

$$\begin{aligned} A = & -K^{-4}\Delta^{2\gamma-\gamma^2+1}\Sigma^{\gamma^2-1}\frac{\partial^2}{\partial r^2}-\frac{K^{-4}\Delta^{2\gamma-\gamma^2}\Sigma^{\gamma^2-1}}{r^2 sin\theta}\frac{\partial}{\partial\theta}\left(sin\theta\frac{\partial}{\partial\theta}\right)-\frac{K^{-4}\Delta^{2\gamma-1}}{r^2\sin^2\theta}\frac{\partial^2}{\partial\varphi^2} \\ & -K^{-4}\Delta^{2\gamma-\gamma^2}\Sigma^{\gamma^2-1}\left(\frac{2\Delta}{r}+\Delta'(r)\right)\frac{\partial}{\partial r}+K^{-2}\Delta^{\gamma}\tilde{m}^2. \end{aligned} \tag{5.1}$$

By plugging in Eq.(5.1) into Eq.(2.27), we get

$$\begin{aligned} & \left[-K^{-4}\Delta^{2\gamma-\gamma^2+1}\Sigma^{\gamma^2-1}\frac{\partial^2}{\partial r^2}-\frac{K^{-4}\Delta^{2\gamma-\gamma^2}\Sigma^{\gamma^2-1}}{r^2 sin\theta}\frac{\partial}{\partial\theta}\left(sin\theta\frac{\partial}{\partial\theta}\right)-\frac{K^{-4}\Delta^{2\gamma-1}}{r^2\sin^2\theta}\frac{\partial^2}{\partial\varphi^2}\right. \\ & \left.-K^{-4}\Delta^{2\gamma-\gamma^2}\Sigma^{\gamma^2-1}\left(\frac{2\Delta}{r}+\Delta'(r)\right)\frac{\partial}{\partial r}+K^{-2}\Delta^{\gamma}\tilde{m}^2\pm i\right]\psi=0. \end{aligned} \tag{5.2}$$

If we suppose that the solution can be separated into the form of $\psi = f(r,\theta)\,e^{\pm ik\varphi}$, where k is associated with the orbital quantum number and can take any integer value, then we can rewrite Eq.(5.2) in the following manner

[6] All the analyses to be performed in this chapter have been published in [67]

$$\left[-K^{-4}\Delta^{2\gamma-\gamma^2+1}\Sigma^{\gamma^2-1}\frac{\partial^2 f}{\partial r^2}-\frac{K^{-4}\Delta^{2\gamma-\gamma^2}\Sigma^{\gamma^2-1}}{r^2 sin\theta}\frac{\partial}{\partial\theta}\left(sin\theta\frac{\partial f}{\partial\theta}\right)\pm\frac{K^{-4}\Delta^{2\gamma-1}fk^2}{r^2\sin^2\theta}\right.$$
$$\left.-K^{-4}\Delta^{2\gamma-\gamma^2}\Sigma^{\gamma^2-1}\left(\frac{2\Delta}{r}+\Delta'(r)\right)\frac{\partial f}{\partial r}+fK^{-2}\Delta^{\gamma}\tilde{m}^2\pm if\right]=0. \tag{5.3}$$

Our aim is to investigate the farthest singularity located at a distance of $r_\Delta = m(1+p)$. To accomplish this, we will limit the direction of our investigation to specific values of θ by setting $f(r,\theta_0 = constant) = R(r)$. At first, we will check the $\theta = \pi/2$ case, in which Eq.(5.3) takes the form

$$(\Delta(r)\Sigma^{-1}(r,\pi/2))^{1-\gamma^2}\left[\frac{r^2\Delta(r)}{R}\frac{d^2R}{dr^2}+\frac{r^2}{R}\left(\frac{2\Delta(r)}{r}+\Delta'(r)\right)\frac{dR}{dr}\right.$$
$$\left.-r^2K^2(r)\Delta^{\gamma^2-\gamma}(r)\Sigma^{1-\gamma^2}(r,\pi/2)\tilde{m}^2\mp ir^2K^4(r)\Delta^{\gamma^2-2\gamma}(r)\Sigma^{1-\gamma^2}(r,\pi/2)\right]\mp k^2=0. \tag{5.4}$$

In the subsequent phase, we will investigate the outermost singularity using waves that propagate along the axis of symmetry, specifically, $\theta = 0$ or $\theta = \pi$. However, in this phase, Eq.(5.3) becomes undefined for all values of k except for $k = 0$, which corresponds to the s-wave mode. To address this limitation, we will only consider the restricted condition of $k = 0$, which allows us to express Eq.(5.3) in the following form

$$\left[\frac{r^2\Delta(r)}{R}\frac{d^2R}{dr^2}+\frac{r^2}{R}\left(\frac{2\Delta(r)}{r}+\Delta'(r)\right)\frac{dR}{dr}\right.$$
$$\left.-r^2K^2(r)\Delta^{\gamma^2-\gamma}(r)\Sigma^{1-\gamma^2}(r,0)\tilde{m}^2\mp ir^2K^4(r)\Delta^{\gamma^2-2\gamma}(r)\Sigma^{1-\gamma^2}(r,0)\right]=0. \tag{5.5}$$

To verify the square integrability of the solutions of Eqs.(5.4) and (5.5) for both positive and negative signs, we calculate the squared norm, where the function space on each hypersurface Σ_t at constant time t is defined as $\mathcal{H} = \{R : \| R \| < \infty\}$. The line element describing the static spacetime in a general $(n+2)$-dimensional scenario is given by

$$ds^2 = -V^2dt^2 + h_{ij}dx^i dx^j, \tag{5.6}$$

where V is the metric function of time component. The squared norm for the generic metric is given by [30]

$$\|R\|^2 = \frac{q_0^2}{2} \int_{\Sigma_t} V^{-1} R R^* d^{n+1}x\sqrt{h}. \tag{5.7}$$

Here, q_0^2 is a positive constant and h_{ij} represents the spatial component of the line element, where h denotes the determinant of the spatial part. In this context, if neither of the solutions to Equations (5.4) and (5.5) can be integrated over all space, then the spatial operator A has a distinct self-adjoint extension.

It is crucial to highlight the function space chosen for the analysis. Our selection is the standard square integrable L^2 Hilbert space used in quantum mechanics. Alternatively, Ishibashi and Hosoya proposed the first Sobolev space H^1 [30]. However, Sobolev space differs from the conventional quantum-mechanical Hilbert space in terms of the norm definition. In Sobolev space, the norm must be square integrable for both the wave function and its derivative. On the other hand, the natural linear function space of quantum mechanics, which we employ in this study, only considers the wave function in the norm calculation. Consequently, the self-adjointness of the spatial part of the Hamiltonian operator A is subject to a stringent condition. In contrast, using Sobolev space weakens this condition by incorporating derivatives. The square-integrability of the wave function does not always guarantee that the same should hold true for its derivative [30, 32, 68].

In the subsequent subsections, we will examine the quantum nature of the non-trivial naked singularities that emerge in the charged and uncharged ZV metrics. We will study the outermost singularity on the equatorial plane, which is valid for all γ values, except for zero and one. This analysis will be followed by investigating the quantum

properties of the directional singularities that form at the poles.

5.1 Probing The Outermost Singularity at $\theta = \pi/2$ Plane

The goal of this subsection is to examine the outermost singularity at $r_\Delta = m(1+p)$, for both the charged and uncharged ZV metrics.

5.1.1 For The Charged *ZV* Solution

If we put $\theta = \pi/2$ into Eq.(5.4), Eq.(5.4) becomes

$$R'' + \frac{\left(r^2\Delta\right)'}{\Delta r^2}R' - \Delta^{\gamma^2-1}\sigma^{1-\gamma^2}\left[\pm\frac{k^2}{\Delta r^2} + K^2\Delta^{-\gamma}\tilde{m}^2 \pm iK^4\Delta^{-2\gamma}\right]R = 0, \tag{5.8}$$

in which $\Sigma(r,\pi/2) = \sigma(r) = 1 - \frac{2m}{r} + \frac{m^2}{r^2}$. We will analyse the solution to Eq.(5.8) in two distinct limiting scenarios, namely $r \to \infty$ and $r \to m(1+p)$ (in the vicinity of the singularity).

When $r \to \infty$, the metric functions exhibit the following behavior:

$$\begin{aligned} &\sigma(r) = \Delta(r) \approx 1 - \frac{2m}{r}, \\ &K \approx 2p. \end{aligned} \tag{5.9}$$

For this limiting case, Eq.(5.8) reduces to

$$R'' + \frac{2}{r}R' + \left((2p)^2\tilde{m}^2 \pm (2p)^4 i\right)R = 0. \tag{5.10}$$

The solution of the Eq.(5.10) is provided by

$$R(r) = \frac{C_1}{r}\sin\kappa r + \frac{C_2}{r}\cos\kappa r, \tag{5.11}$$

in which $\kappa = \sqrt{(2p)^2\tilde{m}^2 \pm (2p)^4 i}$ and C_1, C_2 are integration constants. By inserting Eq. (5.11) into Eq. (5.7), we obtain

$$\|R\|^2 \sim \int_{const}^{\infty} \frac{(RR^*)dr}{\left(1-\frac{2m}{r}\right)^{2\gamma-1}}. \tag{5.12}$$

For practical purposes, it is assumed that $C_1 = C_2 = 1$. To evaluate the integral, the denominator is first expanded using the binomial expansion for large values of r, considering only the dominant terms. Since $\sin(\kappa r)$ and $\cos(\kappa r)$ are complex-valued trigonometric functions, RR^* is transformed into the following form using the expression $\sqrt{a+bi} = \pm\left(\sqrt{\frac{|z|+a}{2}} + i\sqrt{\frac{|z|-a}{2}}\right)$, where $|z| = \sqrt{a^2+b^2}$,

$$\|R\|^2 \sim \int_{const}^{\infty} \frac{rcosh(2\bar{\kappa}_1 r)}{r-2m(2\gamma-1)}dr + \int_{const}^{\infty} \left(\frac{r\sin(2\bar{\kappa}_2 r)}{r-2m(2\gamma-1)}\right)dr, \tag{5.13}$$

where $\bar{\kappa}_1 = \pm\sqrt{2p\sqrt{\tilde{m}^2+(2p)^4}-2p\tilde{m}^2}$ and $\bar{\kappa}_2 = \pm\sqrt{2p\sqrt{\tilde{m}^2+(2p)^4}+2p\tilde{m}^2}$. To analyze the convergence of the first integral in Eq. (5.13), we can apply the comparison test. The hyperbolic function can be expressed as a series expansion given by

$$\cosh(2\bar{\kappa}_1 r) = \sum_{n=0}^{\infty} \frac{(2\bar{\kappa}_1 r)^{2n}}{(2n)!}. \tag{5.14}$$

The first integral can be written as

$$\begin{aligned}\int_{const}^{\infty} \frac{rcosh(2\bar{\kappa}_1 r)}{r-2m(2\gamma-1)}dr &= \int_{const}^{\infty} \left(\frac{r}{r-2m(2\gamma-1)}\right)\left\{\sum_{n=0}^{\infty}\frac{(2\bar{\kappa}_1 r)^{2n}}{(2n)!}\right\}dr \\ &= \sum_{n=0}^{\infty}\frac{(2\bar{\kappa}_1)^{2n}}{(2n)!}\int_{const}^{\infty}\left(\frac{r^b}{r-2m(2\gamma-1)}\right)dr,\end{aligned} \tag{5.15}$$

in which $b = 2n+1$. To determine the convergence behavior of the final integral, we can apply the comparison test. To do so, we examine the following inequality

$$0 \leq \frac{t+2m(2\gamma-1)}{t} \leq \frac{(t+2m(2\gamma-1))^b}{t}. \tag{5.16}$$

Here, $t = r-2m(2\gamma-1)$. We can evaluate the integral of $\frac{t+2m(2\gamma-1)}{t}$ as

$$\int_c^{\infty} \left(\frac{t+2m(2\gamma-1)}{t} \right) dt = (t+2m(2\gamma-1)\ln|t|)\,|_{const}^{\infty} \to \infty. \tag{5.17}$$

According to the comparison test, if the integral $\int_c^{\infty} \left(\frac{t+2m(2\gamma-1)}{t} \right) dt$ diverges, then the integral $\int_c^{\infty} \frac{(t+2m(2\gamma-1))^b}{t} dt$ also diverges. Additionally, we can analyze the convergence of the series in front of the integral using the ratio test. By constructing the expression $\rho = \lim_{n\to\infty} |\frac{a_{n+1}}{a_n}| = \lim_{n\to\infty} \frac{(2\bar{\kappa}_1)^2}{2n+1} = 0$ and examining the value of ρ for convergence analysis, we see that when $0 = \rho < 1$, the limit converges and hence the series converges according to the ratio test. To evaluate the second integral, which is an improper integral, we can use the comparison test. We replace $\sin(2\bar{\kappa}_2 r)$ with its power series expansion,

$$\sin(2\bar{\kappa}_2 r) = \sum_{n=0}^{\infty} (-1)^n \, sign(\bar{\kappa}_2) \frac{(2\omega_2 r)^{2n+1}}{(2n+1)!}, \tag{5.18}$$

in which $\omega_2 = \sqrt{2p\sqrt{\tilde{m}^2+(2p)^4}+2p\tilde{m}^2}$ and *sign* is the signum function. The second integral can be expressed as

$$\begin{aligned} I &= \int_{const}^{\infty} \left(\frac{r}{r-2m(2\gamma-1)} \right) \left\{ \sum_{n=0}^{\infty} (-1)^n \, sign(\bar{\kappa}_2) \frac{(2\omega_2 r)^{2n+1}}{(2n+1)!} \right\} dr \\ &= \sum_{n=0}^{\infty} (-1)^n \, sign(\bar{\kappa}_2) \frac{(2\omega_2)^{2n+1}}{(2n+1)!} \int_{const}^{\infty} \left(\frac{r^a}{r-2m(2\gamma-1)} \right) dr, \end{aligned} \tag{5.19}$$

where $a = 2n+2$. Similar to the previous calculations, applying the integral comparison test for the second integral also yields divergence. However, since $\rho = \lim_{n\to\infty} |\frac{a_{n+1}}{a_n}| = \lim_{n\to\infty} \frac{(2\omega_1)^2}{(2n+3)(2n+2)} = 0 < 1$, it is convergent according to the ratio test.

When the value of r approaches $r_\Delta = m(1+p)$, Eq. (5.8) reduces to

$$\frac{d^2R}{dr^2}+\frac{1}{r-r_\Delta}\frac{dR}{dr}-\frac{p^2}{(1+p)^2}\left[\frac{\pm k^2\Delta^{\gamma^2-2}}{r^2}+K^2\tilde{m}^2\Delta^{\gamma^2-\gamma-1}\pm iK^4\Delta^{\gamma^2-2\gamma-1}\right]R=0. \tag{5.20}$$

We will split this equation into three separate equations by taking into account the rate of change in relation to the deformation parameter γ. For this purpose, we have

$$\frac{d^2R}{dr^2}+\frac{1}{r-r_\Delta}\frac{dR}{dr}+iH_\gamma(r)R=0, \tag{5.21}$$

where

$$H_\gamma(r)=\begin{cases}\frac{\beta_1}{(r-r_\Delta)^{2-\gamma^2}} & ,0<\gamma<1/2\\ \frac{\beta_2}{(r-r_\Delta)^{1+2\gamma-\gamma^2}} & ,\gamma>1/2\\ \frac{\beta_3}{(r-r_\Delta)^{7/4}} & ,\gamma=1/2\end{cases}, \tag{5.22}$$

in which

$$\begin{aligned}\beta_1&=\frac{\pm ip^2k^2(2mp)^{\gamma^2-2}}{(1+p)^2r_\Delta^{2\gamma^2-2}}\\ \beta_2&=\pm\left(\frac{2p}{1+p}\right)^{4\gamma}\frac{p^2(1+p)^2(2mp)^{\gamma^2-2\gamma-1}}{r_\Delta^{2\gamma^2-4\gamma-2}}\\ \beta_3&=\frac{p^2r_\Delta^{7/4}}{(2mp)^{7/4}}\left[(1+p)^4\left(\frac{2p}{1+p}\right)^{4\gamma}\mp\frac{k^2}{m^2(1+p)^2)}\right].\end{aligned} \tag{5.23}$$

The solutions of Eq. (5.21) for each interval are

$$R(r)=\begin{cases}a_1K_0(\eta_1(r-r_\Delta)^{\gamma^2/2})+(a_2)_0F_1(;1;\eta_2(r-r_\Delta)^{\gamma^2}) & ,0<\gamma<1/2\\ a_3K_0(\eta_3(r-r_\Delta)^{\frac{\gamma^2-2\gamma+1}{2}})+(a_4)_0F_1(;1;\eta_4(r-r_\Delta)^{\gamma^2-2\gamma+1}) & ,\gamma>1/2\\ a_5K_0(\eta_5(r-r_\Delta)^{1/8})+(a_6)_0F_1(;1;\eta_6(r-r_\Delta)^{1/4}) & ,\gamma=1/2\end{cases} \tag{5.24}$$

In this equation, a_1 through a_6 represent integration constants, K_0 refers to the first

kind modified Bessel function, ${}_0F_1$ refers to the confluent hypergeometric function, $\eta_1 = \frac{2(-1)^{7/4}\sqrt{\beta_1}}{\gamma^2}$, $\eta_2 = \frac{-i\beta_1}{\gamma^4}$, $\eta_3 = \frac{2(-1)^{3/4}\sqrt{\beta_2}}{2\gamma-1-\gamma^2}$, $\eta_4 = \frac{-i\beta_2}{(2\gamma-1-\gamma^2)^2}$, $\eta_5 = 8\sqrt{\beta_3}$ and $\eta_6 = -16\beta_3$.

The square norm for each case can be written as

$$\|R\|^2 \sim \begin{cases} \left(\frac{2p}{1+p}\right)^{4\gamma} \frac{p^{2-2\gamma^2}(1+p)^{2\gamma^2-1}}{(2mp)^{2\gamma-\gamma^2} r_\Delta^{2\gamma^2-4\gamma-2}} \int_{const}^{r_\Delta} \frac{RR^* dr}{(r-r_\Delta)^{2\gamma-\gamma^2}} & ,0<\gamma<1/2 \\ \left(\frac{2p}{1+p}\right)^{4\gamma} \frac{p^{2-2\gamma^2}(1+p)^{2\gamma^2-1}}{(2mp)^{-2\gamma+\gamma^2} r_\Delta^{2\gamma^2-4\gamma-2}} \int_{const}^{r_\Delta} (r-r_\Delta)^{\gamma^2-2\gamma} RR^* dr & ,\gamma>1/2 \\ \left(\frac{2p}{1+p}\right)^{2} \frac{p^{3/2}(1+p)^{-1/2} r_\Delta^{7/2}}{(2mp)^{3/4}} \int_{const}^{r_\Delta} \frac{RR^* dr}{(r-r_\Delta)^{3/4}} & ,\gamma=1/2 \end{cases} \tag{5.25}$$

To conduct the integration operation, the content of RR^* for each integral in Eq. (5.25) is expressed by using the series expansion of each respective special function, as described in [69],

$$\begin{aligned} I_0(z) &= \sum_{k=0}^{\infty} \frac{\left(\frac{z}{2}\right)^{2k}}{(k!)^2}, \\ K_0(z) &= -ln\frac{z}{2} I_0(z) + \sum_{k=0}^{\infty} \frac{(z)^{2k}}{2^{2k}(k!)^2} \psi(k+1), \\ {}_0F_1(;b;z) &= \sum_{k=0}^{\infty} \frac{(z)^k}{(b)_k k!}, \end{aligned} \tag{5.26}$$

where ψ is the psi function. To evaluate the integrals near the singularity ($r \to r_\Delta$), the variable of integration is changed to $u = r - r_\Delta$. As a result, the new variable u becomes very small. Since the integrand involves the multiplication of power series, we can utilize the Cauchy product law of power series to perform an analytic calculation of these integrals. Moreover, since u is small, we can approximate the dominant term as $K_0(z) \sim -ln\frac{z}{2} I_0(z)$. Let us define the Cauchy product that we will use below.

Definition 5.1 (The Cauchy Product of Power Series): Consider the power series

$\sum_{n=0}^{\infty} a_n z^n$, and $\sum_{n=0}^{\infty} b_n z^n$. Thus, the Cauchy product of these series can be defined as

$$\left(\sum_{n=0}^{\infty} a_n z^n\right)\left(\sum_{n=0}^{\infty} b_n z^n\right) = \sum_{n=0}^{\infty}\left(\left(\sum_{j=0}^{n}\left(a_j b_{n-j}\right)\right) z^n\right) = \sum_{n=0}^{\infty} c_n z^n, \tag{5.27}$$

in which $c_n = \sum_{j=0}^{n} a_j b_{n-j}$ [70].

To simplify the analysis, we set the integration constants a_1 through a_6 equal to 1. By using the Cauchy product of power series, we can perform analytic calculations of the integrals.

FirstIy, we analyze the integral for which the deformation parameter lies within the range of $0 < \gamma < 1/2$. The corresponding square norm can be written as

$$\begin{aligned}\|R\|^2 \sim & \alpha_1 \sum_{k=0}^{\infty} c_k \int_{const}^{0} \left(ln^2 \frac{\eta_1 u^{\gamma^2/2}}{2}\right)\left(\frac{\eta_1 u^{\gamma^2/2}}{2}\right)^k \frac{du}{u^{2\gamma-\gamma^2}} \\ & + \alpha_1 \sum_{l=0}^{\infty} c_l \int_{const}^{0} \left(\eta_2 u^{\gamma^2}\right)^l \frac{du}{u^{2\gamma-\gamma^2}} \\ & - 2\alpha_1 \sum_{n=0}^{\infty} c_n \int_{const}^{0} \left(ln \frac{\eta_1 u^{\gamma^2/2}}{2}\right)\left(u^{\gamma^2}\right)^n \frac{du}{u^{2\gamma-\gamma^2}},\end{aligned} \tag{5.28}$$

where $\alpha_1 = \left(\frac{2p}{1+p}\right)^{4\gamma} \frac{p^{2-2\gamma^2}(1+p)^{2\gamma^2-1}}{(2mp)^{2\gamma-\gamma^2} r_+^{2\gamma^2-4\gamma-2}}$, $c_k = \sum_{l=0}^{k} \frac{1}{(l!(k-l)!)^2}$, $c_l = \sum_{t=0}^{l} \frac{1}{(1)_t t! (1)_{l-t}(l-t)!}$ and $c_n = \sum_{j=0}^{n} \left\{\left(\frac{\eta_1}{2}\right)^j \frac{1}{(j!)^2}\right\}\left\{\frac{(\eta_2)^{n-j}}{(1)_{n-j}(n-j)!}\right\}$.

The first and third integrals are both convergent, as shown by the expressions

$$\int_c^0 x^k ln(bx) dx = \frac{c^{1+k}(1-(1+k)\ln[bc])}{(1+k)^2} \tag{5.29}$$

and

$$\int_c^0 x^k ln^2(bx) dx = -\frac{c^{1+k}(2+(1+k)\ln[bc](-2+(1+k)\ln[bc]))}{(1+k)^3}, \tag{5.30}$$

which are both finite. The convergence of the second integral can be established by using the comparison test. For this purpose, u is very small and positive, the following inequality can be defined as

$$u^{\gamma^2 l-(2\gamma-\gamma^2)} \leq u^{-(2\gamma-\gamma^2)}. \tag{5.31}$$

Furthermore, since $\int_{const}^{0} u^{-(2\gamma-\gamma^2)}du = \frac{u^{(\gamma-1)^2}}{(\gamma-1)^2}\big|_{const}^{0} < \infty$, it follows that the integral $\int_{const}^{0} u^{\gamma^2 l-(2\gamma-\gamma^2)}du$ also converges. Therefore, for $0<\gamma<1/2$, the solution is square integrable and the spacetime singularity remains quantum singular.

Moving on, let us examine the scenario where $\gamma > 1/2$ but not equal to 1. In this instance, the square norm takes

$$\begin{aligned}\|R\|^2 \sim & \alpha_2 \sum_{k=0}^{\infty} c_k \int_{const}^{0} \left(ln^2 \frac{\eta_3 u^{\gamma^2-2\gamma+1}}{2}\right)\left(\frac{\eta_3 u^{\gamma^2-2\gamma+1}}{2}\right)^k u^{\gamma^2-2\gamma}du \\ & + \alpha_2 \sum_{l=0}^{\infty} c_l \int_{const}^{0} \left(\eta_4 u^{\gamma^2-2\gamma+1}\right)^l u^{\gamma^2-2\gamma}du \\ & - 2\alpha_2 \sum_{n=0}^{\infty} c_n \int_{const}^{0} \left(ln\frac{\eta_3 u^{\gamma^2-2\gamma+1}}{2}\right)\left(u^{\gamma^2-2\gamma+1}\right)^n u^{\gamma^2-2\gamma}du\end{aligned} \tag{5.32}$$

in which $\alpha_2 = \left(\frac{2p}{1+p}\right)^{4\gamma} \frac{p^{2-2\gamma^2}(1+p)^{2\gamma^2-1}}{(2mp)^{-2\gamma+\gamma^2} r_+^{2\gamma^2-4\gamma-2}}$. The first and third integrals exhibit a close resemblance to the previous case and thus converge. As for the second integral, we can evaluate it using the expression $\int_{const}^{0} u^{l(\gamma-1)^2+(\gamma^2-2\gamma)}du = \frac{u^{(l+1)(\gamma-1)^2}}{(l+1)(\gamma-1)^2}|_{const}^{0}$, which can be shown to be square integrable. Hence, the spacetime singularity is quantum mechanically singular as long as $1/2<\gamma<1$.

Lastly, we will examine the scenario where $\gamma = 1/2$. In this case, the square norm equation can be written as

$$\begin{aligned}\|R\|^2 \sim & \alpha_3 \sum_{k=0}^{\infty} c_k \int_{const}^{0} \left(ln^2 \frac{\eta_5 u^{1/8}}{2} \right) \left(\frac{\eta_5 u^{1/8}}{2} \right)^k \frac{du}{u^{3/4}} \\ & + \alpha_3 \sum_{l=0}^{\infty} c_l \int_{const}^{0} \left(\eta_6 u^{1/4} \right)^l \frac{du}{u^{3/4}} \\ & - 2\alpha_3 \sum_{n=0}^{\infty} c_n \int_{const}^{0} \left(ln \frac{\eta_5 u^{1/8}}{2} \right) \left(u^{1/4} \right)^n \frac{du}{u^{3/4}}.\end{aligned} \tag{5.33}$$

Here, $\alpha_3 = \left(\frac{2p}{1+p}\right)^2 \frac{p^{3/2}(1+p)^{-1/2} r_+^{7/2}}{(2mp)^{3/4}}$. Similar to the prior situations, the first and third integrals are square integrable for the case when $\gamma = 1/2$. The second integral can be evaluated using the comparison test. To do this, we establish the following inequality

$$u^{l/4-3/4} \leq u^{-3/4}. \tag{5.34}$$

Using this inequality, we can show that $\int_{const}^{0} u^{l/4-3/4} du$ is also square integrable. Specifically, we can evaluate this integral as $\int_{const}^{0} u^{-3/4} du = 4u^{1/4} \left|_{const}^{0} \right\langle \infty$. As a result, the spacetime singularity is quantum mechanically singular for $\gamma = 1/2$.

5.1.2 The Uncharged *ZV* Solution

If we set q to zero and apply a scaling factor of $t \to 2t$ to the time coordinate, we can express Eq. (5.4) in the following form

$$R'' + \frac{\left(r^2 \Delta_{zv}\right)'}{\Delta_{zv} r^2} R' - \Delta_{zv}^{\gamma^2 - 1} \sigma_{zv}^{1-\gamma^2} \left[\frac{\pm k^2}{\Delta_{zv} r^2} + \Delta_{zv}^{-\gamma} \tilde{m}^2 \pm i \Delta_{zv}^{-2\gamma} \right] R = 0, \tag{5.35}$$

where $\Delta_{zv} = 1 - \frac{2m}{r}$, $\sigma_{zv} = 1 - \frac{2m}{r} + \frac{m^2}{r^2}$ and "$\prime$" denotes the derivation with respect to r. We will analyze the solution to Eq. (5.35) separately in two limits: as r approaches infinity, and as r approaches the singularity at $r = 2m$.

When $r \to \infty$ and using the approximate metric functions provided in Eq. (5.9), Eq. (5.35) becomes simplified to

$$R'' + \frac{2}{r}R' + \left(\tilde{m}^2 \pm i\right) R = 0. \tag{5.36}$$

The solutions of Eq. (5.36) is

$$R(r) = \frac{C_5}{r}\sin \nu r + \frac{C_6}{r}\cos \nu r, \tag{5.37}$$

in which $\nu = \sqrt{\tilde{m}^2 \pm i}$ and C_5, C_6 are integration constants. Given that the solution obtained is analogous to the solution derived in Eq. (5.11), it is clear that it is non-square integrable.

When considering the scenario where $r \to 2m$, a new variable x can be introduced, defined by $x \equiv r - 2m \to 0$. Subsequently, the metric functions can be represented in terms of this new variable as

$$\begin{aligned} \sigma_{zv}(x) &= \frac{x}{x+2m} + \frac{m^2}{(x+2m)^2}, \\ \Delta_{zv}(x) &= \frac{x}{x+2m}. \end{aligned} \tag{5.38}$$

By inserting the metric functions outlined previously into the differential equation (5.35), and by considering the leading terms while also taking into account the varying range of the parameter γ, the differential equation (5.35) can be transformed into

$$R'' + \frac{1}{x}R' + ax^{\mu}R = 0, \tag{5.39}$$

where

$$ax^{\mu} = \begin{cases} \pm i(4m^2)^{\gamma}\left(\frac{2}{m}\right)^{\gamma^2-1} x^{\gamma^2-2\gamma-1} & ,\frac{1}{2} < \gamma < \infty \ \ and \ \ \gamma \neq 1 \\ \left(\frac{2}{m}\right)^{\gamma^2-1}\left(\frac{k^2}{2m}\right) x^{\gamma^2-2} & ,0 < \gamma < \frac{1}{2} \\ \left(\frac{2}{m}\right)^{\gamma^2-1}\left(\pm i(4m^2)^{\gamma} \pm \frac{k^2}{2m}\right) x^{-7/2} & ,\gamma = \frac{1}{2} \end{cases} \tag{5.40}$$

The general solution of Eq. (5.39) can be written as

$$R(x) = C_7 J_0\left(\frac{2\sqrt{a}sign(\mu+1)}{\mu+2} x^{\frac{\mu+2}{2}}\right) + C_8 Y_0\left(\frac{2\sqrt{a}sign(\mu+1)}{\mu+2} x^{\frac{\mu+2}{2}}\right). \tag{5.41}$$

It should be noted that C_7 and C_8 represent constants of integration, while J and Y denote the Bessel functions of the first and second kinds, respectively. Additionally, the signum function $sing(\mu+1)$ is also present in the expression. The properties of the Bessel functions as x approaches 0 for real $\nu \geq 0$ are described in [71] as

$$\begin{aligned} J_{\nu}(x) &\sim \frac{1}{\Gamma(\nu+1)}\left(\frac{x}{2}\right)^{\nu} \\ Y_{\nu}(x) &\sim \begin{cases} \frac{2}{\pi}\left[ln\left(\frac{x}{2}\right) + \tilde{\gamma}\right] & ,\nu = 0 \ and \ \tilde{\gamma} \cong 0.5772 \\ -\frac{\Gamma(\nu)}{\pi}\left(\frac{2}{x}\right)^{\nu} & ,\nu \neq 0 \end{cases} \end{aligned} \tag{5.42}$$

Consequently, the solution can be expressed as

$$R(x) \sim \bar{C}_1 + \bar{C}_2 ln(x), \tag{5.43}$$

where $\bar{C}_1 = \frac{C_7}{\Gamma(1)} + \frac{2\tilde{\gamma}C_8}{\pi} + \frac{2C_8}{\pi} ln\left(\frac{\sqrt{a}sing(\mu+1)}{\mu+2}\right)$ and $\bar{C}_2 = \frac{C_8}{\pi}(\mu+2)$. If we substitute Eq. (5.43) into the squared norm (5.7), Eq. (5.7) becomes

$$\begin{aligned} \|R\|^2 &\sim (m)^{2\gamma-\gamma^2+2}(2)^{\gamma^2+2\gamma} \int_{const.}^{0} x^{\gamma^2-2\gamma} |\bar{C}_1 + \bar{C}_2 ln(x)|^2 dx \\ &\sim (m)^{2\gamma-\gamma^2+2}\left\{A\int_{const.}^{0} x^{\gamma^2-2\gamma}dx + B\int_{const.}^{0} x^{\gamma^2-2\gamma} ln(x)dx + C\int_{const.}^{0} x^{\gamma^2-2\gamma} ln^2(x)dx\right\} \end{aligned} \tag{5.44}$$

in which $A = (2)^{\gamma^2+2\gamma}\bar{C_1}^2$, $B = (2)^{\gamma^2+2\gamma+1}\bar{C_1}\bar{C_2}$ and $C = (2)^{\gamma^2+2\gamma}\bar{C_2}^2$. The spatial component of the Hamiltonian operator A is not essentially self-adjoint for the following reasons: Firstly, the results of integrals are dependent on terms of the form $x^a ln^b(x)$. Secondly, $lim_{x\to 0} x^a ln^b(x)$ is convergent for $a > 0$. Finally, the square norm converges only when $\gamma \neq 1$.

To sum up we can draw the conclusion that we have not found any quantum mechanical healing for $\theta = \pi/2$ direction for both ZV cases.

5.2 Quantum Singularities on The North-Pole $(\theta = 0)$:

The direction dependence of singularities is important for ZV solution. We know that the solution regularity depends on the distortion parameter. Some important symmetry directions can be noted as the north and south poles in which $\theta = 0$ and $\theta = \pi$, respectively. We indicate the quantum probe of outermost singularity $r_\Delta = m(1+p)$ from the north pole.

5.2.1 For The Charged *ZV* Solution:

As previously mentioned, directional singularities along the symmetry axis will only be studied using s-waves. In this specific scenario, where $k = 0$, Eq.(5.5) can be expressed as

$$R'' + \frac{\left(r^2\Delta\right)'}{\Delta r^2}R' - K^2\left[\Delta^{-\gamma}\tilde{m}^2 \pm iK^2\Delta^{-2\gamma}\right]R = 0. \tag{5.45}$$

Let us begin by examining the situation where $r \to \infty$. In this case, we use the approximate metric functions described in Eq.(5.9) and Eq.(5.45), resulting in the following expression

$$R'' + \frac{2}{r}R' + \left((2p)^2\tilde{m}^2 \pm (2p)^4 i\right)R = 0. \tag{5.46}$$

Eq.(5.46) is identical to Eq.(5.10), which has already been analyzed and determined to have a divergent square norm. As a result, the spatial wave operator is not square integrable.

Let us now analyze the scenario where $r \to r_\Delta = m(1+p)$. By focusing on the dominant terms in relation to the value of γ, Eq.(5.45) can be expressed as

$$\frac{d^2R}{dr^2} + \frac{1}{r-r_\Delta}\frac{dR}{dr} + U_\gamma(r)R = 0, \tag{5.47}$$

where

$$U_\gamma(r) = \frac{ib_2}{(r-r_\Delta)^{2\gamma}}, \tag{5.48}$$

in which $b_2 = \pm(1+p)^4 \left(\frac{2p}{1+p}\right)^{4\gamma} \frac{r_\Delta^{4\gamma}}{(2mp)^{2\gamma}}$.

The solution of Eq.(5.47) can be written as

$$R(r) = d_3 K_0(\nu_1 (r-r_\Delta)^{1-\gamma}) + (d_4)_0F_1(;1;\nu_2(r-r_\Delta)^{2-2\gamma}), \tag{5.49}$$

where $\nu_1 = \frac{\sqrt{b_2}(-1)^{3/4}}{\gamma-1}$ and $\nu_2 = \frac{-ib_2}{4(\gamma-1)^2}$. The square norm becomes

$$\|R\|^2 \sim \left(\frac{2p}{1+p}\right)^{4\gamma} (1+p)^4 (2mp)^{2\gamma-1} r_\Delta^{4\gamma} \int_{const}^{r_\Delta} \frac{RR^* dr}{(r-r_\Delta)^{2\gamma-1}}. \tag{5.50}$$

Here, d_3 and d_4 are taken to be one for simplicity of calculations. By substituting the variable of integration with $u = r - r_\Delta$ and utilizing the fact that u approaches zero in the proximity of $r \to r_\Delta$, the integrals are evaluated. If we use the Cauchy product as in the previous case, the square norm can be written as

$$\begin{aligned}\|R\|^2 \sim & \bar{\alpha}_2 \sum_{k=0}^{\infty} c_k \int_{const}^{0} \left(ln^2 \frac{\nu_1 u^{1-\gamma}}{2} \right) \left(\frac{\nu_1 u^{1-\gamma}}{2} \right)^k \frac{du}{u^{2\gamma-1}} \\ & + \bar{\alpha}_2 \sum_{l=0}^{\infty} c_l \int_{const}^{0} \left(\nu_2 u^{2-2\gamma} \right)^l \frac{du}{u^{2\gamma-1}} \\ & - 2\bar{\alpha}_2 \sum_{n=0}^{\infty} c_n \int_{const}^{0} \left(ln \frac{\nu_1 u^{1-\gamma}}{2} \right) \left(u^{2-2\gamma} \right)^n \frac{du}{u^{2\gamma-1}}\end{aligned} \tag{5.51}$$

in which $\bar{\alpha}_2 = \left(\frac{2p}{1+p} \right)^{4\gamma} (1+p)^4 (2mp)^{2\gamma-1} r_{\Delta}^{4\gamma}$. Due to the significance of the power of u in the analysis, we divide the deformation parameter γ into two distinct subcategories: $0 < \gamma < 1$ and $\gamma > 1$. It is worth noting that the other components comprising the ln function are also convergent, as demonstrated in the previous section.

Let us begin by analyzing the scenario where $0 < \gamma < 1$. In this situation, the power of u, which is $(1-\gamma)$, is consistently positive. As u is both positive and exceedingly small, we can establish the inequality $u^{2l(1-\gamma)-(2\gamma-1)} \leq u^{-(2\gamma-1)}$. Since the integral $\int_{const}^{0} u^{1-2\gamma} du = \frac{u^{2-2\gamma}}{2-2\gamma} \left| const^0 \right\rangle \infty$ is convergent, the integral $\int const^0 u^{2l(1-\gamma)-(2\gamma-1)} du$ is also convergent, as required by the comparison test. Consequently, when the deformation parameter falls within the interval of $0 < \gamma < 1$, the directional singularities along the axis transform into quantum singularities.

Let us now turn our attention to the case where $\gamma > 1$. Here, $(1-\gamma)$ is negative, and the comparison test inequality can be expressed as $u^{-(2\gamma-1)} \leq u^{2l(1-\gamma)-(2\gamma-1)}$. Upon careful examination, it is revealed that for $\gamma > 1$, the integral $\int_{const}^{0} u^{1-2\gamma} du = \frac{u^{2-2\gamma}}{2-2\gamma} |_{const}^{0} \to \infty$ fails to be square integrable. The solution came out to be classically regular for $\gamma \geq 2$ and quantum regular when $\gamma > 1$.

5.2.2 For The Uncharged *ZV* Solution

When $q = 0$, Eq.(5.45) becomes

$$R'' + \frac{\left(r^2\Delta_{zv}\right)'}{\Delta_{zv}r^2}R' - \left[\Delta_{zv}^{-\gamma}\tilde{m}^2 \pm i\Delta_{zv}^{-2\gamma}\right]R = 0. \tag{5.52}$$

When $r \to \infty$ Eq.(5.52) transforms into

$$R'' + \frac{2}{r}R' + \left(\tilde{m}^2 \pm i\right)R = 0. \tag{5.53}$$

This equation is identical to Eq.(5.10), for which it has been shown that the solution is not square integrable.

Now, we consider the case of $r \to 2m \Leftrightarrow x \equiv r - 2m \to 0$. If we substitute the metric functions into Eq.(5.53), Eq.(5.53) reduces to

$$R'' + \frac{1}{x}R' + bx^{-2\gamma}R = 0, \tag{5.54}$$

where $b = \pm i(4m^2)^{\gamma}$. The solution of Eq.(5.54) is

$$R(x) = q_3 J_0\left(\frac{2\sqrt{b}sign(1-2\gamma)}{2-2\gamma}x^{1-\gamma}\right) + q_4 Y_0\left(\frac{2\sqrt{b}sign(1-2\gamma)}{2-2\gamma}x^{1-\gamma}\right), \tag{5.55}$$

in which q_3 and q_4 are integration constants. If we employ the asymptotic approximations of the Bessel functions as given in Eq.(5.42), then Eq.(5.55) can be simplified to

$$R(x) \sim \bar{q_3} + \bar{q_4}ln(x). \tag{5.56}$$

Here, $\bar{q_3} = \frac{q_3}{\Gamma(1)} + \frac{2\tilde{\gamma}q_4}{\pi} + \frac{2q_4}{\pi}ln\left(\frac{\sqrt{b}sing(1-2\gamma)}{2-2\gamma}\right)$ and $\bar{q_4} = \frac{q_4}{\pi}(2-2\gamma)$. The squared norm for solution (5.56) can be written as

$$\begin{aligned} \|R\|^2 &\sim (2m)^{2\gamma+1}\int_{const.}^{0} x^{1-2\gamma}|\bar{q_3} + \bar{q_3}ln(x)|^2 dx \\ &\sim \bar{A}\int_{const.}^{0} x^{1-2\gamma}dx + \bar{B}\int_{const.}^{0} x^{1-2\gamma}ln(x)dx + \bar{C}\int_{const.}^{0} x^{1-2\gamma}ln^2(x)dx \end{aligned} \tag{5.57}$$

in which $\bar{A} = (2m)^{2\gamma+1}\,\bar{q_3}^2$, $\bar{B} = (2m)^{2\gamma+1}\,\bar{q_3}\bar{q_4}$ and $\bar{C} = (2m)^{2\gamma+1}\,\bar{q_4}^2$. Due to the $x^a ln^b(x)$ terms in the last two integrals being proportional, with $b = 1,2$, the limit of $lim_{x\to 0} x^a ln^b(x)$ is finite. Additionally, since $\gamma \neq 1$, the square norm of the solution converges, indicating quantum mechanical singularity. It has also been found that the solution is not square integrable for $\gamma > 1$. For the choice $\gamma < 1$ on the other hand, the square-integrability condition is satisfied.

Based on this analysis, the classically singular region within the directional singularity of the uncharged ZV metric, specifically within the range $1 < \gamma < 2$, is transformed into a quantum mechanically regular region.

Finally, Fig.5.1 summarizes the results of quantum probes made from the equatorial plane and north pole, respectively, in ZV spacetime with and without charge.

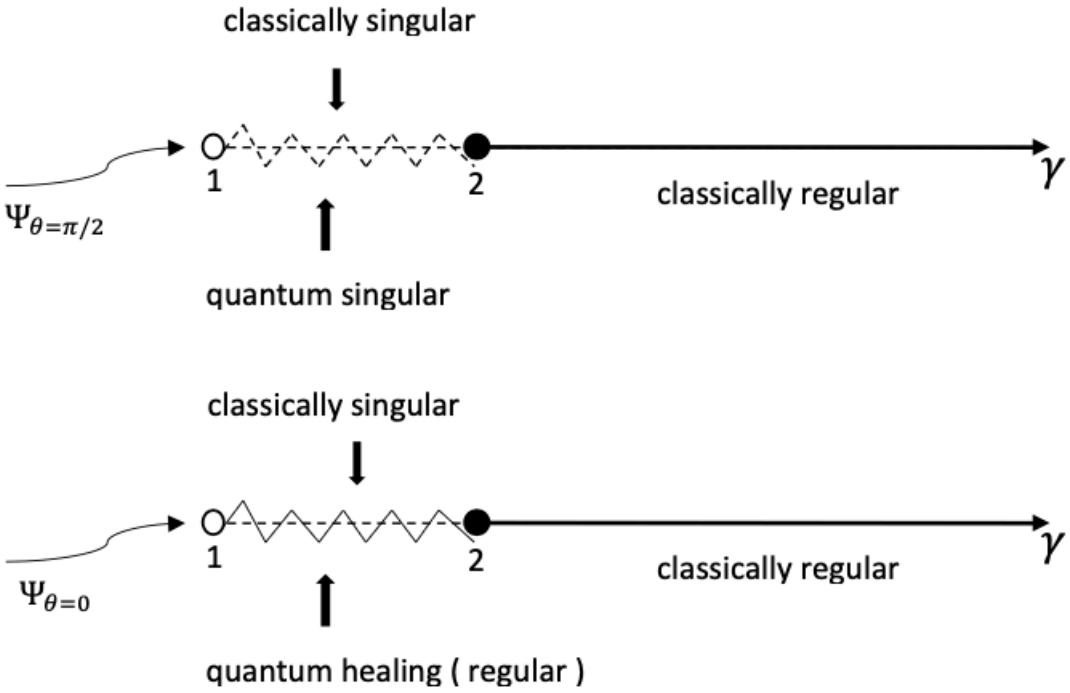

Figure 5.1: As shown in Figure 5.1, spinless waves sent from the equatorial plane $(\theta = \pi/2)$ and the north pole $(\theta = 0)$ to both charged and uncharged ZV spacetimes do not generate quantum regularity in the equatorial plane $(\theta = \pi/2)$ in both ZV spacetimes. However, s-waves sent from the north pole $(\theta = 0)$ generate regularity in the region $1 < \gamma < 2$, which is classically singular, in both ZV spacetimes.

Chapter 6

KERR-NEWMAN (ANTI) DE SITTER (KN(A)dS) SPACETIME

This section is about gravitational lensing analysis via RI approach in a non-AF KNAdS spacetime. It is aimed to use the theoretically evaluated bending angle formulae for two different black holes. [7]

6.1 The Briefly Mathematical and Physical Structures of Kerr-Newman (anti) de Sitter (KN(A)dS) Spacetime

The corresponding metric in the Boyer-Lindquist coordinates is given by [73]

$$ds^2 = -\frac{\Delta_r}{\rho^2}\left(dt - \frac{a\sin^2\theta}{\Xi}d\varphi\right)^2 + \frac{\Delta_\theta \sin^2\theta}{\rho^2}\left(adt - \frac{r^2+a^2}{\Xi}d\varphi\right)^2 + \rho^2\left(\frac{dr^2}{\Delta_r} + \frac{d\theta^2}{\Delta_\theta}\right), \tag{6.1}$$

in which

$$\begin{aligned} &\rho^2 = r^2 + a^2\cos^2\theta, \quad \Delta_\theta = 1 - \frac{a^2}{l^2}\cos^2\theta, \quad \Xi = 1 - \frac{a^2}{l^2}, \\ &\Delta_r = \left(r^2+a^2\right)\left(1+\frac{r^2}{l^2}\right) - 2mr + e^2. \end{aligned} \tag{6.2}$$

Here, the parameter a represents rotation, while e and m denote charge and mass, respectively. The curvature radius, l, is determined by $\Lambda = -3l^{-2}$ [73, 74]. The mass M and angular momentum L of the KN(A)dS can be calculated using Komar integrals with the assistance of Killing vectors ∂_t/Ξ and ∂_ϕ [75]. By referencing AdS space as the background, one can derive

[7] The material of this chapter was published in [72]

$$M = \frac{m}{\Xi^2}, \quad L = \frac{am}{\Xi^2}. \tag{6.3}$$

It is possible to also figure out the charge of KNAdS line element via finding the em field tensor flux for $r \to \infty$ [76] as

$$Q_e = \frac{e}{\Xi}. \tag{6.4}$$

The Einstein-Maxwell field equations are satisfied by the metric ((6.1)) when coupled with the em vector potential (1-form) given by

$$A_t = -\frac{er}{\rho^2}, \quad A_\varphi = \frac{ae\sin^2\theta}{\rho^2\Xi}, \tag{6.5}$$

where A_φ is angular component of the em vector potential. Alternatively, one could verify that the em potential produces the resultant field strength tensor: In addition, the vierbein fields [74] for the metric (6.1) may be defined by

$$\begin{aligned} \mathrm{e}^0 &= \frac{\sqrt{\Delta_r}}{\rho}\left(\mathrm{d}t - \frac{a\sin^2\theta}{\Xi}\mathrm{d}\varphi\right), \quad \mathrm{e}^1 = \frac{\rho}{\sqrt{\Delta_r}}\,\mathrm{d}r, \\ \mathrm{e}^2 &= \frac{\rho}{\sqrt{\Delta_\theta}}\mathrm{d}\theta, \quad \mathrm{e}^3 = \frac{\sqrt{\Delta_\theta}\sin\theta}{\rho}\left(a\,\mathrm{d}t - \frac{r^2+a^2}{\Xi}\mathrm{d}\varphi\right). \end{aligned} \tag{6.6}$$

Alternatively, it is possible to verify that the em potential equation (6.5) produces the resultant field strength tensor as

$$F = \frac{e\left(\rho^2 - 2r^2\right)}{\rho^4}\left(dt - \frac{a\sin^2\theta}{\Xi}d\varphi\right)\wedge dr + \frac{era\sin 2\theta}{\rho^4}\left(adt - \frac{r^2+a^2}{\Xi}d\varphi\right)\wedge d\theta, \tag{6.7}$$

on the other hand

$$F = \frac{e\left(\rho^2 - 2r^2\right)}{\rho^4}(\mathrm{e}^0\wedge\mathrm{e}^1) - \frac{2era\cos\theta}{\rho^4}(\mathrm{e}^2\wedge\mathrm{e}^3). \tag{6.8}$$

To determine the magnetic fields generated by the KN(A)dS spacetime, one may calculate the non-zero contravariant components of the em field tensor:

$$F^{tr} = \frac{e\left(r^2+a^2\right)}{\rho^6}\left(2r^2-\rho^2\right), \quad F^{t\theta} = -\frac{ea^2 r}{\rho^6}\sin 2\theta,$$
$$F^{r\varphi} = \frac{ea\left(2r^2-\rho^2\right)}{\rho^6}\Xi, \qquad F^{\theta\varphi} = \frac{2ear}{\rho^6}\Xi\cot\theta. \tag{6.9}$$

The magnetic field elements of the KN(A)dS solution can be extracted from equation (6.9) by employing the subsequent formula, as cited in references [77, 78]:

$$B_\mu = \frac{1}{2}E_{\mu\nu\alpha\tau}u^\nu F^{\alpha\tau} \tag{6.10}$$

in which u^ν represents the 4-velocity vector and the covariant Levi-Civita tensor (Riemannian volume form) is defined by $E_{\mu\nu\alpha\tau} \equiv |g|^{1/2}\varepsilon_{\mu\nu\alpha\tau}$ with $\varepsilon_{tr\theta\phi} = +1$ [79, 80]. To sum up, the non-zero components of the magnetic fields can be written as

$$B_r = \frac{2ear\left(r^2+a^2\right)\cos\theta}{\rho^4\Delta_r}. \tag{6.11}$$

$$B_\theta = \frac{eal^2\left(\rho^2-2r^2\right)\sin\theta}{\rho^4(a^2\cos^2\theta-l^2)}, \tag{6.12}$$

in which the net magnetic field relation: $B = \sqrt{B_r^2+B_\theta^2}$. It is important to highlight that the formulas describing the magnetic and electric field components in the Kerr-Newman spacetime with the inclusion of the cosmological constant for a zero-angular-momentum observer (ZAMO) were derived in Ref. [81]. When the cosmological constant Λ is extremely small and the detector is located far away from the black hole, such that $a << r$, Eq. (6.11) can be approximated as

$$B_r \approx \frac{2ea\cos\theta}{r^3} + \frac{4eam\cos\theta}{r^4} + O\left(\frac{1}{r^5}\right), \tag{6.13}$$

where this simplification leads to the radial component of the magnetic field in the Kerr-Newmann solution, as described in the Ref. [82]. It is important to mention that the Biot-Savart law in electrodynamics states that a charged particle with mass m and charge e moving in a circular orbit with angular momentum $\vec{L}$ possesses the magnetic dipole moment given by

$$\vec{\mu} = \mathcal{X}\frac{e\vec{L}}{2m}, \tag{6.14}$$

in which $\mathcal{X}$ is the gyromagnetic moment [82]. The magnetic dipole moment $\vec{\mu}$ can be written as

$$\vec{B} = \frac{3\left(\vec{\mu}\cdot\vec{e}_r\right)\vec{e}_r - \vec{\mu}}{r^3}. \tag{6.15}$$

Consequently, the radial component of this field can be expressed as $B_r = \vec{B}\cdot\vec{e}r = 2\vec{\mu}\cdot\vec{e}r/r^3$. By comparing the leading-order term of the radial magnetic field derived from Eq. (6.13) with the expression given in Eq. (6.15), we obtain

$$\vec{\mu} = e\vec{a} = \frac{e\vec{L}}{m} = 2\frac{e\vec{L}}{2m}. \tag{6.16}$$

Note that, $\mathcal{X} = 2$ for the charged slow-rotating KN(A)dS spacetime.

The (positive) roots of the metric function $\Delta_r = 0$ gives the horizons of metric (6.1). Therefore, the horizons are found by [74]

$$\begin{aligned}\Delta_r &= \left(r^2+a^2\right)\left(1-\frac{1}{3}\Lambda r^2\right) - 2mr + e^2 \\ &= -\frac{1}{3}\Lambda\left[r^4 - \left(\frac{3}{\Lambda}-a^2\right)r^2 + \frac{6M}{\Lambda}r - \frac{3}{\Lambda}\left(a^2+e^2\right)\right] \\ &= -\frac{1}{3}\Lambda\left(r-r_{++}\right)\left(r-r_{--}\right)\left(r-r_{+}\right)\left(r-r_{-}\right) = 0,\end{aligned} \tag{6.17}$$

in which the roots r_{++} and r_{--} form a pair of complex conjugates, while r_+ and

r_- are two distinct positive real roots, where r_+ is greater than r_-. As a result, the value $r = r_+$ corresponds to the event horizon. Also, the Hawking temperature of the KN(A)dS space time can be written as

$$T_H = \frac{3r_+^4 + \left(a^2+\ell^2\right) r_+^2 - \ell^2\left(a^2+e^2\right)}{4\pi\ell^2 r_+\left(r_+^2+a^2\right)}. \tag{6.18}$$

6.1.1 Gravitational Lensing in KN(A)*d*S Spacetime

The generic light ray equation of metric (2.35) can be written as

$$\frac{d^2u}{d\varphi^2} = 2u^3\kappa(u) + \frac{u^4}{2}\frac{d\kappa(u)}{du}, \tag{6.19}$$

where $u = \frac{1}{r}$ and $\kappa(u)$ is given by

$$\kappa(u) = \frac{g^2(r) + p(r)f(r)}{h(r)\left[g(r)E + f(r)L\right]^2}\left[p(r)E^2 - f(r)L^2 - 2g(r)LE\right], \tag{6.20}$$

in which E and L are the energy and angular momentum of photon, respectively.

If we put the metric function in (6.1) into the generic null geodesic equation formula Eq. (6.19), Eq. (6.19) reduces to

$$\frac{d^2u}{d\varphi^2} + \beta u = \frac{3Mu^2}{\alpha^2} - \frac{2e^2u^3}{\alpha^2}, \tag{6.21}$$

in which $\beta = -\frac{\Lambda a^2}{3\alpha^2} + \frac{L+Ea}{\alpha^2(L-Ea)}$ and $\alpha = 1 + \frac{1}{3}\Lambda a^2$.

By using the linear solution of Eq. (6.21) as $u = \frac{\sin(\sqrt{\beta}\varphi)}{R}$, where R denotes the impact parameter, an approximate solution can be obtained. Upon substituting this solution into Eq. (6.21), the approximate solution of the differential equation is derived as

$$\begin{aligned} u(\varphi) = \frac{\sin(\sqrt{\beta}\varphi)}{R} + \frac{1}{4R^3}\Bigg\{\Big(\left(1+\cos^2(\sqrt{\beta}\varphi)\right)4MR + e^2\Bigg(\frac{3\varphi\cos(\sqrt{\beta}\varphi)}{\sqrt{\beta}\alpha^2} \\ - \frac{sin(\sqrt{\beta}\varphi)\cos^2(\sqrt{\beta}\varphi)}{\beta\alpha^2} - \frac{2\sin(\sqrt{\beta}\varphi)}{\beta\alpha^2}\Bigg)\Bigg\}. \end{aligned} \tag{6.22}$$

And, Eq. (2.38) gives

$$A(r,\varphi) = \frac{r^2}{4R^3}\left\{4MR\sqrt{\beta}\sin(2\sqrt{\beta}\varphi) + e^2\left(\frac{\cos^3(\sqrt{\beta}\varphi)}{\sqrt{\beta}\alpha^2} - \frac{sin(2\sqrt{\beta}\varphi)sin(\sqrt{\beta}\varphi)}{\sqrt{\beta}\alpha^2}\right.\right.$$
$$\left.\left.\frac{3\varphi\sin(\sqrt{\beta}\varphi)}{\alpha^2} - \frac{cos(\sqrt{\beta}\varphi)}{\sqrt{\beta}\alpha^2}\right)\right\} - \frac{r^2}{R}\sqrt{\beta}cos(\sqrt{\beta}\varphi). \tag{6.23}$$

In order to analyze the influence of the black hole model's geometry and physical parameters (such as charge, mass, and spin) on the equation for the closest approach distance, denoted as r_0, an analysis is conducted at $\varphi = \pi/2$. Subsequently, the reciprocal of the closest approach distance is evaluated as

$$\frac{1}{r_0} = \frac{sin(\sqrt{\beta}\pi/2)}{R} + \frac{1}{4R^3}\left\{\left((1+cos^2(\sqrt{\beta}\pi/2)\right)4MR + \right.$$
$$\left. e^2\left(\frac{3\pi cos(\sqrt{\beta}\pi/2)}{2\sqrt{\beta}\alpha^2} - \frac{sin(\sqrt{\beta}\pi/2)cos^2(\sqrt{\beta}\pi/2)}{\beta\alpha^2} - \frac{2sin(\sqrt{\beta}\pi/2)}{\beta\alpha^2}\right)\right\}. \tag{6.24}$$

In order for being able to check astrophysical applications of our results, let us investigate what happens for $\varphi = 0$. For the cases when $\frac{M}{R} << 1$ and $\Lambda R^2 << 1$ [41, 83, 84], the radial coordinate and its first derivative with respect to φ can be written as

$$r \approx \frac{\beta\alpha^2 R^2}{2M}, \qquad A(r,\varphi=0) \approx -r^2\frac{\sqrt{\beta}}{R}. \tag{6.25}$$

Then, Eq. (2.39) gives

$$\tan\varepsilon = \tan\Psi_0 \simeq \frac{2M}{\beta^{3/2}\alpha^3 R}\left\{1 - \frac{\beta^2\alpha^5 R^4\Lambda}{12M^2} - \frac{4M^2}{\alpha^2\beta R^2} - \frac{a^2\Lambda}{3}\left[1+\frac{2}{3\alpha^2}\right]\right.$$
$$\left. + \frac{4M^2}{\beta^2\alpha^4 R^4}\left[a^2 + e^2 + \frac{2a^2}{\alpha^2} - \frac{2a^4\Lambda}{3\alpha^2} - \frac{2a^4\Lambda}{3\beta^2}\right]\right\}^{1/2}. \tag{6.26}$$

When we apply the standard approximate expansion of square root, Eq. (6.26) reduces to

$$\tan\varepsilon = \tan\Psi_0 \simeq \frac{2M}{\beta^{3/2}\alpha^3 R}\left\{1-\frac{\beta^2\alpha^5 R^4\Lambda}{24M^2}-\frac{2M^2}{\alpha^2\beta R^2}-\frac{a^2\Lambda}{6}\left[1+\frac{2}{3\alpha^2}\right]\right.$$
$$\left.+\frac{2M^2}{\beta^2\alpha^4 R^4}\left[a^2+e^2+\frac{2a^2}{\alpha^2}-\frac{2a^4\Lambda}{3\alpha^2}-\frac{2a^4\Lambda}{3\beta^2}\right]\right\}+O\left(\frac{M^9a^4}{\alpha^{19}\beta^{19/2}R^{17}}\right). \tag{6.27}$$

Note that, If $a \to 0$, Eq.(6.27) gives the same result for the linear case in [65].

At this stage, it is necessary to decide how to handle the parameter β. As evident from Eq. (6.21), this dimensionless parameter contains information about the propagation of light rays through the spacetime under consideration. By using the definition of the impact parameter and considering $R \equiv L/E$ [85], we can express β as

$$\beta = -\frac{\Lambda a^2}{3\alpha^2}+\frac{R+a}{R-a}. \tag{6.28}$$

Now, we explore significant astrophysical implementations. We conduct a numerical examination to observe the impact of electric charge in the presence of a cosmological constant by analyzing the bending angles obtained for different rotation limits, denoted as $j\ (=ac^2/GM)$. The numerical analysis is specifically focused on two black holes, and their respective characteristics are documented in [72].

In our numerical analysis, we adopt $\varphi = 0$ as the reference point for measuring the one-sided bending angle. This reference point corresponds to a significantly large distance from the source. We plot the bending angle ε as a function of $x = R/R_*$, where R_* represents the radius of the charged compact star. It is worth noting that we convert the geometrized units to standard international units (SI units). The mass (M) and electric charge (Q) are converted to SI units by multiplying the mass by Gc^{-2} and the charge by $G^{1/2}c^{-2}\left(4\pi\varepsilon_0\right)^{-1/2}$. Here, $G = 6.67408\times10^{-11}m^3kg^{-1}s^{-2}$ denotes

the gravitational constant, $c = 3 \times 10^8 ms^{-1}$ represents the speed of light, and $\varepsilon_0 = 8.85418 \times 10^{-12} C^2 N^{-1} m^2$ corresponds to the free space permittivity. Consequently, the one-sided bending angle is measured in radians.

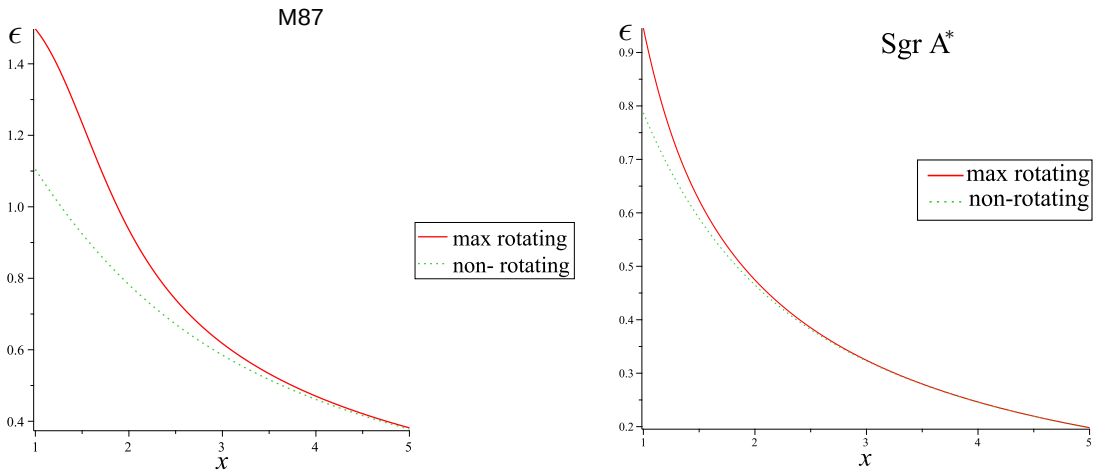

Figure 6.1: The plots illustrate the bending angles ε as a function of $x = R/R_*$ for both the $M87$ and $Sgr\ A^*$ black holes. In the case of $Sgr\ A^*$, the graphs are generated assuming a mass of $4.1 \times 10^6 M_\odot$. The Schwarzschild radius is taken as $1.27 \times 10^{10} m$, and the charge is approximately $10^{15} C$. For the $M87$ black hole, the graphs are plotted based on a mass of $6.5 \times 10^9 M_\odot$, an observable radius of $16.8 Mpc$, and a tidal charge of $9.35 \times 10^{22} C$. Additionally, as mentioned earlier, $j = 1$ represents the maximum-rotation scenario, while $j = 0$ corresponds to the non-rotating case.

Chapter 7

CONCLUSION

In this thesis, we have used the Ernst formalism to generate the Maxwell extensions of ZV metrics. The *ZV* metrics are known to arise from the interaction of aligned, static rods [86]. However, our approach surpasses the concept of finite rods and explores the realm of infinite plane waves. By exploiting the symmetry in this limit, we are able to discover additional exact solutions using the power of the Ernst formalism. It is worth mentioning that the relationship between the two dimensional colliding wave spacetime and the three dimensional spherical coordinates can be viewed as a holographic manifestation.

Furthermore, it is important to emphasize that our study also paves the way for transforming the infinite class of EM solutions with the second polarization [55] into the ZV space, as we have demonstrated in this paper. This transformation will also involve the spinning of the source.

Regarding non-spherical, charged compact objects, the obtained solution (3.26) is significant for astrophysical implications. The observable universe indicates that most planets and stellar objects possess magnetic fields. Our Earth, for instance, possesses a relatively weak magnetic field on the order of $B \sim 0.5G$, which is nonetheless crucial for supporting life. Similarly, most of other planets exhibit magnetic fields that are either stronger or weaker than the Earth's. On the other hand, gravastars possess extremely high magnetic fields on the order of $\sim 10^{14}G$. When we combine the

existence of these magnetic fields with the non-spherical topology of planets/stars, we naturally encounter the case of the charged *ZV* metric. This metric is characterized by three parameters: m, q, and γ. For $\gamma > 1$, the object is oblate; whereas for $\gamma < 1$, it is prolate. Notably, the spherically symmetric *RN* solution is obtained at $\gamma = 1$, and its uniqueness dictates that any other class of *EM* solutions must agree at $\gamma = 1$ as well. The source of our metric can be purely electric or purely magnetic. The motion of test particles in the effective potential has been investigated for both cases. Combining electric and magnetic fields in a more realistic scenario, which requires a separate study, can further enhance our understanding. Furthermore, in the calculation of the Newtonian potential in the charged ZV spacetime, the charge contributed to the quadrupole moment, along with the contribution of the dipole moment and singularity analysis resulted in the charge shifting the ZV singularity.

Gravitational lensing analysis was performed in this thesis as an astrophysical application, utilizing the GB theorem with the aid of geodesic analysis in the equatorial plane, based on compact objects with known physical parameters. The effect of the geometric deformation parameter on the lensing of charged ZV and uncharged ZV, as well as stationary ZV spacetimes, was investigated using the limit obtained. Additionally, the gravitational redshift value was calculated in the charged ZV spacetime.

To use the CX theorem, is investigated the stationary charged ZV spacetime and the expansions of all metric functions and EM potentials of this new solution are up to the quadrupole moment term. Moreover, it is observed that the stationary solution reduces to the charged ZV, ZV, RN, and Schwarzschild limits under certain conditions.

In this theses, the possibility of traversing backward in time within our newfound universe is contemplated. However, it is important to emphasize that this speculation is limited to our physical realm alone, as the preservation of chronological order should prohibit such a phenomenon within the context of biological time.

After performing a quantum probe using two different directions of scalar waves on the ZV charged singularity located beyond the outermost regions of ZV spacetime, it has been observed that quantum healing is direction dependent in both spacetimes. It is found that only in the $\theta = 0$ plane and $0 < \gamma < 1$ range, both solutions, which are classically singular, are quantum mechanically regular for s-wave mode.

Finally, in the lensing analysis performed using the RI method in the well known non-spherically symmetric KN(A)DS spacetime, the general lensing formula obtained has been calculated in the limit where rotation and charge are zero, matching the expression found by RI in the Schwarzschild-de Sitter spacetime. This derived general formula has been applied to $M87$ and $Sgr\,A^*$ black holes to investigate the effect of rotation on gravitational lensing. The astrophysical analyse confirmed the theoretical prediction that rotation enhances the lensing effect. Additionally, it is observed that the impact of the cosmological constant on lensing is quite small in this analysis, depending on the chosen value.

REFERENCES

[1] T. Gangopadhyay, S. Ray, X.-D. Li, J. Dey, and M. Dey, "Strange star equation of state fits the refined mass measurement of 12 pulsars and predicts their radii," *Monthly Notices of the Royal Astronomical Society*, vol. 431, no. 4, pp. 3216–3221, 2013.

[2] O. Gurtug, M. Mangut, and M. Halilsoy, "Gravitational lensing in rotating and twisting universes," *Astroparticle Physics*, vol. 128, p. 102558, 2021.

[3] K. Schwarzschild, "Über das gravitationsfeld eines massenpunktes nach der einsteinschen theorie," *Sitzungsberichte der königlich preussischen Akademie der Wissenschaften*, pp. 189–196, 1916.

[4] H. Weyl, "Zur gravitationstheorie," *Annalen der physik*, vol. 359, no. 18, pp. 117–145, 1917.

[5] K. Schwarzschild, "On the gravitational field of a mass point according to einstein's theory," *Gen. Relativ. Gravit*, vol. 35, no. 5, pp. 951–959, 2003.

[6] H. Weyl, "The theory of gravitation," *Annalen Phys*, vol. 54, p. 117, 1917.

[7] D. M. Zipoy, "Topology of some spheroidal metrics," *Journal of Mathematical Physics*, vol. 7, no. 6, pp. 1137–1143, 1966.

[8] B. Voorhees, "Static axially symmetric gravitational fields," *Physical Review D*, vol. 2, no. 10, p. 2119, 1970.

[9] E. T. Newman, E. Couch, K. Chinnapared, A. Exton, A. Prakash, and R. Torrence, "Metric of a rotating, charged mass," *Journal of mathematical physics*, vol. 6, no. 6, pp. 918–919, 1965.

[10] W. Israel, "Event horizons in static vacuum space-times," *Physical review*, vol. 164, no. 5, p. 1776, 1967.

[11] B. Carter, "Hamilton-jacobi and schrodinger separable solutions of einstein's equations," *Communications in Mathematical Physics*, vol. 10, pp. 280–310, 1968.

[12] J. F. Plebanski and M. Demianski, "Rotating, charged, and uniformly accelerating mass in general relativity," *Annals of Physics*, vol. 98, no. 1, pp. 98–127, 1976.

[13] F. Kottler, "Über die physikalischen grundlagen der einsteinschen gravitationstheorie," *Annalen der Physik*, vol. 361, no. 14, pp. 401–462, 1918.

[14] B. Carter, "Black hole equilibrium states in c dewitt and bs dewitt, eds, black holes: Les astres occlus," 1973.

[15] M. Misra, "Some axially symmetric empty gravitational fields," *Proc. Nat. Acad. Sci. India*, vol. Sect. A 26, pp. 673–680, 1960.

[16] F. J. Ernst, "New formulation of the axially symmetric gravitational field problem," *Physical Review*, vol. 167, no. 5, p. 1175, 1968.

[17] Ö. Gurtug, H. Mustafa, and M. Mangut, "The charged zipoy–voorhees metric with astrophysical applications," *The European Physical Journal C*, vol. 82, no. 8, p. 671, 2022.

[18] K. Destounis, G. Huez, and K. D. Kokkotas, "Geodesics and gravitational waves in chaotic extreme-mass-ratio inspirals: the curious case of zipoy-voorhees black-hole mimickers," *General Relativity and Gravitation*, vol. 55, no. 6, p. 71, 2023.

[19] B. Narzilloev, D. Malafarina, A. Abdujabbarov, and C. Bambi, "On the properties of a deformed extension of the nut space-time," *The European Physical Journal C*, vol. 80, pp. 1–11, 2020.

[20] F. W. Dyson, A. S. Eddington, and C. Davidson, "Ix. a determination of the deflection of light by the sun's gravitational field, from observations made at the total eclipse of may 29, 1919," *Philosophical Transactions of the Royal Society of London. Series A, Containing Papers of a Mathematical or Physical Character*, vol. 220, no. 571-581, pp. 291–333, 1920.

[21] A. Einstein, "Lens-like action of a star by the deviation of light in the gravitational field," *Science*, vol. 84, no. 2188, pp. 506–507, 1936.

[22] K. P. Rauch and R. D. Blandford, "Optical caustics in a kerr spacetime and the origin of rapid x-ray variability in active galactic nuclei," *Astrophysical Journal, Part 1 (ISSN 0004-637X), vol. 421, no. 1, p. 46-68*, vol. 421, pp. 46–68, 1994.

[23] R. V. Pound and G. A. Rebka Jr, "Apparent weight of photons," *Physical review*

letters, vol. 4, no. 7, p. 337, 1960.

[24] J. L. Greenstein and M. Schmidt, "The quasi-stellar radio sources 3c 48 and 3c 273." *Astrophysical Journal, vol. 140, p. 1*, vol. 140, p. 1, 1964.

[25] F. Ernst, "New formulation of the axially symmetric gravitational field problem ii," *Physical Review*, vol. 168, no. 5, p. 1415, 1968.

[26] A. Papapetrou, "Eine rotationssymmetrische lösung in der allgemeinen relativitätstheorie," *Annalen der Physik*, vol. 447, no. 4-6, pp. 309–315, 1953.

[27] T. Lewis, "Some special solutions of the equations of axially symmetric gravitational fields," *Proceedings of the Royal Society of London. Series A, Containing Papers of a Mathematical and Physical Character*, vol. 136, no. 829, pp. 176–192, 1932.

[28] G. Ellis and B. Schmidt, "Classification of singular space-times," *General Relativity and Gravitation*, vol. 10, pp. 989–997, 1979.

[29] R. Penrose, "Gravitational collapse and space-time singularities," *Physical Review Letters*, vol. 14, no. 3, p. 57, 1965.

[30] A. Ishibashi and A. Hosoya, "Who's afraid of naked singularities? probing timelike singularities with finite energy waves," *Physical Review D*, vol. 60, no. 10, p. 104028, 1999.

[31] R. M. Wald, "Dynamics in nonglobally hyperbolic, static space-times," *Journal*

of Mathematical Physics, vol. 21, no. 12, pp. 2802–2805, 1980.

[32] G. T. Horowitz and D. Marolf, "Quantum probes of spacetime singularities," *Physical Review D*, vol. 52, no. 10, p. 5670, 1995.

[33] H. Weyl, "Über gewöhnliche differentialgleichungen mit singularitäten und die zugehörigen entwicklungen willkürlicher funktionen. (mit 1 figur im text)," *Mathematische Annalen*, vol. 68, pp. 220–269, 1910. [Online]. Available: http://eudml.org/doc/158437

[34] J. v. Neumann, "Allgemeine eigenwerttheorie hermitescher funktionaloperatoren," *Mathematische Annalen*, vol. 102, pp. 49–131, 1930. [Online]. Available: http://eudml.org/doc/159371

[35] M. Reed and B. Simon, "Functional analysis and fourier analysis, self-adjointness," *Methods of Modem Mathematical Physics, Vols. I & II, Academic Press, New York*, 1972.

[36] G. W. Gibbons and M. C. Werner, "Applications of the gauss–bonnet theorem to gravitational lensing," *Classical and Quantum Gravity*, vol. 25, no. 23, p. 235009, nov 2008. [Online]. Available: https://dx.doi.org/10.1088/0264-9381/25/23/235009

[37] M. Werner, "Gravitational lensing in the kerr-randers optical geometry," *General Relativity and Gravitation*, vol. 44, pp. 3047–3057, 2012.

[38] M. P. Do Carmo, *Differential geometry of curves and surfaces: revised and*

updated second edition. Courier Dover Publications, 2016.

[39] A. Ishihara, Y. Suzuki, T. Ono, T. Kitamura, and H. Asada, "Gravitational bending angle of light for finite distance and the gauss-bonnet theorem," *Phys. Rev. D*, vol. 94, p. 084015, Oct 2016. [Online]. Available: https://link.aps.org/doi/10.1103/PhysRevD.94.084015

[40] M. C. Werner, *Gravitational Lensing and Optical Geometry*. MDPI, Basel, 2020.

[41] W. Rindler and M. Ishak, "Contribution of the cosmological constant to the relativistic bending of light revisited," *Physical Review D*, vol. 76, no. 4, p. 043006, 2007.

[42] K. S. Thorne, J. A. Wheeler, and C. W. Misner, *Gravitation*. Freeman San Francisco, CA, 2000.

[43] N. K. Glendenning, *Compact stars: Nuclear physics, particle physics and general relativity*. Springer Science & Business Media, 2012.

[44] O. Zubairi, A. Romero, and F. Weber, "Static solutions of einstein's field equations for compact stellar objects," in *Journal of Physics: Conference Series*, vol. 615, no. 1. IOP Publishing, 2015, p. 012003.

[45] F. Frutos-Alfaro and M. Soffel, "On relativistic multipole moments of stationary space–times," *Royal Society open science*, vol. 5, no. 7, p. 180640, 2018.

[46] H. Kodama and W. Hikida, "Global structure of the zipoy–voorhees–weyl spacetime and the δ= 2 tomimatsu–sato spacetime," *Classical and Quantum Gravity*, vol. 20, no. 23, p. 5121, 2003.

[47] G. Lukes-Gerakopoulos, "Nonintegrability of the zipoy-voorhees metric," *Physical Review D*, vol. 86, no. 4, p. 044013, 2012.

[48] S. Chandrasekhar and B. C. Xanthopoulos, "On colliding waves that develop time-like singularities: A new class of solutions of the einstein-maxwell equation," *Proceedings of the Royal Society of London. Series A, Mathematical and Physical Sciences*, vol. 410, no. 1839, pp. 311–336, 1987. [Online]. Available: http://www.jstor.org/stable/2398210

[49] S. Chandrasekhar and B. Xanthopoulos, "On colliding waves in the einstein-maxwell theory," *Proceedings of the Royal Society of London. Series A, Mathematical and Physical Sciences*, vol. 398, no. 1815, pp. 223–259, 1985. [Online]. Available: http://www.jstor.org/stable/2397513

[50] M. Halilsoy, "Interpolation of the schwarzschild and bertotti-robinson solutions," *General relativity and gravitation*, vol. 25, pp. 275–280, 1993.

[51] M. Yamazaki, "On the charged kerr-tomimatsu-sato family of solutions," *Journal of Mathematical Physics*, vol. 19, no. 6, pp. 1376–1378, 1978.

[52] M. Halilsoy, M. Mangut, and C.-L. Hsieh, "Stationary, charged zipoy–voorhees metric from colliding wave spacetime," *General Relativity and Gravitation*,

vol. 55, no. 103, 2023.

[53] S. Chandrasekhar and B. C. Xanthopoulos, "A new type of singularity created by colliding gravitational waves," *Proceedings of the Royal Society of London. A. Mathematical and Physical Sciences*, vol. 408, no. 1835, pp. 175–208, 1986.

[54] M. Halilsoy, "Similarity solution for the ernst equation with electromagnetic fields," *Lettere Al Nuovo Cimento, Italian Physical Society*, vol. 37, no. 231, 1983.

[55] M.Halilsoy, "Large family of colliding waves in the einstein–maxwell theory," *Journal of mathematical physics*, vol. 31, no. 11, pp. 2694–2698, 1990.

[56] M. Halilsoy, "New metrics for spinning spheroids in general relativity," *Journal of mathematical physics*, vol. 33, no. 12, pp. 4225–4230, 1992.

[57] A. Al-Badawi and M. Halilsoy, "On the physical meaning of the nut parameter," *General Relativity and Gravitation*, vol. 38, pp. 1729–1734, 2006.

[58] E. Newman, L.Tamburino, and T. Unti, "Empty space generalization of the schwarzschild metric," *J. Math. Phys. (N.Y)*, vol. 4, no. 915, 1963.

[59] K. Gödel, "An example of a new type of cosmological solutions of einstein's field equations of gravitation," *Reviews of modern physics*, vol. 21, no. 3, p. 447, 1949.

[60] M. Halilsoy and Ö. Gürtuğ, "On some properties of the nut-curzon space-time," *Il Nuovo Cimento B (1971-1996)*, vol. 109, no. 9, pp. 963–972, 1994.

[61] I. Robinson, "A solution of the maxwell-einstein equations," *Bull. Acad. Pol. Sci. Ser. Sci. Math. Astron. Phys*, vol. 7, p. 351, 1959.

[62] B. Bertotti, "Uniform electromagnetic field in the theory of general relativity," *Physical Review*, vol. 116, no. 5, p. 1331, 1959.

[63] E. Newman and R. Penrose, "An approach to gravitational radiation by a method of spin coefficients," *Journal of Mathematical Physics*, vol. 3, no. 3, pp. 566–578, 1962.

[64] L. Herrera, F. M. Paiva, and N. Santos, "Geodesics in the γ spacetime," *International Journal of Modern Physics D*, vol. 9, no. 06, pp. 649–659, 2000.

[65] O. Gurtug and M. Mangut, "Effect of power-law maxwell field to the gravitational lensing," *Physical Review D*, vol. 99, no. 8, p. 084003, 2019.

[66] Ö. Gurtug and M. Mangut, "Gravitational lensing in a model of nonlinear electrodynamics: The case for electrically and magnetically charged compact objects," *Annalen der Physik*, vol. 532, no. 3, p. 1900576, 2020.

[67] O. Gurtug, M. Halilsoy, and M. Mangut, "Probing naked singularities in the charged and uncharged $\gamma-$ metrics with quantum wave packets," *General Relativity and Gravitation*, vol. 55, no. 98, 2023.

[68] O. Unver and O. Gurtug, "Quantum singularities in (2+ 1) dimensional matter coupled black hole spacetimes," *Physical Review D*, vol. 82, no. 8, p. 084016, 2010.

[69] I. S. Gradshteyn and I. M. Ryzhik, *Table of integrals, series, and products*. Academic press, 2014.

[70] W. Rudin *et al.*, *Principles of mathematical analysis*. McGraw-hill New York, 1976, vol. 3.

[71] M. Abramowitz, I. A. Stegun, and R. H. Romer, "Handbook of mathematical functions with formulas, graphs, and mathematical tables," 1988.

[72] M. Mangut, H. Gürsel, and İ. Sakallı, "Gravitational lensing in kerr–newman anti de sitter spacetime," *Astroparticle Physics*, vol. 144, p. 102763, 2023.

[73] S. Zhang, Y. Liu, and X. Zhang, "Kerr–de sitter and kerr–anti–de sitter black holes as accelerators for spinning particles," *Physical Review D*, vol. 99, no. 6, p. 064022, 2019.

[74] A. N. Aliev, "Electromagnetic properties of kerr–anti-de sitter black holes," *Physical Review D*, vol. 75, no. 8, p. 084041, 2007.

[75] A. Belhaj, M. Chabab, H. El Moumni, L. Medari, and M. Sedra, "The thermodynamical behaviors of kerr—newman ads black holes," *Chinese Physics Letters*, vol. 30, no. 9, p. 090402, 2013.

[76] V. A. Kostelecký and M. J. Perry, "Solitonic black holes in gauged n= 2 supergravity," *Physics Letters B*, vol. 371, no. 3-4, pp. 191–198, 1996.

[77] G. F. Ellis, R. Maartens, and M. A. MacCallum, *Relativistic cosmology*.

Cambridge University Press, 2012.

[78] C. G. Tsagas and J. D. Barrow, "A gauge-invariant analysis of magnetic fields in general-relativistic cosmology," *Classical and Quantum Gravity*, vol. 14, no. 9, p. 2539, 1997.

[79] G. Clement, D. Gal'tsov, and C. Leygnac, "Linear dilaton black holes," *Physical Review D*, vol. 67, no. 2, p. 024012, 2003.

[80] M. Halilsoy and I. Sakalli, "Collision of electromagnetic shock waves coupled with axion waves: An example," *Classical and Quantum Gravity*, vol. 20, no. 8, p. 1417, 2003.

[81] G. Kraniotis, "Gravitational lensing and frame dragging of light in the kerr–newman and the kerr–newman (anti) de sitter black hole spacetimes," *General Relativity and Gravitation*, vol. 46, pp. 1–44, 2014.

[82] M. Bartelmann, *General Relativity, Lecture Notes*. Heidelberg University Publishing, 2019.

[83] S. Hilbert, S. D. White, J. Hartlap, and P. Schneider, "Strong-lensing optical depths in a λcdm universe–ii. the influence of the stellar mass in galaxies," *Monthly Notices of the Royal Astronomical Society*, vol. 386, no. 4, pp. 1845–1854, 2008.

[84] G. Bisnovatyi-Kogan and O. Y. Tsupko, "Gravitational lensing in plasmic medium," *Plasma Physics Reports*, vol. 41, pp. 562–581, 2015.

[85] T. Hsieh, D.-S. Lee, and C.-Y. Lin, "Strong gravitational lensing by kerr and kerr-newman black holes," *Physical Review D*, vol. 103, no. 10, p. 104063, 2021.

[86] F. P. Esposito and L. Witten, "On a static axisymmetric solution of the einstein equations," *Physics Letters B*, vol. 58, no. 3, pp. 357–360, 1975.

APPENDICES

Appendix A: Asymptotic Expansion Coefficients for Metric Functions and em Potentials

The coefficients of the metric functions asymptotically expanded in $(A.1-A.5)$ are shown below.

$$
\begin{aligned}
a_1 &= -4mp^2\gamma \\
a_2 &= -\left(2p^2(k+1)+\gamma k\left(k\left(p^2+1\right)^2+p^4-1\right)+2k-8\gamma p^2-2\right)2m^2p^2\gamma \\
a_3 &= 8m^3p^4\gamma^3\left(5k^2\left(p^2+1\right)^2+4k\left(p^4-1\right)-\left(p^2+22\right)p^2-1\right) \\
&-\frac{4}{3}\gamma m^3p^2\left(p^2+3\right)r_0^2-4\gamma^2m^3p^2\left(k\left(k\left(p^2+1\right)^2+p^4-1\right)-8p^2\right)
\end{aligned}
\tag{A.1}
$$

$$
\begin{aligned}
b_0 &= 2mp\gamma c(\theta) \\
c(\theta) &= (p^2+1)\sqrt{k^2-1}\cos(\theta) \\
b_1 &= -4m\gamma p^2 \\
b_2 &= -2m^2p^2\gamma\left(2p^2(k+1)+\gamma k\left(k\left(p^2+1\right)^2+p^4-1\right)+2k-8\gamma p^2-2\right) \\
b_3 &= -\frac{8}{3}p^4m^3\gamma^3\left(-5k^2\left(p^2+1\right)^2-4k\left(p^4-1\right)+p^4+22p^2+1\right) \\
&+\frac{4}{3}r_0p^2m^3\gamma\left(\left(p^2+3\right)\left((k+1)p^2+k-1\right)+3\gamma\left(k\left(k\left(p^2+1\right)^2+p^4-1\right)-8p^2\right)\right)
\end{aligned}
\tag{A.2}
$$

$$
\begin{aligned}
c_0 &= \frac{1}{4}r_0^2 \\
c_1 &= 4m\gamma p^2 \\
c_2 &= \frac{1}{2}m^2p^2r_0\left(k\left(3\gamma^2+1\right)\left(p^2+1\right)-\left(\gamma^2-1\right)p^2-1\right) \\
&+\frac{1}{2}m^2p^2r_0\left(\gamma(\gamma+8)+r_0\left(\gamma^2-1\right)\cos(2\theta)\right) \\
c_3 &= -2m^3p^2r_0^2\left(\gamma^2-1\right)\left(kp^2+k+2\gamma p^2+p^2-1\right)\sin^2(\theta) \\
&-\frac{4}{3}m^3p^2r_0^2\gamma\left(3\gamma k+p^2\left(2\gamma^2+3\gamma k+1\right)+3\right)
\end{aligned}
\tag{A.3}
$$

$$
\begin{aligned}
d_{-2} &= \frac{1}{4} \\
d_{-1} &= -\frac{1}{2}m\left(kp^2+k-2\gamma p^2+p^2-1\right) \\
d_0 &= +\frac{1}{8}m^2p^2r_0^2\left(\gamma^2-1\right)\cos(2\theta) \\
&+\frac{1}{8}m^2r_0\left(k\left(p^2+1\right)\left(\left(3\gamma^2-1\right)p^2+2\right)-\left(\gamma^2+1\right)p^4+((\gamma-8)\gamma+3)p^2-2\right) \\
d_1 &= \frac{1}{6}(3\cos(2\theta)+1)\left(\gamma^2-1\right)\gamma m^3p^4r_0^2 \\
d_2 &= \frac{r_0^3}{196}\left(\left(\gamma^2-1\right)\gamma m^4p^4\left(32-\gamma\left((7k-9)p^2+7k+9\right)\right.\right. \\
&\left.\left.+12\cos(2\theta)\left(\gamma+3\gamma k+p^2\gamma(3k-1)+8\right)\right)\right)+\frac{3}{196}\left(\gamma^2-1\right)\gamma^2m^4p^4r_0^4\cos(4\theta) \\
d_3 &= \frac{1}{480}r_0^4\gamma\left(\gamma^2-1\right)m^5p^4\left(80-5\gamma(7k+9)-p^2(\gamma(6\gamma+35k-45)+16)\right) \\
&+\frac{1}{24}r_0^4\gamma\left(\gamma^2-1\right)m^5p^4\left(3(\gamma+3\gamma k+4)+p^2(\gamma(2\gamma+9k-3)+4)\right)\cos(2\theta) \\
&+\frac{1}{32}r_0^4\gamma\left(\gamma^2-1\right)m^5p^4\gamma\left(kp^2+k+2\gamma p^2+p^2-1\right)\cos(4\theta)
\end{aligned}
\tag{A.4}
$$

$$
\begin{aligned}
e_{-2} &= \frac{1}{4r_0}\sin^2(\theta) \\
e_{-1} &= -\frac{1}{2}(-1+k+p^2+kp^2-2p^2\gamma)sin^2(\theta) \\
e_0 &= -(-1+k^2)(1+p^2)^2m^2p^2\gamma^2cos^2(\theta) \\
&+\frac{1}{2}m^2r_0\left(k\left(p^2+1\right)\left(\left(2\gamma^2-1\right)p^2+1\right)-p^2\left(4\gamma+p^2-2\right)-1\right)\sin^2(\theta) \\
e_1 &= \frac{2}{3}m^3p^4\gamma\left(6\gamma^2\left(k^2-1\right)\left(p^2+1\right)^2\cos^2(\theta)+\left(\gamma^2-1\right)r_0^2\sin^2(\theta)\right) \\
e_2 &= 12\gamma^2\left(k^2-1\right)\left(p^2+1\right)^2\left(2(k+1)p^2+\gamma k\left(k\left(p^2+1\right)^2+p^4-1\right)\right. \\
&\left.+2k-8\gamma p^2-2\right)\cos^2(\theta)+r_0^3\left(\gamma^2-1\right)\left(\gamma k\left(p^2+1\right)+4\right)\sin^2(\theta) \\
e_3 &= \frac{16}{3}\gamma^5m^5p^6\left(k^2-1\right)\left(p^2+1\right)^2\left(-5k^2\left(p^2+1\right)^2-4k\left(p^4-1\right)\right. \\
&\left.+p^4+22p^2+1\right)\cos^2(\theta)+\frac{8}{3}\gamma^3m^5p^4r_0^2\left(k^2-1\right)\left(p^2+1\right)^2\cos^2(\theta) \\
&+\frac{24}{3}\gamma^4m^5p^4r_0\left(k^2-1\right)\left(p^2+1\right)^2\left(k\left(k\left(p^2+1\right)^2+p^4-1\right)-8p^2\right)\cos^2(\theta) \\
&+\frac{2}{15}\gamma m^5p^4r_0^4\left(\gamma^2-1\right)\left(5(\gamma k+2)+p^2\left(2\gamma^2+5\gamma k+2\right)\right)\sin^2(\theta)
\end{aligned}
\tag{A.5}
$$

The coefficients of the em potentials are given by

$$
\begin{aligned}
\alpha_0 &= \frac{p(k+1)}{(k+1)p^2+k-1}q \\
\alpha_1 &= \frac{2\gamma m}{k+1}\left(k\left(p^2-1\right)+p^2+1\right) \\
\alpha_2 &= \frac{2\gamma m^2 p}{k+1}\left(2\gamma p^2\left(k^2+(k-2)(k+1)p^2+k-2\right)+k\left((k+2)p^4-k+2\right)+p^4-1\right) \\
\alpha_3 &= \frac{2\gamma m^3 r_0}{3(k+1)}\left(r_0\left(p^2+3\right)\left(k\left(p^2-1\right)+p^2+1\right)+12\gamma p^2\left(k^2+(k-2)(k+1)p^2+k-2\right)\right) \\
&- \frac{4\gamma^3 p^6 m^3}{3}\left((k(2k+15)-23)+(k+1)(2k-1)p^2\right) \\
&+ \frac{4\gamma^3 p^2 m^3(k-1)}{3(k+1)}\left((-1+k)(1+2k)+(-23+k(-15+2k))p^2\right)
\end{aligned}
\tag{A.6}
$$

$$
\begin{aligned}
\beta_0 &= \frac{\sqrt{k^2-1}}{(k+1)p^2+k-1}q \\
\beta_1 &= 4\gamma m p^2 \\
\beta_2 &= 2\gamma m^2 p^2\left(\gamma+k\left(p^2+1\right)\left(\gamma\left(p^2-1\right)-2\right)+p^2\left(\gamma\left(p^2+6\right)-2\right)+2\right) \\
\beta_3 &= -\frac{4r_0\gamma m^3 p^2}{3}\left(\left(p^2+3\right)r_0-3\gamma\left(k\left(p^4-1\right)+p^4+6p^2+1\right)\right) \\
&+ \frac{16\gamma^3 m^3 p^4(k-2)}{3}\left(2\left(k-2\right)p^2+k^2+(k+1)p^4+1\right)
\end{aligned}
\tag{A.7}
$$